



**University of
Zurich**^{UZH}

Comparative Analysis of the Flood Models HEC-RAS and BASEMENT

ESS 511 Master's Thesis

Author

Navjot Kaur Sidhu
16-719-577

Supervised by

Remo Solèr (r.soler@bs-ing.ch)

Faculty representative

Prof. Dr. Jan Seibert

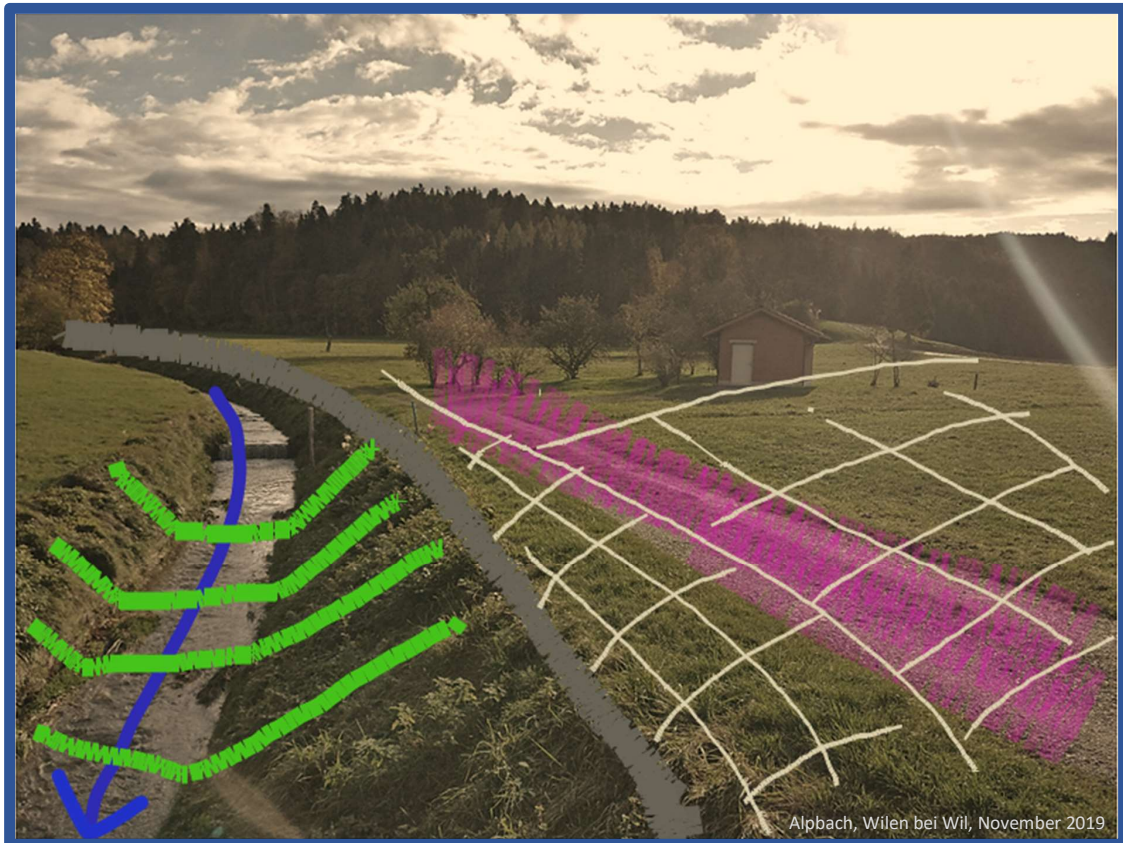
01.10.2020

Department of Geography, University of Zurich

A Comparative Analysis of Flood Modeling HEC-RAS and BASEMENT

Thesis

To obtain the degree of Master of Science in Earth System Science



Author
Navjot Sidhu
16-719-577

Supervisor
Remo Solèr
dipl. Bauingenieur FH

B+S
INGENIEURE UND PLANER

Faulty Representative
Prof. Dr. Jan Seibert

 **Universität
Zürich**^{UZH}

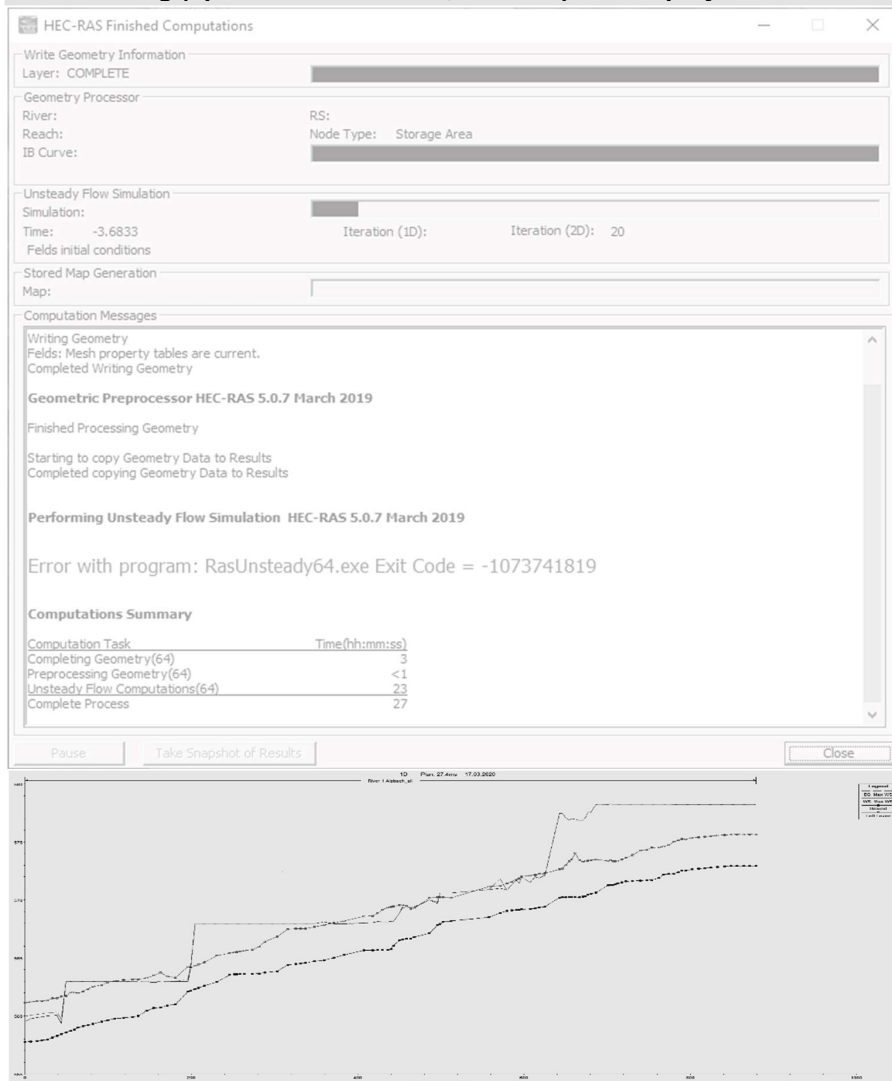
Submitted to the Department of Geography, University of Zurich
September 2020

Acknowledgements

While working on this thesis I was fortunate to have assistance and support. I would like to express bottomless gratitude to Remo Solèr at B+S AG for accepting me as a thesis student and offering his time, wisdom and patience to support the hydraulic modeling process, which was a new topic for me. This thesis was an admittedly ambitious endeavour and could not have been realised without his knowledge and guidance. I would also like to thank Andrea Waser at B+S AG for her time and sharing results.

Thank you to Prof. Dr. Jan Seibert for being my faculty representative and facilitating this thesis and thank you to Dr. Daniel Viviroli for his time and providing clarifications when I was at the early stages.

Many thanks to Johanna Theilmann for her LaTeX tutorial and resources. And thank you to friends -new and old, near and far- for sending an abundance of encouragement, good vibes and positive energy as I trucked along (uphill and backwards, at times) on this project.



Abstract

Due to the extreme damages, dangers and costs associated with flood events, hazard maps are produced to help understand the risk involved and make decisions. In Switzerland, generating hazard maps are a requirement for each canton. This task is carried out by a modeler via the use of a flood modeling software. Flood models are tested and compared often in research to assist modelers in determining which tool to utilise for their project and generate trust in the outputs. This thesis aimed to compare two freely available models: HEC-RAS and BASEMENT. As well as explore the latest version of HEC-RAS, which recently added 2D modeling capabilities. The HEC-RAS and BASEMENT comparison was done using a fully 2D approach, while the intra-model comparisons for HEC-RAS were done using 1D, 2D and linked 1D2D models, as well as testing parameters. The outputs from BASEMENT and HEC-RAS in the case study area were found to be similar, as well as when utilising extreme hydrology inputs. For the flood plain in the case study area, a 1D2D modeling approach could be utilised over a fully 2D to save on computation time as outputs were also similar. Geometry representation was found to be very important, especially grid cell alignment in HEC-RAS.

Contents

List of Figures	5
List of Tables	8
1 Introduction	9
1.1 Flooding in Switzerland	9
1.1.1 Recent Events – Costs and Dangers	9
1.1.2 Future outlooks	10
1.1.3 Hazard Mapping System	11
1.2 Flood Modeling - Link to industry	12
1.3 Flood Modeling in Research	12
1.3.1 Parameter - Manning’s n	13
1.3.2 Inputs	14
1.3.3 Validation Data	14
1.3.4 Model Structure - Modeling Approach	14
1.4 Tools for Modeling – Software	15
1.5 Research Questions	16
1.5.1 Question 1	16
1.5.2 Question 2	16
1.5.3 Question 3	16
2 Study Site	17
2.1 Hochwasserschutz Projekt	17
2.2 Catchment Characteristics	19
2.3 Study Site	22
3 Methodology	24
3.1 Models	24
3.1.1 HEC-RAS	25
3.1.2 BASEMENT	25
3.1.3 Computations	25
3.2 HWS Results	26
3.3 Input Data	27
3.3.1 Terrain	27

3.3.2 Hydrology	28
3.4 Calibration and Validation	30
3.5 Model Set-ups	30
3.5.1 2D Models	31
3.5.2 Models to explore dimensionality	32
3.5.3 Exploring parameters	34
4 Results and Discussion Q1	38
4.1 1:1 1st 2D	38
4.1.1 Peak Values	38
4.1.2 Metrics and Statistics	39
4.1.3 Residuals	41
4.2 1:1 NACH 2D	49
4.2.1 Peak Values	49
4.2.2 Metrics and Statistics	50
4.2.3 Residuals	51
4.2.4 Intense Hydrology	57
5 Results and Discussion Q2	68
5.1 1D and 2D - Channel	68
5.2 1D2D and 2D - Floodplain	71
6 Results and Discussion Q3	76
6.1 Roughness	76
6.2 Time	78
6.3 2D Equation	79
6.4 Junction Equation	79
6.5 Weir Setup	79
6.6 Grid Size	79
6.7 Grid Alignment	82
7 Discussion	86
7.1 Further Discussion	86
8 Conclusion	87
9 References	89
Appendices	96
Appendix A	97
A.1 BASEMENT Computational Meshes	97
A.2 Flood area maps: start-, end-, and post-peak flow	100

List of Figures

1.1	Krebsbach A1 Flood (Wil, SG)	10
1.2	Hazard Mapping	12
2.1	HWS Location	18
2.2	HWS Modifications	19
2.3	Catchments of HWS	21
2.4	Study Site Terrain	22
3.1	Scenario NACH for HWS	27
3.2	DEM	28
3.3	Hydrological Input	29
3.4	Flood Depth HQ30 and HQ100	30
3.5	Model Organisation for Analysis	31
3.6	Mannings Roughness Layer in HEC-RAS	32
3.7	Base Models Setup	34
3.8	Grid Size Adjustment	36
4.1	2D IST - Peak 10% Depth	39
4.2	2D IST - Peak 10% Velocity	39
4.3	Study Areas and Key Areas IST	40
4.4	2D IST Contingency Output	41
4.5	2D IST Depth Residuals	42
4.6	2D IST Velocity Residuals	43
4.7	2D IST Depth Residuals Histogram	43
4.8	2D NACH Velocity Residuals Histogram	44
4.9	2D IST Profile Line Depth at Wilen Outlet	45
4.10	2D IST Profile Line Velocity at Wilen Outlet	46
4.11	2D IST Profile Line Depth at Engistr. 95	47
4.12	2D IST Profile Line Velocity at Engistr. 95	48
4.13	2D NACH - Peak 10% Depth	49
4.14	2D NACH - Peak 10% Depth	49
4.15	Study Areas and Key Areas NACH	50
4.16	2D NACH Contingency Output	51
4.17	2D NACH Depth Residuals	52

4.18	2D NACH Velocity Residuals	52
4.19	2D NACH Depth Residuals Histogram	53
4.20	2D NACH Velocity Residuals Histogram	53
4.21	2D NACH Profile Line Depth at Sooret Field	54
4.22	2D NACH Profile Line Velocity at Sooret Field	55
4.23	2D NACH Profile Line Depth at Overflow Area	56
4.24	2D NACH Profile Line Velocity at Overflow Area	57
4.25	2D NACH Depth Residuals for HQ1000	58
4.26	2D NACH Velocity Residuals for HQ1000	58
4.27	2D NACH Depth Residuals Histogram - HQ1000	59
4.28	2D NACH Velocity Residuals Histogram - HQ1000	59
4.29	2D NACH Depth at Sooret for HQ1000	60
4.30	2D NACH Velocity at Sooret for HQ1000	61
4.31	2D NACH Depth at Overflow Area for HQ1000	62
4.32	2D NACH Velocity at Sooret for HQ1000	63
4.33	Tributary Velocity	64
4.34	Tributary Comparison	65
5.1	Depth along Thalweg	69
5.2	Velocity along Thalweg	69
5.3	Overflow point for 1D and 2D	70
5.4	Depth at Overflow point for 1D and 2D	71
5.5	Floodplain Depth Residuals	72
5.6	Floodplain Depth Residuals Histogram	73
5.7	Floodplain Velocity Residuals	74
5.8	Floodplain Velocity Residuals Histogram	75
6.1	Velocity with Varying Roughness Values	76
6.2	Flow with Varying Roughness Values	77
6.3	Flood Extents with Varying Roughness	78
6.4	Grid Size - Velocity profiles	81
6.5	Grid Size - Flood Extents	82
6.6	Grid Alignment During Setup	83
6.7	GridAlignment	84
6.8	Weir Flow	85
A.1	BASEMENT IST Mesh	98
A.2	BASEMENT NACH Mesh	99
A.3	BASEMENT IST HQ300	101
A.4	BASEMENT NACH HQ300	102
A.5	BASEMENT NACH HQ1000	103

A.6	HEC-RAS 1D2D IST HQ300	104
A.7	HEC-RAS 1D2D NACH HQ300	105
A.8	HEC-RAS 2D IST HQ300	106
A.9	HEC-RAS 2D NACH HQ300	107
A.10	HEC-RAS NACH HQ1000	108

List of Tables

3.1 Manning's n values	37
3.2 Weir Co-efficients	37
4.1 2D IST Metrics and Statistics	66
4.2 2D NACH Metrics and Statistics	67
6.1 Weir co-efficients	80

Chapter 1

Introduction

1.1 Flooding in Switzerland

In Switzerland, a landlocked nation, the threat of floods to a population of 8.5 million is relevant as streams and rivers traverse the country. It is considered a flood prone country, especially in the mountainous regions, but the plateau region also is subject to intense thunderstorms as described by MeteoSwiss precipitation data ([46]). Severe floods have occurred in the past and are likely to occur in the future. It is a natural hazard of such importance that since 1972, the well-maintained National Platform for Natural Hazards (<http://www.planat.ch/> records floods and damages caused in CHF in its database, with floods accounting for 86% of damages in the history of the database.

1.1.1 Recent Events – Costs and Dangers

The effects of flooding vary from minor, to expensive up to dangerous. Examples include traffic delays, property or infrastructure damage, crop losses, population displacement and death [51]. Whether a large river crossing many countries or a first order stream, there is a possibility of flooding to occur and effects to be felt. The relatively small Krebsbach has been spending its recent summers causing the A1 motorway to close, as recently as 2015, 2018 and 2019 (www.hallowil.ch.)

In PLANAT, from 1972 to 2016, 16,800 entries for flood damage were entered [7]. The most expensive damage recorded for an event was 3 billion CHF in 2005 due to intense rainfall across a large part of the country. In October 2000, 669 million CHF of damage was recorded as well as fatalities after several days of rainfall. When damage from flooding can become so expensive, another part of the cost equation is introduced: protection investments. In the same paper the authors reported reported CHF 1.45 is spent annually on natural hazard prevention measures, which includes the development of hazard maps.

Overall flooding becomes of interest for the danger but also for the cost/investment.



Figure 1.1: A portion of the A1 Motorway in the region of Wil was flooded by the Krebsbach after an intense rainfall event in June 2015. Image from the official website for the flood protection project in Wil (www.hws-region-wil.ch).

1.1.2 Future outlooks

It is generally accepted that flooding is a re-occurring theme in Switzerland. There is a diversity in terrain and also in weather patterns, and the benefit of this in terms of flooding is that the “big floods” which cause damage of gross proportions across the country are less likely to occur. ([46] and [9]). The downside is that it makes studying future events and forming projections more complex. Thus studying effects of climate change on flooding is more than a research topic in Switzerland, but rather a large community of scientists working to evolve this subject as more information and research becomes available.

The theory is that warmer temperature will provide more thermal energy to processes which drive extreme events [9]. A warmer air temperature causes the air to be able to hold more moisture, leading to rainfall of a greater intensity. Recent large projects [22, 23] couldn't for certain say the flooding pattern in Europe will change. When not looking at seasonality, but event magnitudes, other work from Switzerland has found generally due to increased temperature, enhanced snowmelt and earlier precipitation that the peak value of mean annual floods is likely to increase for northern Switzerland [9, 28]. And Alpine areas will see a 20% increase [46]. As more information is obtained, more research questions emerge and scientists will re-visit old research to update it [27].

The number of events and their magnitude are one aspect of floods, another aspect is the risk and subsequent costs which can be narrowed down to societal processes [34]. Several studies explicitly note that aside from meteorological or hydrological reasons, risk and damage from floods has increased substantially due to the amount of population or valuables (property and belongings) put in or near risky areas [5, 9, 10, 30]. An interesting finding from Röhliberger et al. [44], when they examined all buildings in the entire country, the newer buildings - the ones built since 1980s - take a greater proportion of the risk exposure. Going forward, to avoid this type of risk or mitigate it as much as possible, it is important for planning to have a hazard map. With hazard maps risk can be accepted and understood and one can choose how much risk to take wisely.

1.1.3 Hazard Mapping System

As long ago as the 19th century Switzerland began to recognise the importance of protection measures by enacting laws in the late 1800s which meant the federal government would support cantons and municipalities with their protection work. Approximately 100 years later they increased the law and mandated cantonal authorities to perform hazard assessments and produce maps [24]. The maps are directly used in many important sectors of administering society: land use planning, zoning, building codes, emergency management and cost efficiency determination for protection measures. They provide the basis for assessment of hazards and are a step toward protection measures to be sufficient [24]. Beyond this they can also aid in the public's perception and can help people realise they live near risk and to take precautions [47]. Several types of maps are generated, which fall into two categories. A hazard map is used to show information related to a natural hazard – like where a flood plain is or areas affected by past events – and a danger map outlines the degree of danger in a particular area. For a flood map the risk is expressed as a combination of intensity (depth and velocity) and probability of occurrence. Overall, this is a long process -as evidenced by cantons being at different stages- that requires experts to produce very detailed outputs [24, 47].



Figure 1.2: Example of a hazard map from the GIS portal of the canton of Thurgau. This map depicts flood water depths and speed

1.2 Flood Modeling – Link to industry

The flood portion of a hazard map is generated by an expert via the means of a flood model.

Traditionally, experts, or practitioners, producing the flood portion of hazard maps have been hydrologists, (water resources) engineers and statisticians [33]. And they often are working with a flood model in order to serve a range of industries who may have commissioned the information: planning, development, construction, emergency services, infrastructure, tourism [Cook 2009]. The information obtained aids decision makers [48] plan for a safer future. While a large interest in flood modeling revolves around development and safety, floods also serve ecological purposes [21] and modeling results combine with research done in the natural sciences on ecosystems. The information can also be required to interface with other models [19, 27].

This imperative need to have the information for modeling, the inherent variation in any modeling (when taking a natural system turning it into numerical computations) and the reliance by many crucial projects in society on flood modeling means that flood modeling becomes a very relevant and also deep topic in research.

1.3 Flood Modeling in Research

“Flood modeling has become a global endeavour” [48]. Just as climate scenarios and hydrological extremes have come together to form a large research community, (which is generating one main part of data that is fed into flood models), the same can be said for flood modelling as a whole. When focusing on a flood model to produce an inundation map, for

example, a simple description of a flood model is hydrology + terrain + boundary conditions + hydraulic process to achieve an inundated area [15], a number of components are present. When cascading from these components a wealth of research has been generated and continues to be generated. This is definitely a topic which changes as developments in technology occur and practitioners should always be on the lookout for the latest scientific work [48].

The research on inundation modeling tends to divide models into 3 broad groups: Empirical – which relies on measurements and more recently remote sensing, Hydrodynamic – which are mathematical models based on physical laws and require input data, and conceptual (sometimes called 0 dimension) which are based on simplified hydraulic concepts and do not involve the actual solving of an equation [48]. The inputs and outputs of these models, and to a large degree the computation time will vary [8]. Users try to seek the model that balances the needs of their project, the computational demand and to some extent their knowledge. The overall process of modelling and its accessibility and a balance between data and computational demands is also important [38, 48].

This thesis will focus on the use of hydrodynamic models. These models can be divided into groups as well, based on the number of dimensions flow is computed for. The focus will be on 2 dimension (2D) and to a lesser extent 1 dimension (1D). This can also be referred to as the model type.

Teng et al. [48] breaks down the most widely studied parts of the model process: model parameters, model inputs, so-called validation data, change in floodplain landscape over time, change in climate conditions and a big part is choice of model structure.

1.3.1 Parameter – Manning's n

An important parameter to set for a numeric hydraulic model is the surface roughness as this value is empirically related to flow velocity and eventually used to derive depth. This value is usually represented by a roughness co-efficient, like Manning's (or Strickler). An earlier paper [20] concluded that the Manning's value should not be relied on for geomorphological research and if used, with extreme caution. The authors however did acknowledge that there are few alternatives that could be used. It is common when modeling to need to find a solution to carry on with the work. Many studies do not stick to focusing on only one portion of the modelling process and often combine processes or parameters as part of one greater study. For example, a later paper by **savage2016**, also examined the roughness parameter but involved the hydrograph input and topographic data as well. Papaioannou et al. [37] focused on roughness coefficient uncertainty but minimising uncertainty from other sources.

1.3.2 Inputs

The major input to a hydrodynamic model is the topographic data as this is often how geometry is represented (although geometry could be collected via field surveys). Geometry is important as it forms the basis of computations. This is one of the larger research topics and if not done as the sole focus of a study [1, 14] it is a part of others [15, 37]. It was generally accepted that a finer resolution DEM is better for accurate results [37] but researchers are also looking at how coarse the DEM can go or realising its full effect to know when to be able to extract useful information but save on computation time or still carry on with modeling when a fine resolution isn't available [savage2016, 41, 45].

Another part of the research is the hydrological input, which could be derived from a separate hydrological model first. The interface/coupling of these models is a topic of study, as well [4, 19].

1.3.3 Validation Data

Several studies must become creative – in an educated way – when it comes to calibration and validation of their models. In many instances the measurements or evidence of past floods simply does not exist. However, it is a clear problem that the observations or measurements needed to perform these steps are not robust and, more often than not, lacking. Research acknowledges this and is actively searching for a solution, or at least robust workarounds to this issue, for example focusing on smaller areas for local calibration [17, 35, 39, 53]. A very novel approach was done by Zischg et al. [53], who sought to validate inundation models using insurance claims and saw good results.

1.3.4 Model Structure – Modeling Approach

Model structure is a very important part of uncertainty on model process, but can be less studied than inputs [18]. What falls under model structure is the choice of tool that the modeler will use and this can also be called the modelling approach. Many modelers opt for a software rather than programming their own computations and utilise research to find which software is suitable for their needs. Often within a study on inputs, different modeling approaches are used to compare those as well [15, 32, 37]. Previously, Apel et al. [8], wanted to see how complex the model approach must be to satisfy a demand, similar to how DEM data was simplified to see what is the minimum needed.

Many researchers who investigated uncertainty in modeling inputs, have also conducted their study using more than one tool to generate a comparison [15, 16, 18, 26, 29, 32, 42]. The Environment Agency of the UK (DEFRA) has conducted a very large investigation on

2D hydraulic models which includes 15 suppliers [36]. The study has the aim of “delivering benefits through evidence” and the main objective is to ensure that the Environment Agency and the flood risk consultants they hire are utilising reliable packages as important decisions are based on the predicted variables. Following the DEFRA report, a benchmarking study for HEC-RAS was released to compare and highlight how this model can stand against the others [13].

Comparison studies are crucial in helping identify strengths and limitations of the modeling approach Alfieri 2018, for example, what was conducted by Ahmadian et al. [3] or Cook and Merwade [15].

1.4 Tools for Modeling – Software

The modeling approach is often chosen or limited based on accessibility – ie cost. A variety of software are publicly available to practitioners for download and are called “freeware”. Modeling approach can also be determined based on usability – ie knowledge required.

One model that is prevalent in research and used around the world is HEC-RAS [31].

The River Analysis System from the Hydrologic Engineering Center of the United States Army Corps of Engineers, commonly known as HEC-RAS, is a freeware model that is one of the most commonly used for hydrodynamic simulations [31, 37]. It has been available for over 2 decades and is capable of performing 1D modeling and is trusted to do so [25, 45]. The 2D modeling capability – and along with this the 1D/2D combined modeling - is relatively new, being first released as part of version 5.0 in spring 2016. Patel et al. [40] list several locations where HEC-RAS 1D was used or used in conjunction with another tool successfully for hydrodynamic simulations, but acknowledge that overflow analysis is limited in 1D and 2D would be more appropriate.

This 2D release opened the door to researchers exploring the 2D capabilities and integrating these capabilities into their projects. For example, Vozinaki et al. [50] immediately used both 1D and 1D/2D to investigate high-res topo data. Patel et al. [40] could apply the results of Vozinaki et al. [50] to integrate the 2D capabilities for assessing inundation in low lying areas of the large Lower Tapi Basin. And the Brunner [13] report compared this release to other models. But perhaps because it is new or because the practitioner/researcher was more comfortable with another approach, Petroselli et al. [42] missed a chance to apply the 2D capability and study intra model variations, even though they conducted 2D modeling using another software.

Another freeware available is BASEMENT, which was created by the Swiss Federal Institute of Technology Zurich (ETHZ). It has been presented in research as a tool among another study [12, 43, 49, 52, 53]. The depth of peer reviewed research of the model

itself is not as far reaching as other models, like HEC-RAS, although BASEMENT was released in 2006. Despite this limitation, it is being applied as the model of choice in a present day flood protection project: the Hochwasserschutz Region Wil Project (HWS) in eastern Switzerland (www.hws-region-wil.ch).

1.5 Research Questions

Within the scope of the latest version of HEC-RAS, and BASEMENT, being featured to a limited extent in research, and keeping in focus a flood modeler's practical needs, 3 research questions are proposed to explore the use and results from these softwares.

1.5.1 Question 1

How do the outputs of BASEMENT and HEC-RAS compare to one another?

1.5.2 Question 2

How do intra-model results from using varying dimensionality in HEC-RAS compare to one another?

1.5.3 Question 3

How do intra-model results from varying parameters in HEC-RAS compare to one another?

Chapter 2

Study Site

This section will outline the location and characteristics of the flood protection project in the region of Wil in East Switzerland and describe the study site used for this thesis.

2.1 Hochwasserschutz Projekt

In East Switzerland a flood protection project is currently underway (fig 2.1). The Hochwasserschutz Region Wil Project (HWS) has been commissioned by the Swiss Federal Roads Office, the Canton of St. Gallen (SG), the Canton of Thurgau (TG), the City of Wil, and the communities of Rickenbach, Sirnach and Wilen. Research relating to HWS began long ago and consultations, optimizations and planning are ongoing - construction has not started.

The HWS studies have been conducted in stages. Deficits in flood protection were already recognised as early as the 1980s and a feasibility report on the area was conducted in 2009. As Hall et al. [23] states, humankind has manipulated rivers for centuries for navigation, flood protection, food production and hydropower production among other purposes. The HWS region is no different. According to the project pre-study [6], the region of the HWS has always undergone some hydrological change. The report examined old maps and concluded that streams had their courses adjusted over time and, in addition, most marsh/swamp areas were drained. This aligns with the fact that the area was mainly used for agriculture. As development started in the 1900s and steadily increased, agricultural area was converted to residential and the natural space available for infiltration decreased. The annual population growth remained at +5% and beginning in 2000 the rate doubled to +10%. At present, there is residential, commercial and industrial properties in the area, as well as the A1 motorway, an SBB track and a regional train track. All of this infrastructure, combined with inhabitants, is of high value and needs to be protected from the dangers of floods.

The pre-study presented an in-depth examination of various combinations of protection

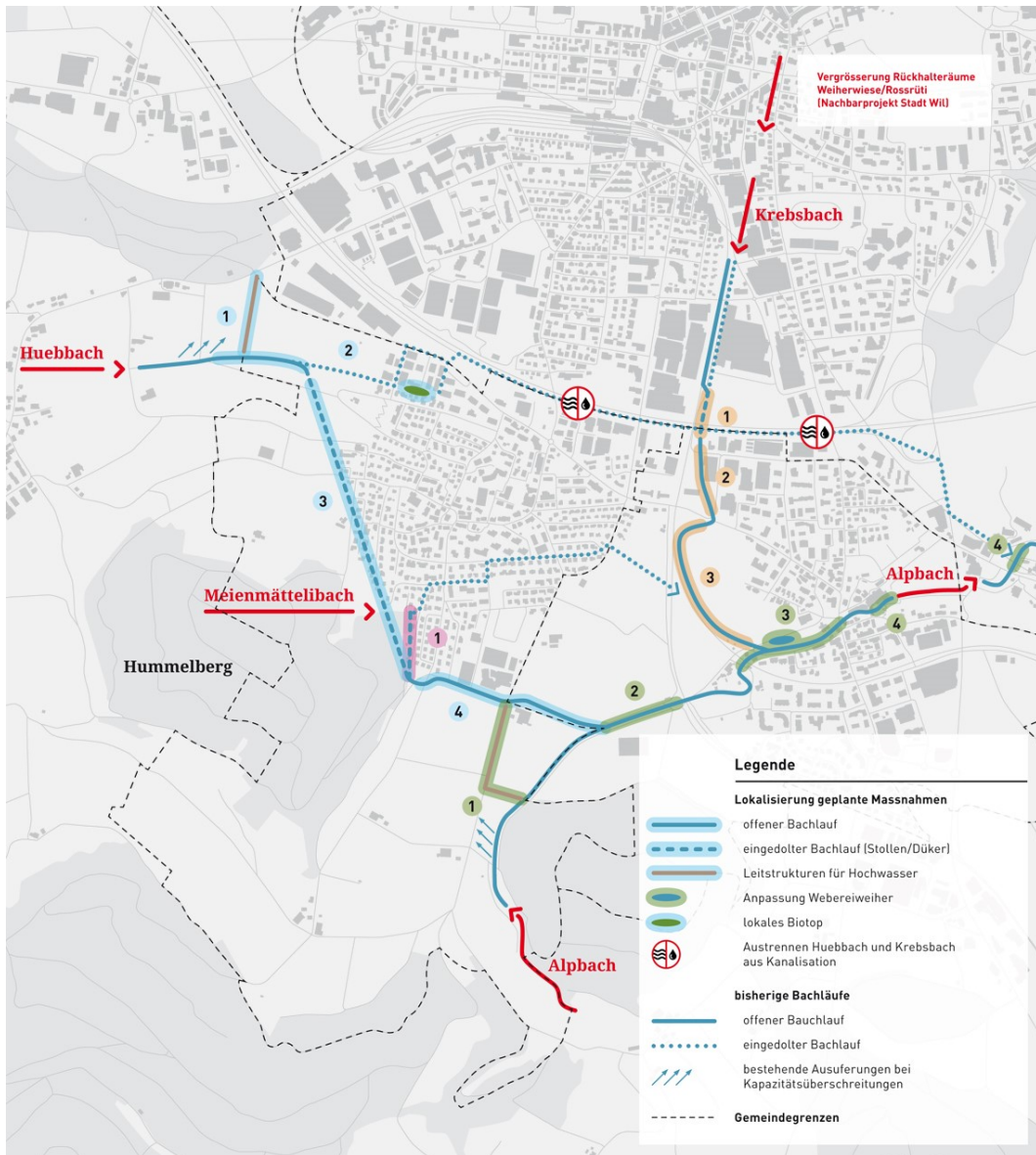


Figure 2.2: HWS measures to be implemented and watercourses to be modified. Image provided for information for public as part of HWS (www.hws-region-wil.ch)

2.2 Catchment Characteristics

The streams in the region -Krebsbach, Meienmättelibach, Huebbach and Alpbach (fig 2.3)- are all sub-catchments of the Thur River and relatively small compared to it. However, it shouldn't be forgotten that they have already proven their ability to exceed their banks and cause damage. For example, the Alpbach was recorded to cause flooding in Wilen in 1972 and the Krebsbach has caused closure of the A1 Motorway 3 times in recent history (www.hws-region-wil.ch). When considering only the 4 streams in the project, the Alpbach is the main channel with the other 3 streams feeding into it as tributaries and the total HWS catchment area is 22.9km². The Meienmaettelibach is the smallest stream and has

been deemed ephemeral in the past. It begins on the Hummelberg hill and flows to the edge of Wilen where a structure is in place to route the flow into a storm water line. The Huebbach begins in the town of Busswil in Thurgau and serves to drain this area, it joins the Alpbach at the water treatment facility Freudenu. The Krebsbach begins near the Hofberg area, north of the City of Wil and flows into the Alpbach along the western edge of the town of Rickenbach. The Alpbach headwaters are in the town of Kirchberg SG. For surface conditions, the streams flow over moraine (*Wiler Niederterrassenschotter* and at the area before the Thur, at the mouth of the Alpbach, is a drained marsh/reed [6]). The time of heaviest precipitation for the region occurs in June, July and August and it is an area which sees thunderstorms.

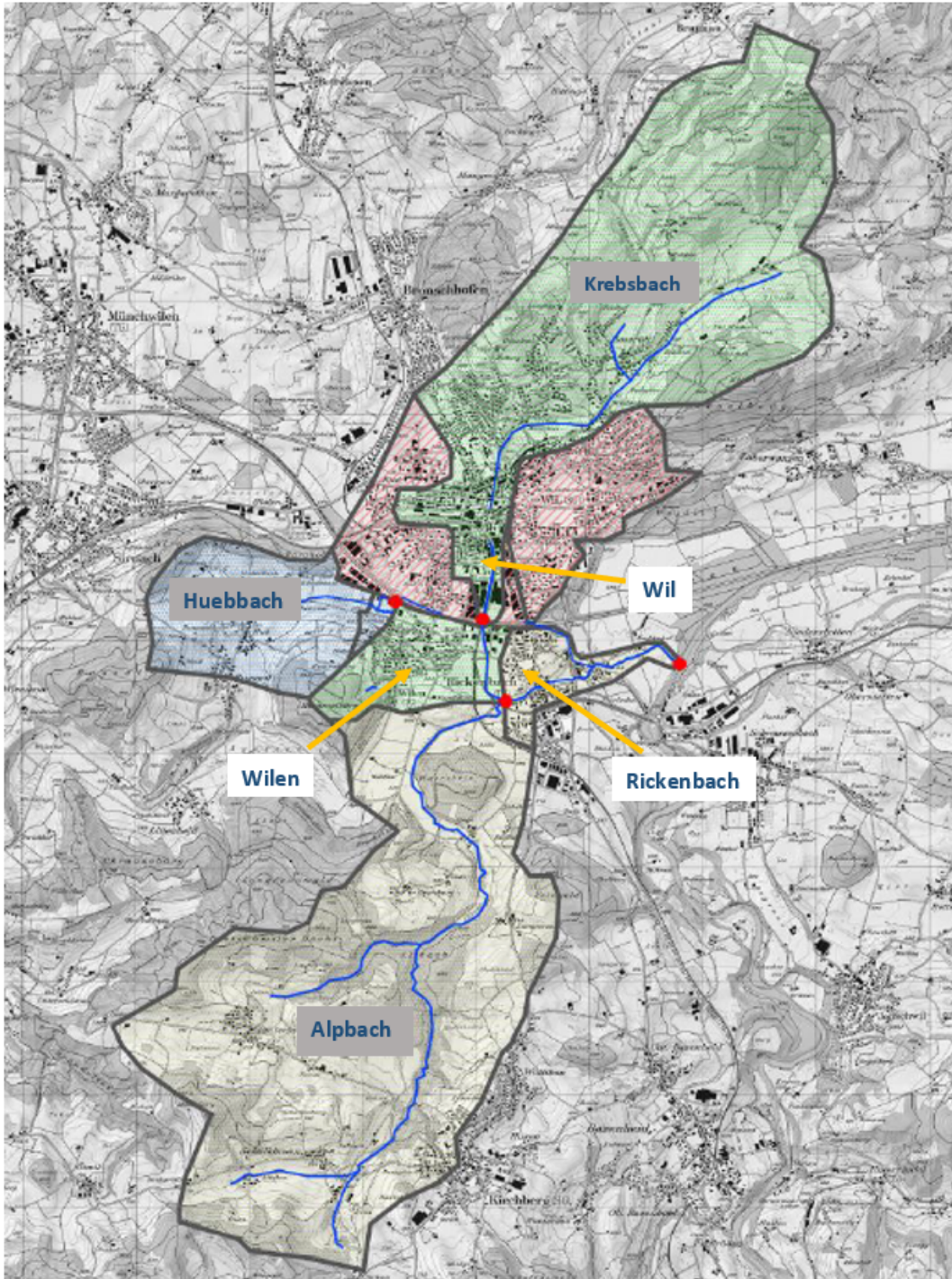


Figure 2.3: This image from the 2015 pre-study delineates the catchments in the HWS. The yellow delineation is the Alpbach catchment, the blue is for the Huebbach. The study area for this thesis is within the Alpbach catchment. After the Huebbach is redirected as part of the HWS, the catchment will terminate within the study area.

2.3 Study Site

The case study for this thesis took place over an area extracted from the area covered by HWS and investigated by B+S AG. The fields Sooret, Bachwis, Flurhof and Engi make-up the case study area and cover approximately 221,642 m². They are bound by Egelsestrasse along the west and south, Bachwissstrasse along the north and the Alpbach along the east. Within the project (sec 2.1) the Huebbach will be relocated to run as an open channel along Alpbachstrasse and join the Alpbach in the region on the eastern corner of the Bachwis (fig. 3.1).

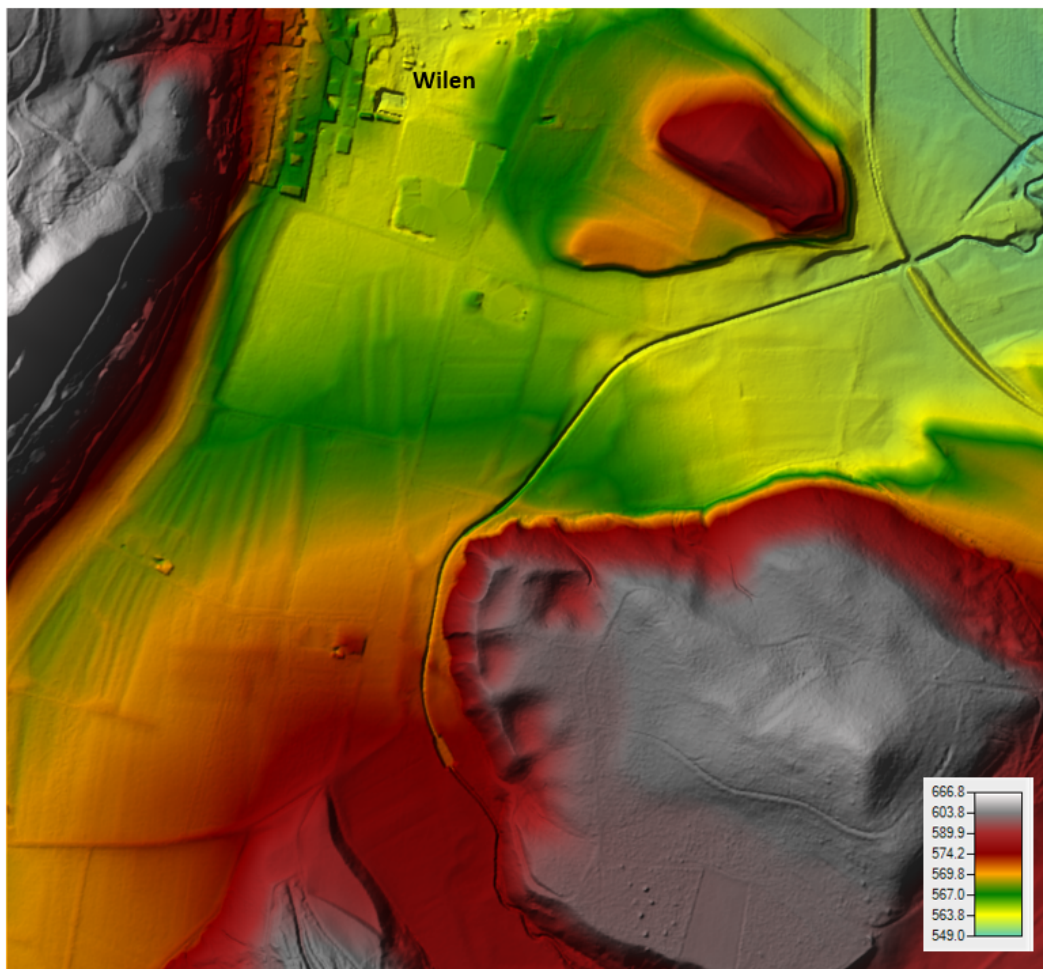


Figure 2.4: From the DEM the general slope of the terrain in the study area can be observed. Water leaving the channel would follow the terrain sloping down toward Wilten.

This area has been selected for both its relatively small size, which allows for faster model computation times, and its hydrological points of interest. The terrain in the area means the town of Wilten has an unfortunate position downslope of the flood plain (fig. 2.4). As the Alpbach runs in a northerly/north-easterly direction, it is predicted to overflow its left bank and water will flow overland in a north-westerly direction, across fields and eventually funneling into the residential area of Wilten. The new layout of the Huebbach running along

the southern edge of Wilen should act to capture this flow and direct it back into the Alpbach at the new junction of the two streams (fig.3.1).

Chapter 3

Methodology

The goal of this thesis was to research similarities and differences between a subset of the results obtained via BASEMENT within HWS, with those obtained via the latest version of HEC-RAS. As well as examining the intra-model aspects and parameters within the latest version of HEC-RAS. This was conducted with model runs in HEC-RAS 2D as similar as possible to those from BASEMENT, while still utilising HEC-RAS, and its features, in an efficient and appropriate manner. Then, further model set-ups with HEC-RAS allowed for an intra-model and parameter investigation. Analysis and presentation of the results was completed using R Programming, QGIS and RAS-MAPPER (a geographic information system built into HEC-RAS that can be used for setting up models and viewing/extracting results). The present day scenario of HWS is referred to as IST and the scenario after protection measures have been implemented is referred to as NACH. The results extracted had to be narrowed down for processing and analysis and the time of end-peak flow was chosen as the flood plain was approximately at max inundation. This time corresponds to 1h50m for IST and 1h20m for NACH. Start-peak flow corresponds to 1h20m and 40m respectively for IST and NACH and post-peak flow corresponds to 2h05m and 1h35m. The results were extracted in GeoTIFF format for post-processing and carried a pixel size of 0.5m x 0.5m.

3.1 Models

The modeling approaches compared are the freeware softwares: HEC-RAS and BASEMENT. The HWS results generated with BASEMENT and received from B+S AG were obtained using a fully 2D modeling approach - called BaseMESH. 1-, 2- and linked 1- and 2- dimensional approaches were utilised in HEC-RAS. In the case of the Alpbach flooding, the flow is considered unsteady and both models contain the capability to model unsteady flow. Streamflow is governed by the Principle of Conservation of Mass and the Principle of

Conservation of Momentum and the computational equations used in both models are based on these principles. They are known as the Shallow Water Equations (SWE).

3.1.1 HEC-RAS

The River Analysis System was created in the Hydrologic Engineering Center of the United States Army Corps of Engineers. Known by its acronym HEC-RAS. It is capable of solving unsteady and steady flow hydraulics, and also includes modules for water temperature, water quality and sediment transport. The latest version of HEC-RAS, version 5.0.7, was available for download in March 2019 and is the version used for this thesis (<https://www.hec.usace.army.mil>). Along with the model documentation, tutorials and example datasets are available as well. Version 5.0.7 allows for 1D and 2D modeling. Support from the creators is not available, however bug reports can be submitted and a considerable community has built up around assisting users and enhancing the model's usability.

3.1.2 BASEMENT

BASEMENT was developed at the Laboratory of Hydraulics, Hydrology and Glaciology (VAW) at the Swiss Federal Institute of Technology (ETH). It stands for BASic EnvironMENT for simulation of environmental flow and natural hazard simulation. It was created as the result of a proposal submitted to build a new software tool for the Rhone-Thur project.

BASEMENT is a freely available numerical software which is a BASic EnvironMENT for the simulation of environmental flow and natural hazard events in 1 and 2 dimensions. It was developed by the Laboratory of Hydraulics, Hydrology and Glaciology (VAW) at the Swiss Federal Institute of Technology (ETH) and the first version was released in autumn 2006. It was created as the result of a proposal submitted to build a new software tool for the Rhone-Thur project (??). A handful of tutorials and sample data are packaged with the model and an online forum is available to potentially provide support. (www.basement.ethz.ch).

3.1.3 Computations

The computations in both HEC-RAS and BASEMENT are based on the Shallow Water Equations (SWE). The reach being modeled needs to be a match for the tool and set-up employed. The requirements for the use of the SWE and, in turn, the models are: a gradually varied bed slope, constant pressure distribution (hydrostatic) and the length of the reach is much greater relative to the water depth. In the case of HWS these assumptions can be met. Furthermore, in the case of using a purely 1D approach for a multi dimensional phenomenon, the flow moving along the overbank area is mainly orientated downstream. The full deriva-

tions for the SWE are provided in the reference manuals of each model [basement, 2]. A unique analytical solution to the SWE equations is only possible for very simple and idealised conditions. Instead the equations must be discretized and turned into a set of algebraic equations and co-efficients. The method of discretization in HEC-RAS is primarily a finite difference scheme, the method in BASEMENT is a finite volume scheme. The points of computation also vary between the models. BASEMENT utilises a triangular mesh to represent the underlying geometry and computations occur at the node points on the mesh where flow variables are determined. HEC-RAS uses a flexible grid composed of cells which can have up to 8 sides and the computational point is the cell center. Although the principles behind the computations are the same for each model, the methods to solve them vary slightly.

3.2 HWS Results

The 2D BASEMENT results were generated by Engineers at B+S AG in late 2018 and serve as a basis for planning for future flood protection measures. 2 results were generated using a 300 year flood event (HQ300). The first result covered the scenario of the current state of the Alpbach and surrounding floodplain (IST scenario). The second result covered a future scenario after protection measures have been implemented (NACH scenario). The main changes for NACH: the Huebbach running as an open channel south of Wilen and joining the Alpbach at an open junction and raising select streets (see figure 3.1).

The results' output files were viewed and extracted as raster files using QGIS with the Crayfish plugin.

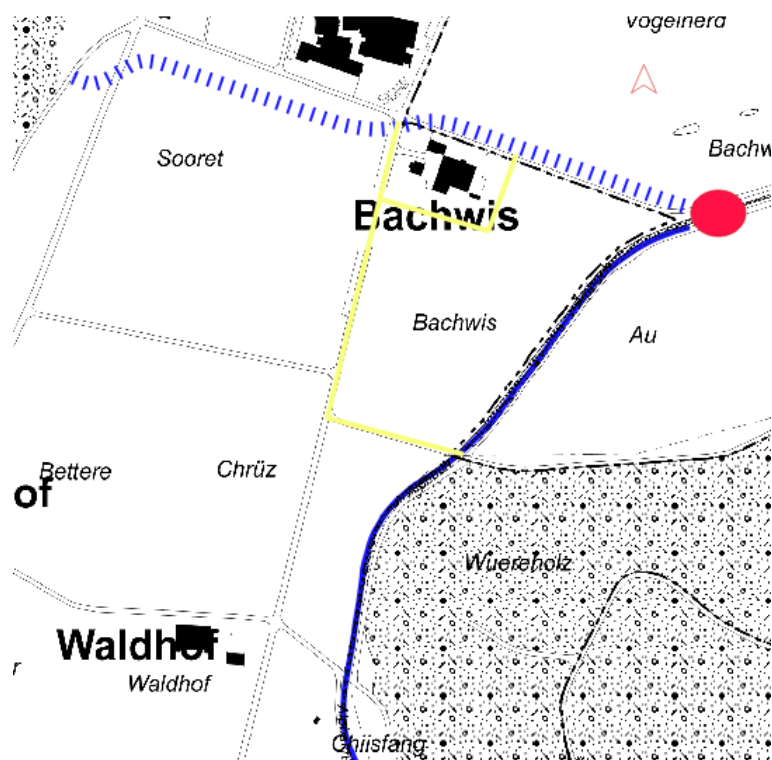


Figure 3.1: The new Huebbach channel (hashed blue line) flows openly east to west along the southern edge of Wilen and joins the Alpbach (solid blue line) at the confluence (red circle) located near the north-eastern corner of the Bachwis field. Selected streets (yellow lines) in the flood plain have been raised compared to the IST scenario.

3.3 Input Data

To conduct the modeling, two sets of input data were required: geometry and boundary conditions. The numerical computations are based on the geometry and this was extracted from a digital elevation model (DEM). Stream flow values for a HQ300 event were used as the input boundary conditions.

3.3.1 Terrain

The DEM needed for the IST and NACH scenarios for this thesis were created using QGIS, from x,y,z files received from B+S AG. As HEC-RAS does not accept DEMs with *No Data* values, these were replaced with a value of 575. The areas lacking a value represented structures (homes, barns, sheds) and there were few structures in the study area, and none are expected to be completely overtopped with flood water from the Alpbach. The BASEMENT models did not lay a mesh over these areas (A.1). As analysing flow around each structure was also not the aim of this thesis, a value of 575 m MSL was tall enough to ensure that these cells would not interfere with the results.

The x,y,z files were generated by the Engineers at B+S AG by overlaying a triangulated mesh over elevation data - which was a combination of Lidar, photogrammetric, drone survey and survey data near the channel - to capture details in the terrain. Then values were extracted on a regular square grid spaced at 0.5m x 0.5m to be able to represent enough terrain detail and create a GeoTIFF file with z values representing elevation.

The final DEMs used for the IST and NACH scenarios are seen in figure 3.2, the new Huebbach channel can be seen in the NACH terrain.

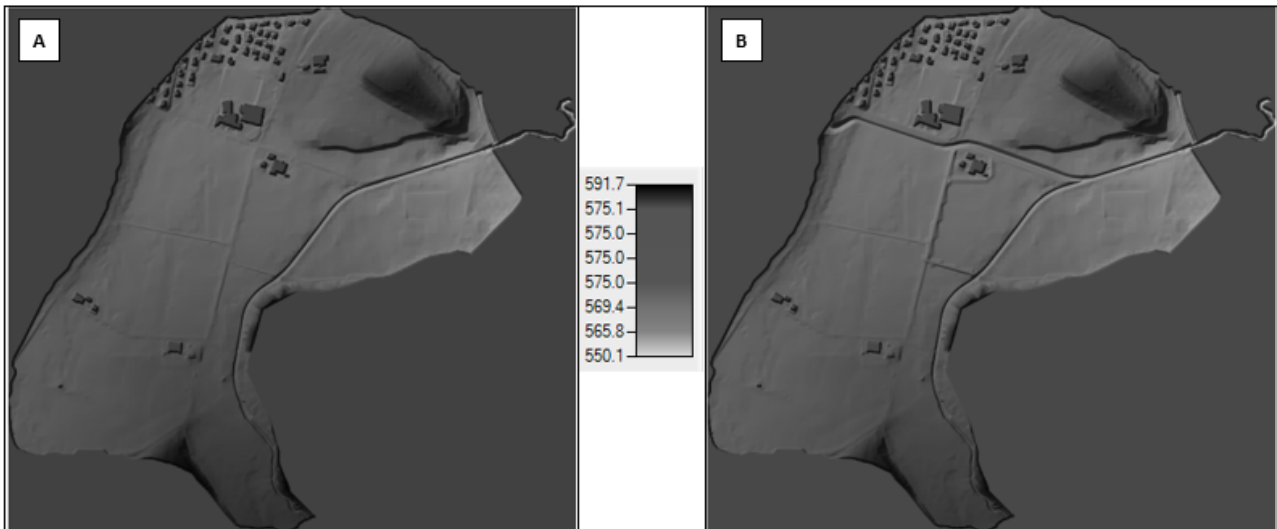


Figure 3.2: Image A shows the input DEM for the IST scenario and Image B shows the input DEM for the NACH scenario as viewed in RAS-MAPPER.

3.3.2 Hydrology

The hydrology for the HQ300 event, as well as HQ30 and HQ100 (see Calibration and Validation, sec.3.4) was provided by B+S AG and is identical to that utilised in BASEMENT. Estimated flow values were available to B+S AG for each stream from the environmental departments responsible in SG and TG. As the HWS region transects these two cantons, and each canton utilised a different method for estimation, two varying sets of data were available and especially the Huebbach had a large discrepancy. The Engineers at B+S AG conducted a thorough hydrological re-analysis using the data available and derived flow values to use in HWS ?? which correspond to peak flow values of 35m³/s for the Alpbach and 6m³/s for the new Huebbach.

Additional hydrology was used for this thesis to examine how the models compared in more extreme situations. An additional hydrograph using HQ1000 values was utilised to see how the models handle larger events. This corresponds to peak flow values of 43.1m³/s and 11.5m³/s for the Alpbach and Huebbach, respectively. Another set of hydrographs was utilised to observe the behaviour at the confluence in extreme events for the NACH

scenario. The Alpbach and Huebbach are separate catchments and there is the possibility that the smaller Huebbach could be hit with a very intense rain cell while other streams in the region are not. This is the type of situation which occurred during the recent Krebsbach flood (sec.1.1.1.) For the Huebbach a hydrograph for HQ1000 + 30% of the peak value and another of HQ1000 + 50% of the peak value were created to be run with only a HQ30 for the Alpbach in a NACH scenario.

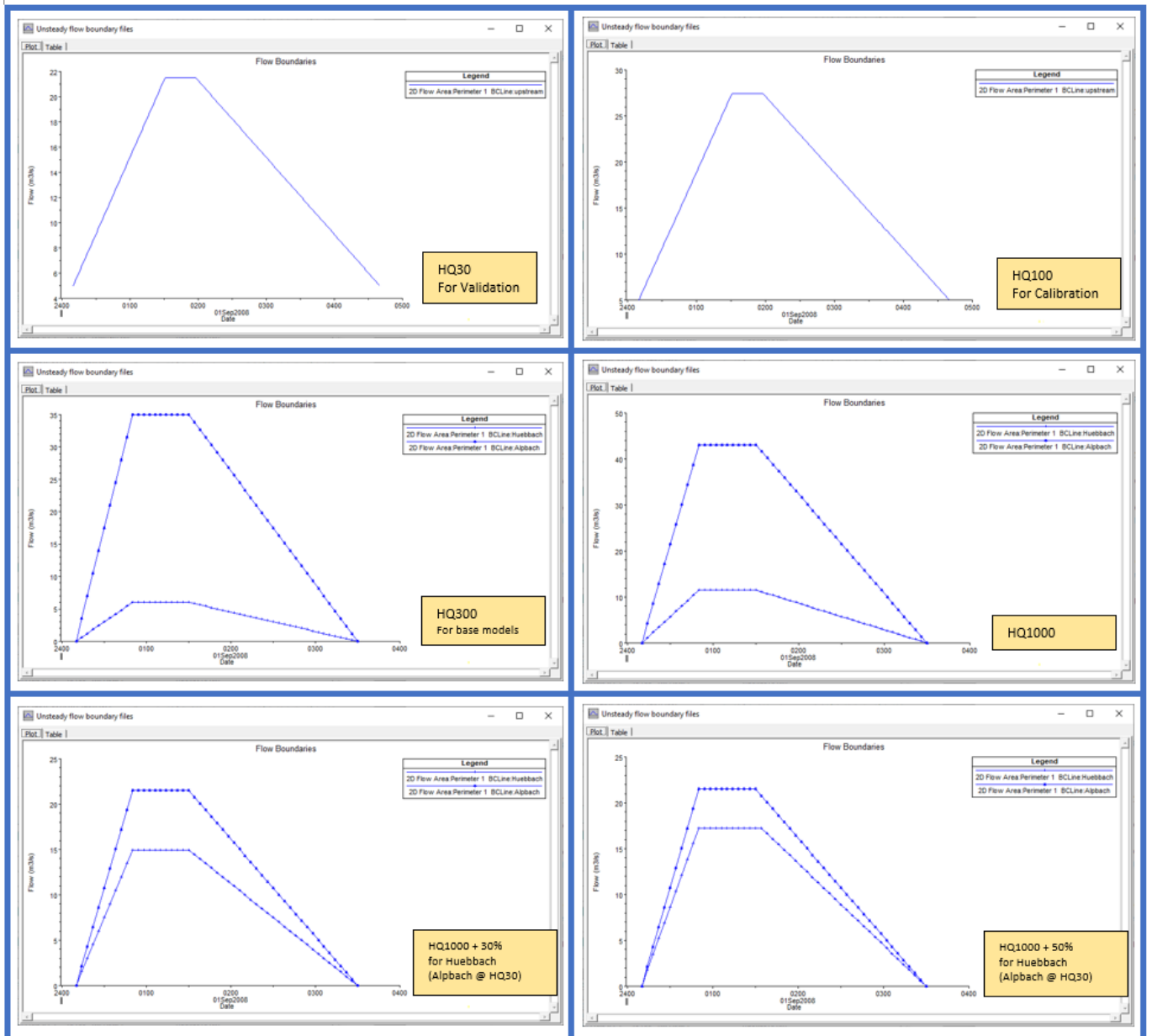


Figure 3.3: Plots of the hydrology used as input data for calibration, validation and different scenarios

3.4 Calibration and Validation

Calibration and validation of a flood model, or any environmental model, is an integral step in the modeling process (sec. 1.3.3) but data is often desperately lacking. For HWS, the same problem exists. There was a lack of past records and the streams are ungauged. To counteract this dilemma, a work around of utilising the information from the present-day hazard maps as calibration and validation data was devised (www.map.geo.tg.ch). At present, these maps are considered *the go-to* and these are the values upon which decisions are made on in the area (section 1.1.3). As different return periods are available, HQ100 was used for calibration and HQ30 was used for validation. This method was in line with the recommendations from a recent validation in flood modeling paper, and, although not as robust as having records from one (or, in a better case, multiple) flooding event, is a suitable method which was complimented by expert opinion from B+S AG ([35]). The focus for calibration and validation was placed locally at the bend along the Alpbach, next to the Wuereholz hill (red circle in figure 3.4), where the majority of overflow into the study area occurs.

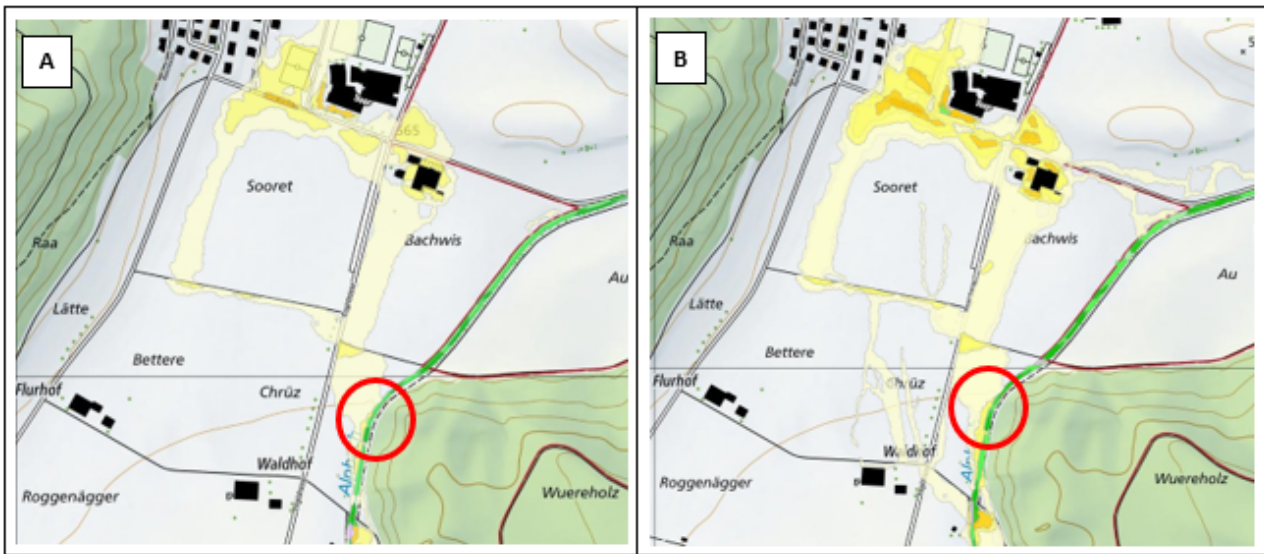


Figure 3.4: The Kanton Thurgau publicly available flood depth hazard maps were employed as calibration (Image B, HQ100) and validation (Image A, HQ30) data. The red circle indicates the location where calibration and validation was focused.

3.5 Model Set-ups

In total, five base models were set-up in HEC-RAS to address research questions 1 and 2 (sec. 1.5). This was comprised of three models using the IST DEM as input and two using the NACH DEM as input. For research question 3, a variation of one of the five models was used and it depended on which parameter was being explored. All of the models could be

created and edited using RAS-MAPPER and the geometry editor GIU in HEC-RAS.

The overarching steps to create stable models were: initiate the model in a small upstream section with a baseflow value hydrograph until a geometry leading to model stability is achieved, expand the geometry to cover to channel and determine the model warm-up time (if applicable), input the HQ100 hydrograph to calibrate, adjust geometry or parameters, and input the HQ30 hydrograph for validation.

Figure 3.5 outlines the grouping of model set-ups per research question and figure 3.7 illustrates the final set-up for the five base models as viewed in RAS-MAPPER.

The following sections describe each model set-up.

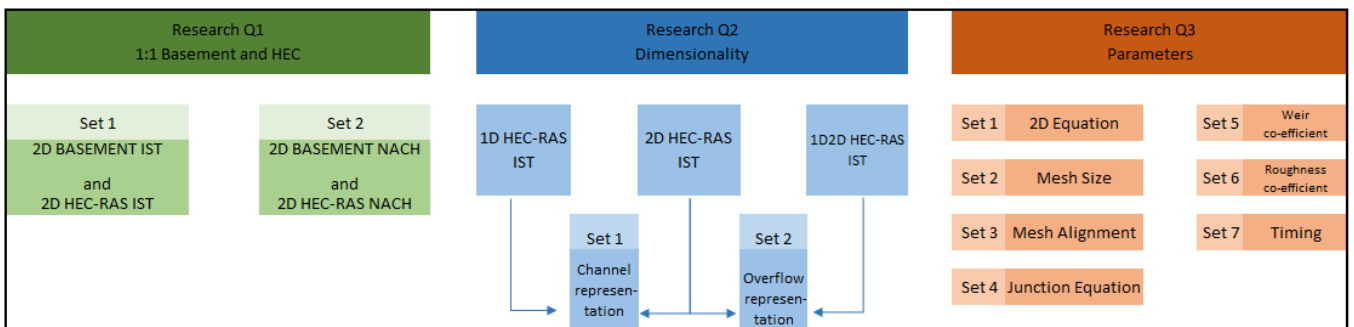


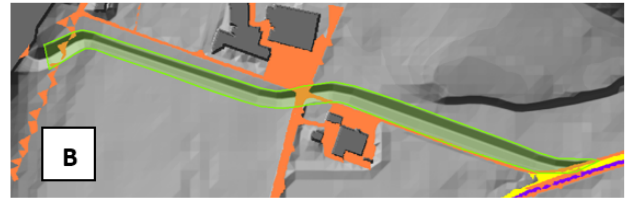
Figure 3.5: Overview of models and scenarios in relation to the research questions

3.5.1 2D Models

2D IST

This model contains a default grid value of 2m x 2m, as it was found to be small enough to capture flow moving along the terrain while allowing for a reasonable computation time. The channel and overflow region along the bend of the Alpbach was refined to a grid size of 1m x 1m as these regions are hydraulically important and require more detail. After trial runs, further refinement was done and areas not being flooded were refined to 4m x 4m to save on computation time. Breaklines were laid to align cell edges along roads. Normal depth boundary conditions were drawn to release flow along the north edge of the study area and also downstream.

Surface roughness was determined by attaching a manning's n layer to the terrain input (fig. 3.6). The roughness layer had to be created in QGIS by georeferencing an image which outlined various roughness patches and then drawing shapefile polygons over these areas. The polygons were converted into raster format and then input into HEC-RAS via RAS-MAPPER. The manning's layer could then be used for subsequent model set-ups which used a 2D flow area.



Legend	
Value 1	0.0303
Value 2	0.0333
Value 3	0.02
Override Region (NACH Only)	0.0333

Figure 3.6: Image A is the Manning's roughness layer for the IST and NACH scenarios. Image B shows the Manning's override polygon used to set a Manning's value for the new channel in the NACH scenario.

2D NACH

The 2D NACH geometry was set-up as the IST, with the exception of additional 1m x 1m refinement regions in the area of the raised road, the new Huebbach channel and the confluence area. As well as applying a manning's n override polygon to the new channel.

3.5.2 Models to explore dimensionality

Additional base models were created to address research question 2.

1D IST

The 1D model was set up by arranging cross sections along 10-20 metre sections of channel at a time, working in the upstream direction. By adjusting the terrain visualisation in RAS-MAPPER, the areas of the channel with steep drops or where the water had carved out the channel bottom could be located and cross sections could be placed strategically to ensure a gradually decreasing slope in the downstream direction. The inflow area terrain was very steep and flow was entering the system with too much energy causing model instability. Mock cross sections had to be used rather than extracting geometry from the terrain to achieve a more gradual inflow slope and model stability. This area is located very far from the study area though and the strategy of applying mock cross sections should not

affect the study area. Bank stations were defined and levees added at high elevation values on the channel edge. A zero-height weir was added along the left bank and set to remove flow out of system.

1D2D IST

Setting up the 1D2D was a combination of what was learned in setting up the 1D and 2D separately. Due to the varying elevation and steepness of the channel bottom, the cross section placement was very sensitive and their positions were not adjusted. A 2D flow area was drawn over the flood plain and refined and then connected to the lateral structure along the left channel bank. The 2D flow area along the structure was then aligned and refined to 1m x 1m.

1D2D NACH

The 1D2D NACH was also a combination of what was learned in setting up the other base models. As the terrain of the newly designed Huebbach was smooth, it was possible to use the cross section interpolation tool in the geometry editor GIU to arrange the new cross sections. These were connected to the 2D flow area via a lateral structure. An additional lateral structure was connected along the left bank of the Huebbach to the cross sections. A junction was added at confluence and set to use the water surface balance method.

The 2D cell alignment was very sensitive along the structure and the 1D2D IST grid needed to be imported to achieve stability. When 2D flow areas are imported, the original refinement regions are blended into the grid and this means they are not available as a separate layer to edit. For these reasons the final geometry of the flood plain appears different. The 1D2D NACH cells along the structure were kept as imported and additional refinement regions were added where the roads were raised and over flow-free areas.

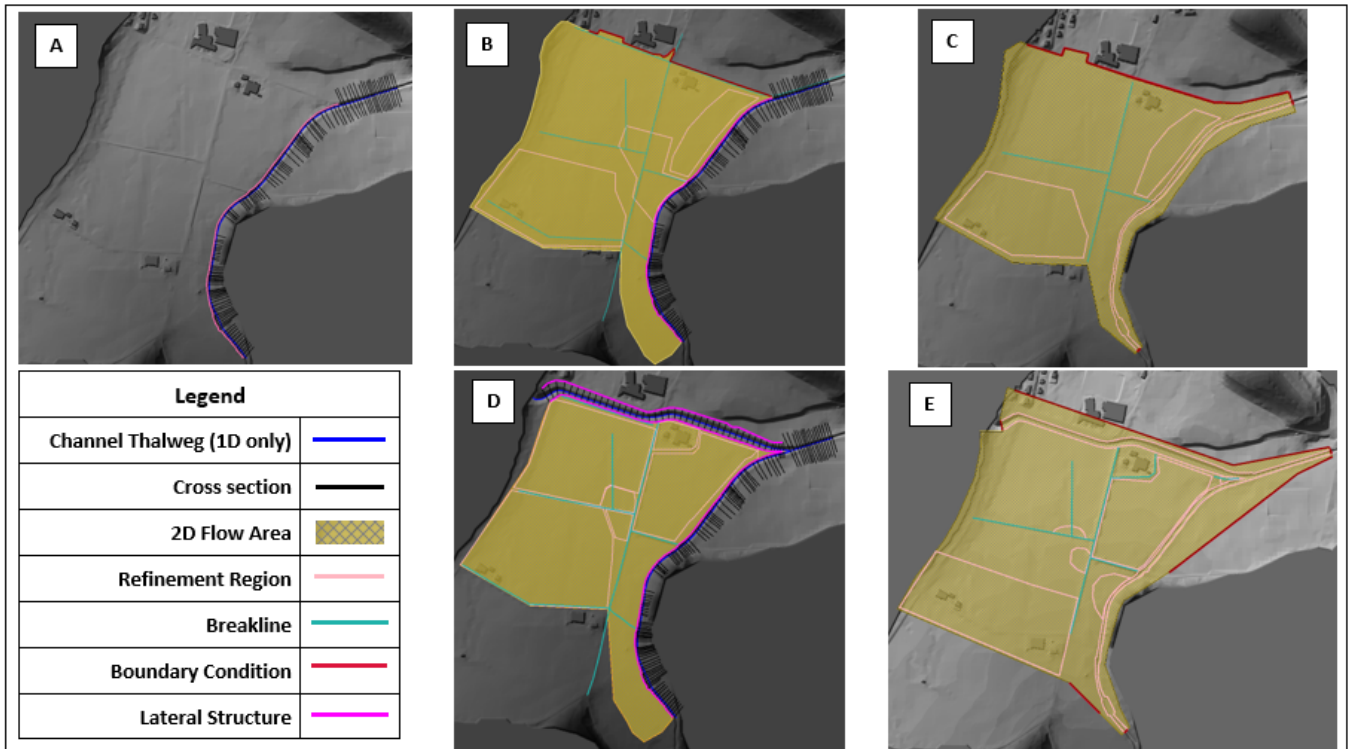


Figure 3.7: Illustration of final geometry and boundary condition layout for each base model. A: 1D IST, B: 1D2D IST, C: 2D IST, D: 1D2D NACH, E: 2D NACH

3.5.3 Exploring parameters

These models were set-up to address research question 3.

Roughness

The 1D2D IST scenario was chosen to vary the surface roughness value. Values were increased and decreased by 30%, in intervals of 10% (see Table 3.1 for values).

Time

Within the calculation options, there is a choice to have a flexible time step for the model run which will be based on the courant condition. A courant value of 1 indicates that a particle of water will move through a grid element in 1 time step [2] and is the ideal courant value. By varying the range of this value the model will alter timesteps. This could shorten or lengthen the computation time depending on the model set-up, but it is also meant to lead to stability as the time step will adjust if the model cannot converge to a water surface value and it is meant to be more efficient and focus the time step value on areas seeing flow. This value was set to the range of 0.5-3.0 to observe the computation time reaction.

2D Equation

The 2D modeling in HEC-RAS offers a setting to use the diffusive wave approximation for the numerical computations. This approximation can speed up processing time and also can help to stabilise a model. This setting is activated in the *Calculation Options and Tolerances* in the Unsteady Flow Simulation settings.

Junction Equation

When two reaches meet at a junction in HEC-RAS, there are two options available to compute the flow at this point. The water surface balance method was utilised in the 1D2D NACH model. This option was changed to the energy balance method in the junction settings dialog.

Weir Co-efficient

Within the lateral structure settings, the weir co-efficient is entered. It is recommended to use low values when the weir is representing the channel bank and not a physical structure [2]. This value was varied systematically from .1 - .5, in .1 intervals.

See table of weir co-efficients 3.2

Grid Size

Default grid size is set in the 2D flow area editor. The default size for the HWS study area was 2m x 2m. Using the 1D2D NACH scenario (faster computation time than fully 2D), this value was adjusted once to 3m x 3m, and 4m x 4m in a subsequent run. An additional model was set-up using a complete 4m x 4m grid, it contained no refinement regions (see B in figure 3.8).

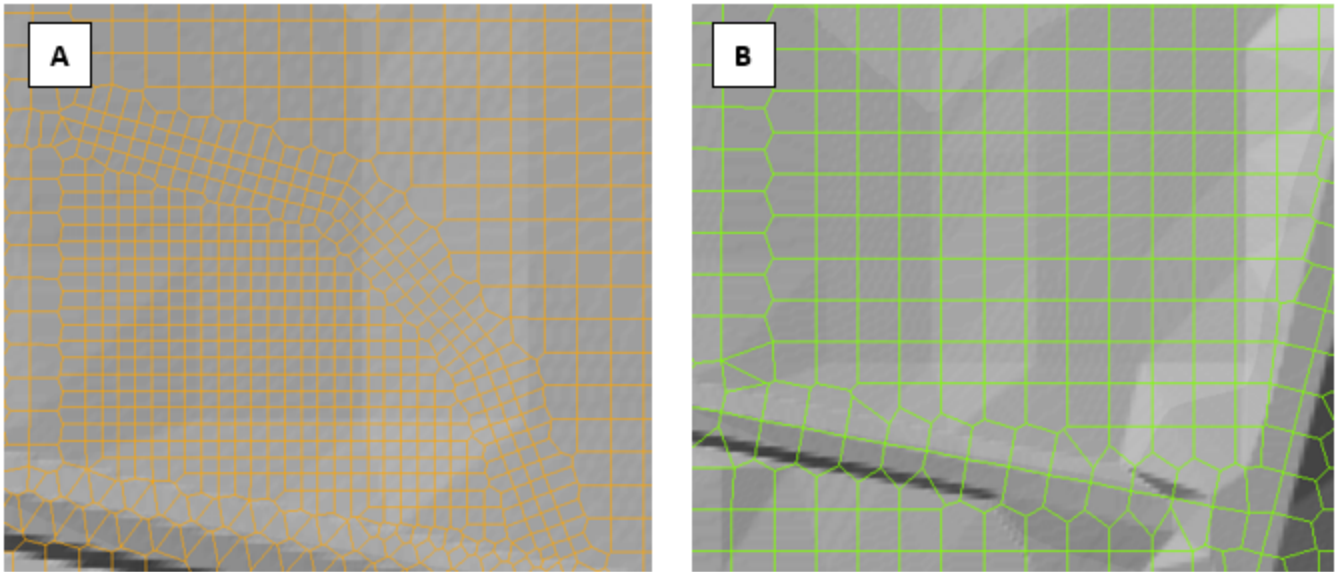


Figure 3.8: Sample of grid from near the raised road. A: Grid with refinement region included. For the 1D2D NACH, 2m x 2m and 3m x 3m runs the refinement region was included. B: One run was conducted with a 4m x 4m grid, breaklines were kept but the refinement region with 1m x 1m cells was not.

Grid Alignment

Grid alignment is a very important part of setting up the geometry. It is a manual process which involves examining the study area and terrain closely and applying breaklines or refinement regions where necessary. Thus, the exploration of grid alignment was realised during the setting up of the base models.

Table 3.1: Table of adjusted Manning's n values

	Default	Value 1	Value 2	Value 3
+30 %	0.039	0.03939	0.04329	0.026
+20 %	0.036	0.03636	0.03996	0.024
+10 %	0.033	0.03333	0.03663	0.022
1D2D IST	0.03	0.0303	0.0333	0.02
-10 %	0.027	0.02727	0.02997	0.018
-20 %	0.024	0.02424	0.02664	0.016
-30 %	0.021	0.02121	0.02331	0.014

Table 3.2: Table of adjusted weir co-efficient values

Plan	Weir Co-eff
Weir Test 6	0.1
Weir Test 5	0.2
Weir Test 4	0.3
Weir Test 3	0.4
1D2D IST	0.5

Chapter 4

Results and Discussion Q1

4.1 1:1 Ist 2D

Results comparison for HEC-RAS 2D IST and BASEMENT 2D IST. As discussed in methodology, have taken the results at end peak flow which is 1h50 for IST scenario and 1h20 for NACH (see sec.A.2 for results at start, end post peak flow)

4.1.1 Peak Values

Location of top 10% values for depth (fig.4.1) and velocity (fig.(4.2)). The peak depth values have a greater concentration at the outlet to Wilen for Basement but velocity peak values are similar. This could be attributed to slightly different terrain elevation representations because the models do not use the same grid to extract elevation values.

Depth

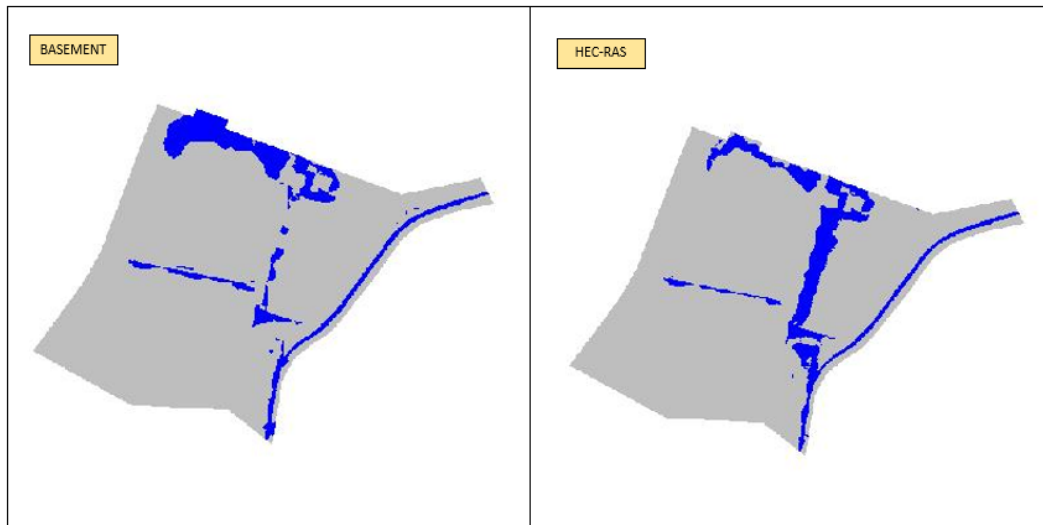


Figure 4.1: Mapping the top 10% of values for depth (blue) for BASEMENT and HEC-RAS 2D IST scenario.

Velocity

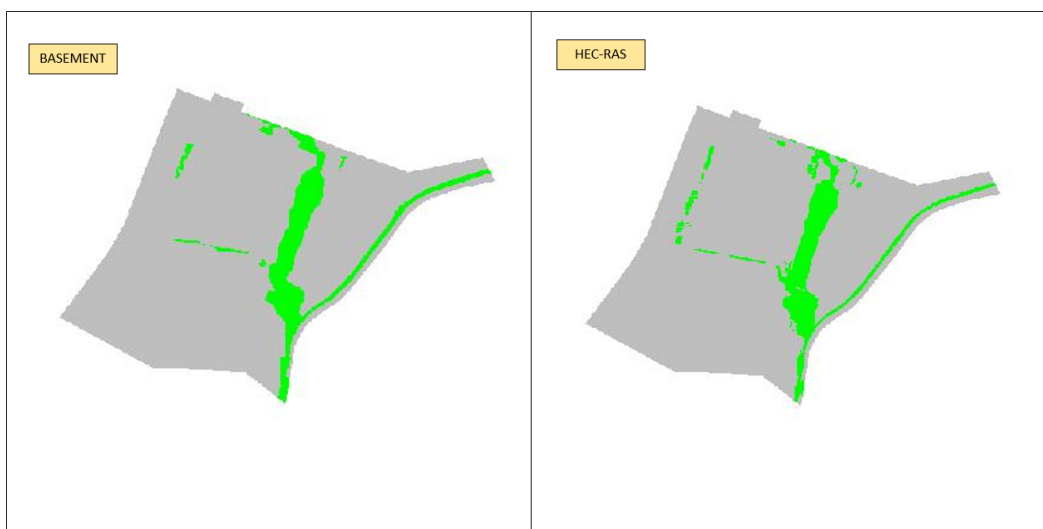


Figure 4.2: Mapping the top 10% of values for velocity (green) for BASEMENT and HEC-RAS 2D IST scenario.

4.1.2 Metrics and Statistics

Accuracy metrics for the performance of HEC-RAS compared to BASEMENT are based on wet/dry cells and do not take into account the actual pixel value. The metrics are modeled after those in Bennett et al. [11].

In addition to the overall study area, two areas of importance are looked at closer (fig. 4.3.)

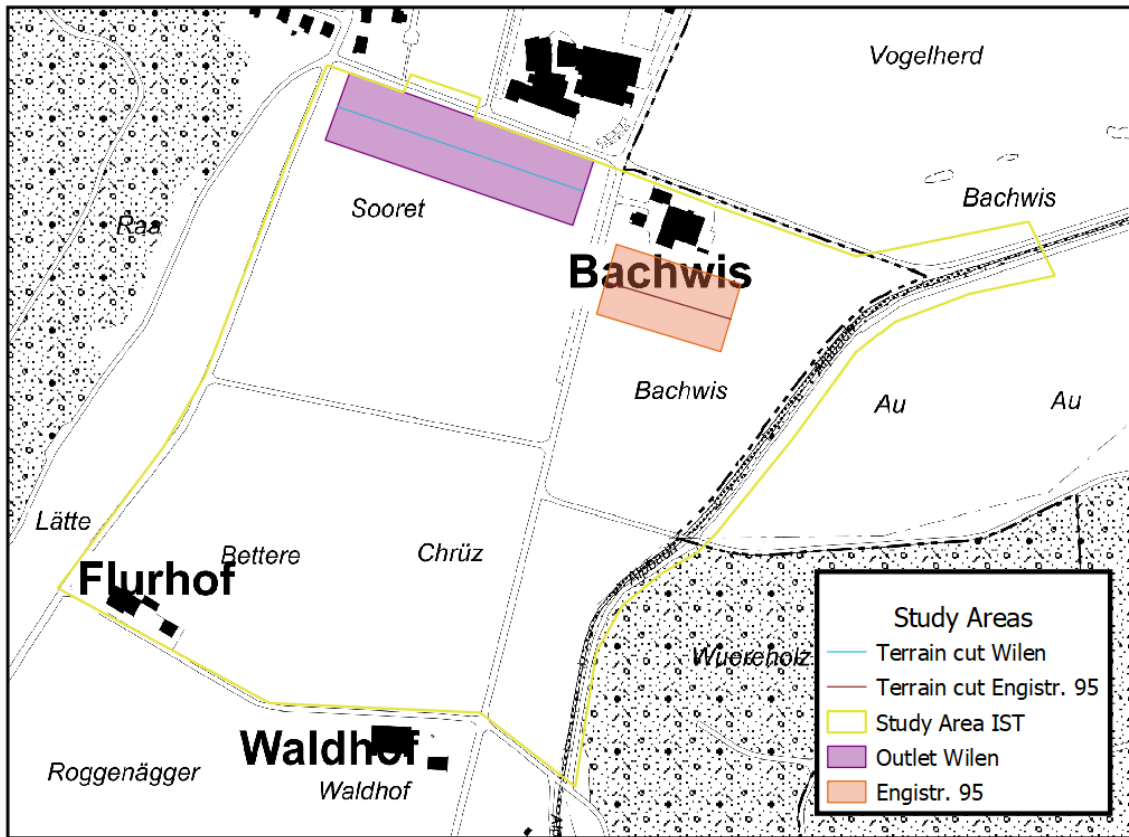


Figure 4.3: Main study area for the IST scenario. The area at the outlet to the village of Wilen and the area in front of Engstrasse 95 are key areas. Profile lines have been extracted from within each of these areas which are used to examine how the models behaved over time.

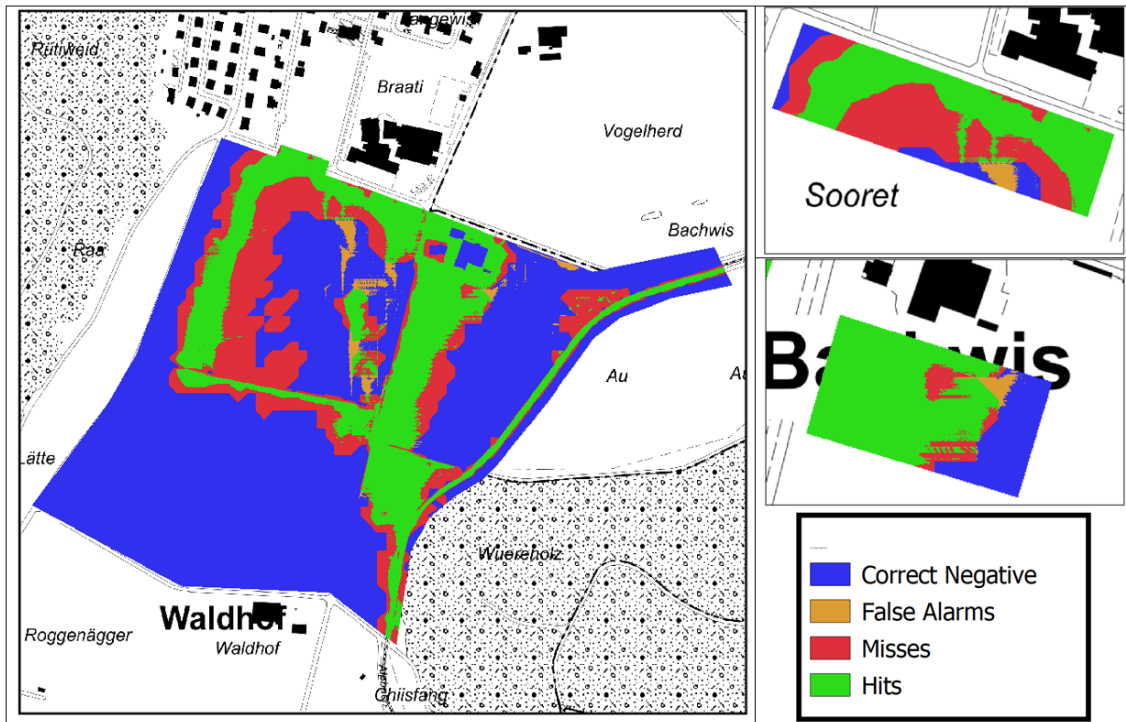


Figure 4.4: Hits, misses, false alarm and correct negatives for HEC-RAS, assessed at 0.5m pixel size

Table 4.1 summarises the accuracy metrics and summary statistics.

The overall flood area index (FAI) is 0.54 but at Engistr. 95, an area of importance because of the residence located there, the FAI increases to 0.86. Overall accuracy is high and false alarm rates are very low. The mean values and ranges for depth and velocity are also similar between both models, with the exception of velocity for the overall study area having a greater range for HEC-RAS.

4.1.3 Residuals

Residuals help to gauge a better understanding if the outputs of the models were similar. In the case of 2D IST, both models produced similar outputs.

Depth

Depth residuals are close to 0, with a slight tendency to being negative

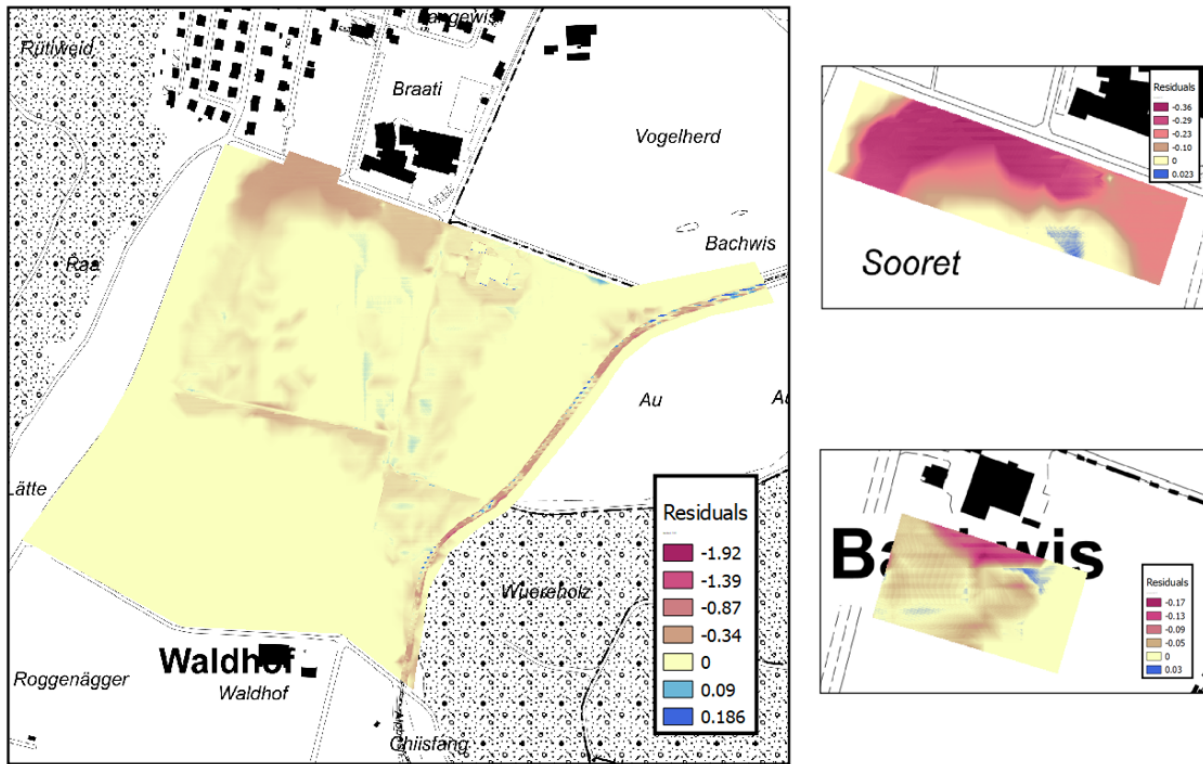


Figure 4.5: Depth residual values in metres for the IST study area and key areas. Based on a pixel size of 0.5m.

Velocity

Velocity residual were close to 0 with a slight tendency to being positive.

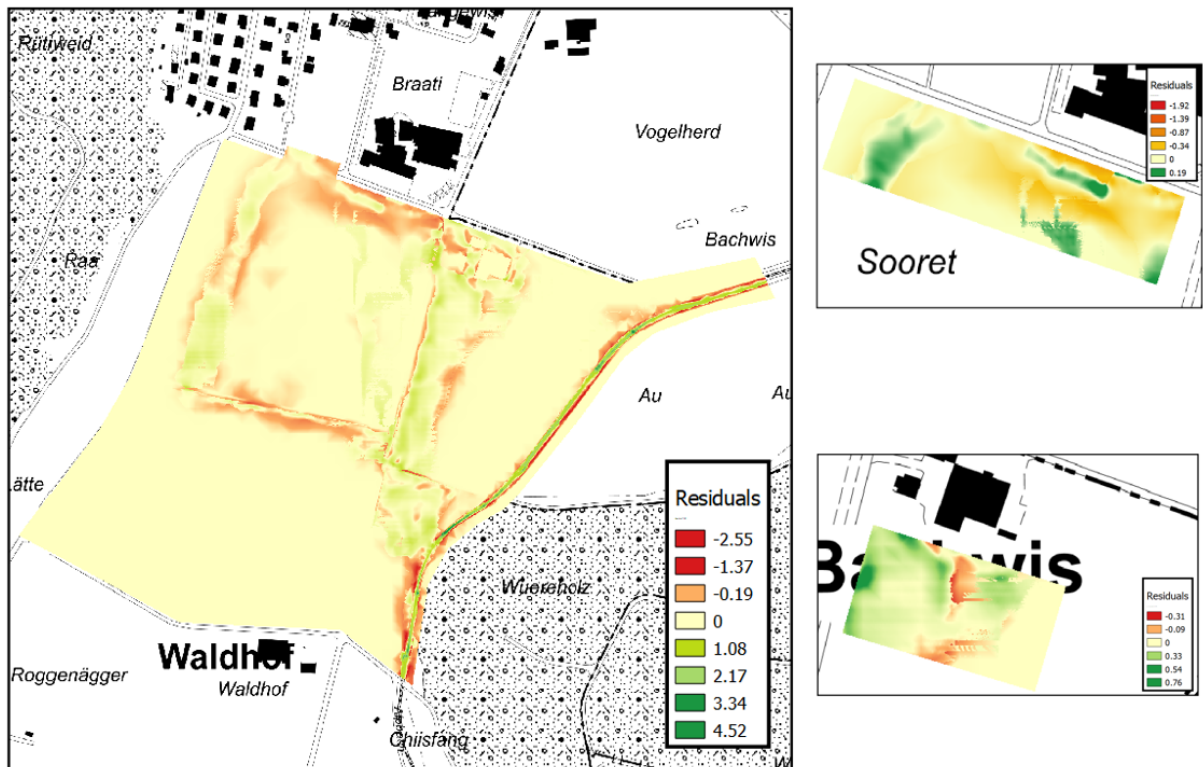


Figure 4.6: Velocity residual values in metres per second for IST study area and key areas. Based on a pixel size of 0.5m.

The histograms for residuals are based on the overall study area.

The histogram of depth residuals 4.7 shows most values were close to 0.

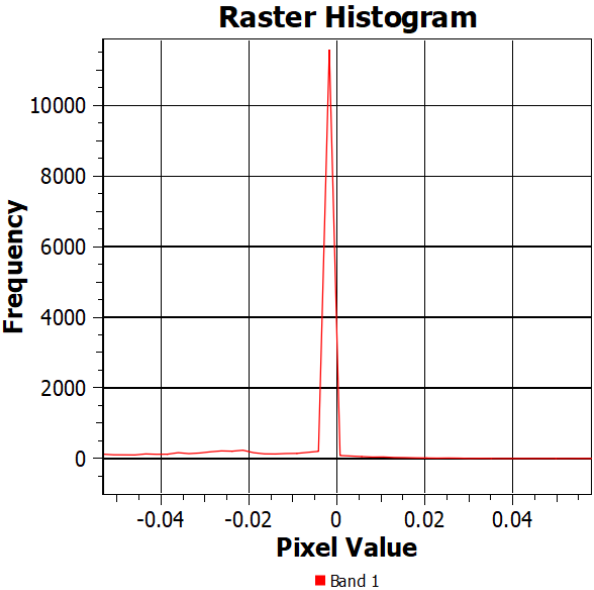


Figure 4.7: Histogram of residuals for depth for the 2D IST scenario. Frequency indicates number of pixels.

And the histogram of velocity residuals 4.8 also shows values being nearly 0.

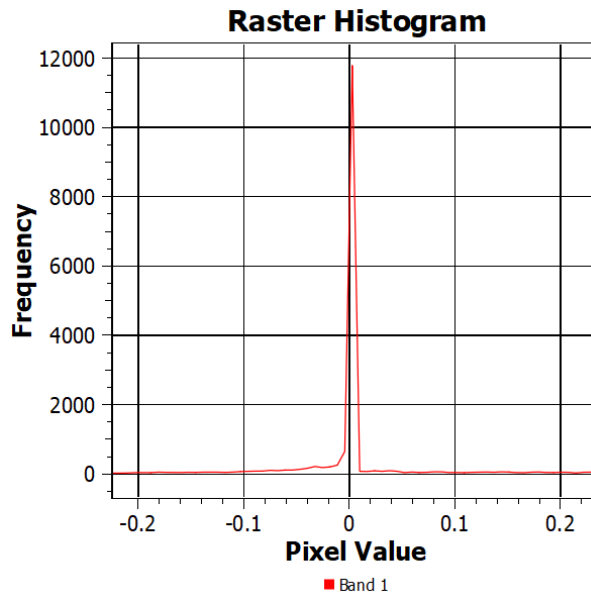


Figure 4.8: Histogram of residuals for velocity for the 2D IST scenario. Frequency indicates number of pixels.

Including Time

In these plots, model run duration is on the y-axis and the x-axis represents a terrain profile. The colour scale represents the value of the variable (depth or velocity) for each model and the third plot represents residuals. The black horizontal lines in the images are marking the start, end and post peak flow times. This visualisation is help gauge how variables were output over time.

In the small valleys in the terrain, the residuals show HEC-RAS is faster on velocity and reduced on depth, especially during the peak flood time.

The depth at Wilen (4.9) is modeled higher by BASEMENT, especially at the lower elevations.

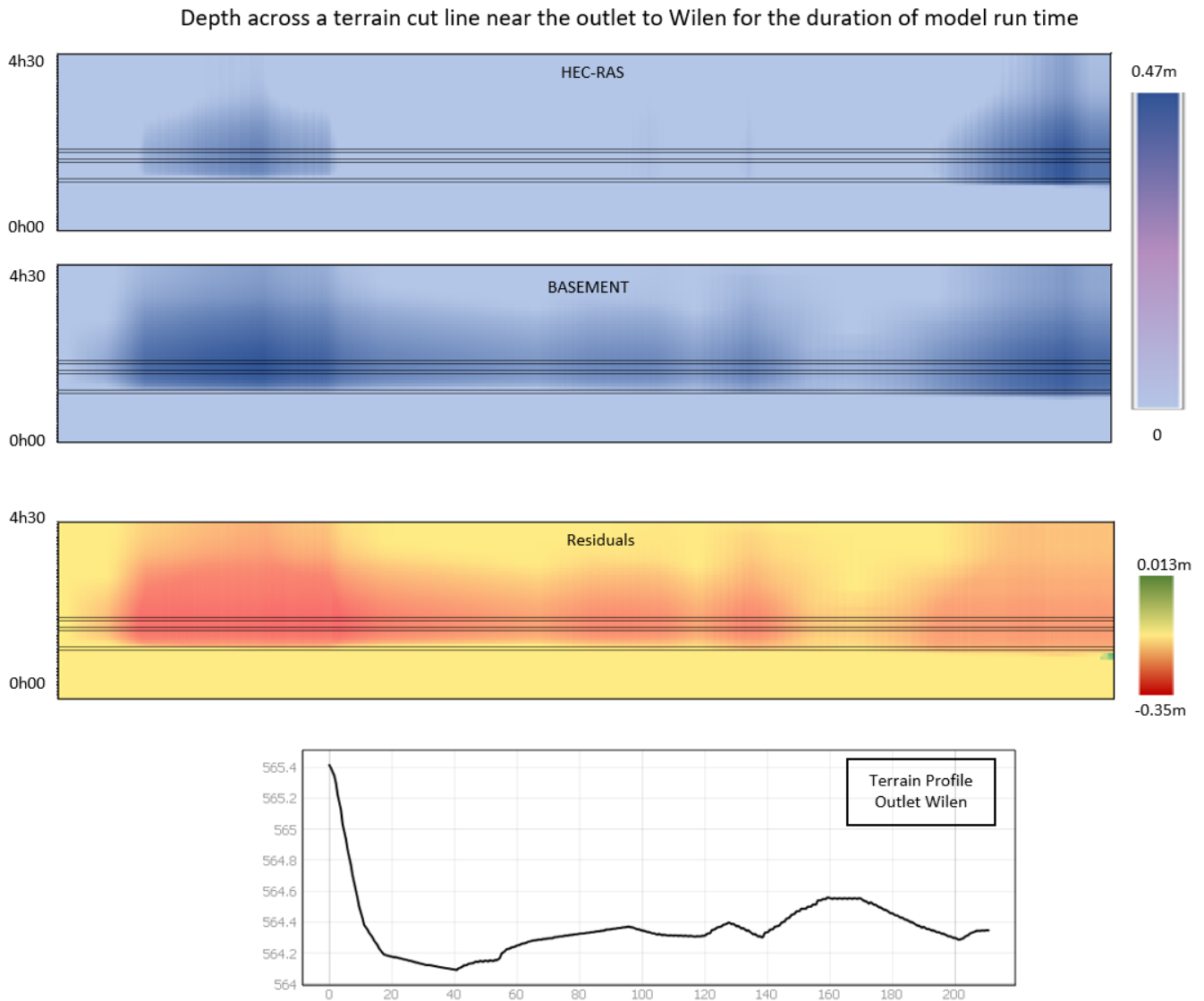


Figure 4.9: The y-axis for the plots represents model run-time and the x-axis represents distance along the profile line at the key area of Wilen. The colour scale indicates the range of values. The horizontal markings are the start-, end- and post-peak flow times. The terrain profile is included for reference in the last plot.

The velocity (4.10) at Wilen varies between the two models, in general it was higher with HEC-RAS.

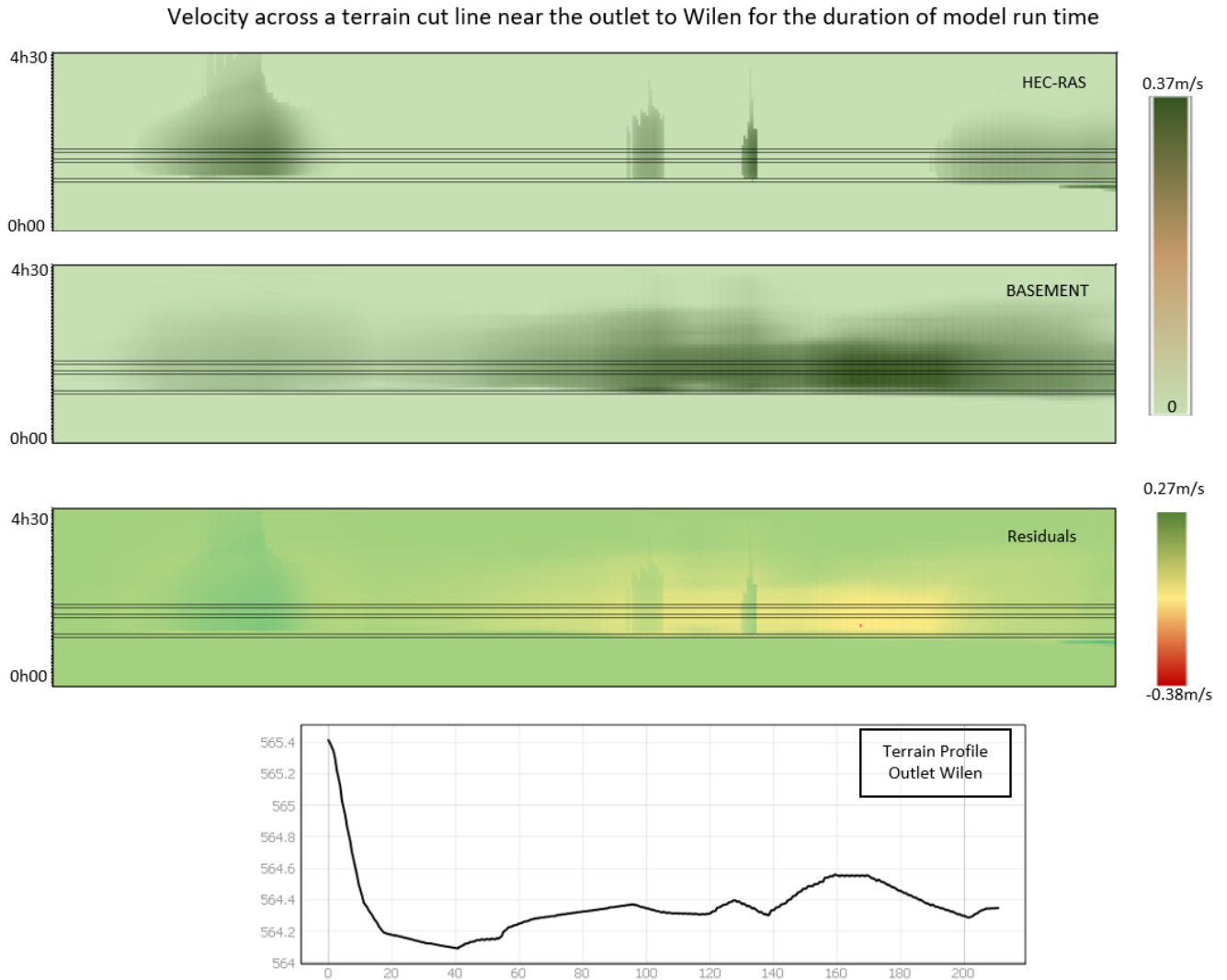


Figure 4.10: The y-axis for the plots represents model run-time and the x-axis represents distance along the profile line at the key area of Wilen. The colour scale indicates the range of values. The horizontal markings are the start-, end- and post-peak flow times. The terrain profile is included for reference in the last plot.

At Engstrasse 95 depth (4.11) was also higher for BASEMENT and velocity (4.12) faster for HEC-RAS.

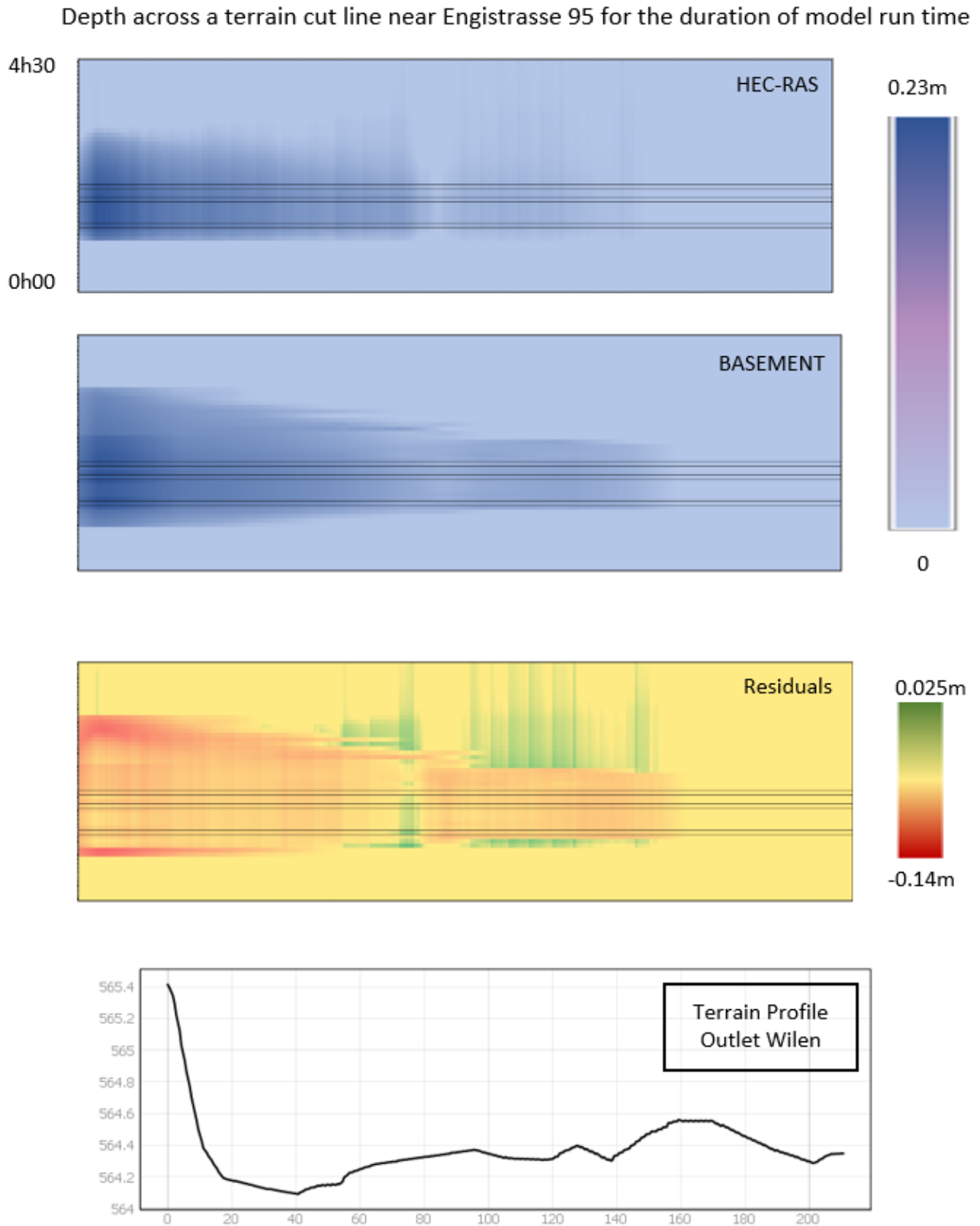


Figure 4.11: The y-axis for the plots represents model run-time and the x-axis represents distance along the profile line at the key area of Engistrasse 95. The colour scale indicates the range of values. The horizontal markings are the start-, end- and post-peak flow times. The terrain profile is included for reference in the last plot.

Velocity across a terrain cut line near Engistrasse 95 for the duration of model run time

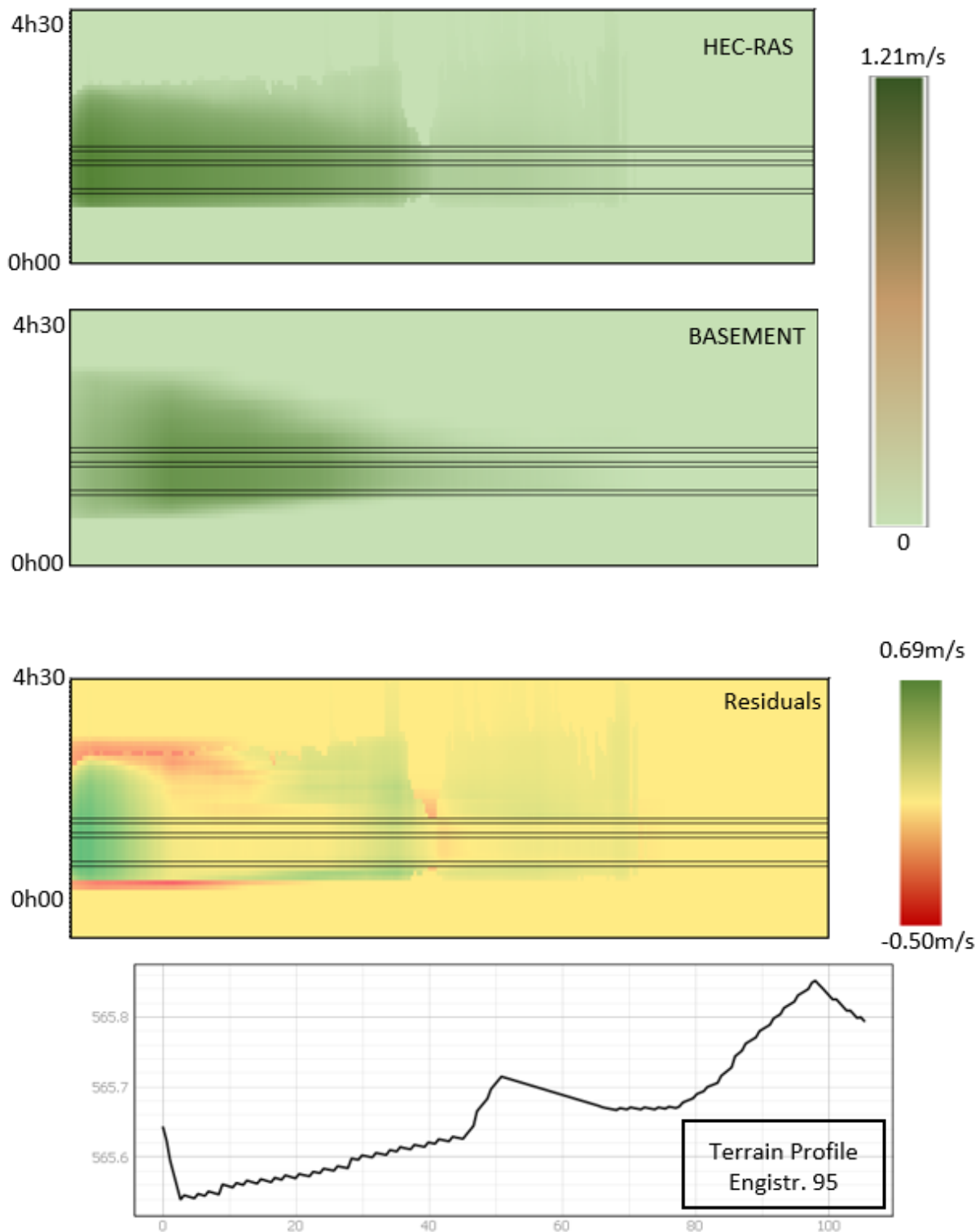


Figure 4.12: The y-axis for the plots represents model run-time and the x-axis represents distance along the profile line at the key area of Engistrasse 95. The colour scale indicates the range of values. The horizontal markings are the start-, end- and post-peak flow times. The terrain profile is included for reference in the last plot.

4.2 1:1 NACH 2D

4.2.1 Peak Values

Depth

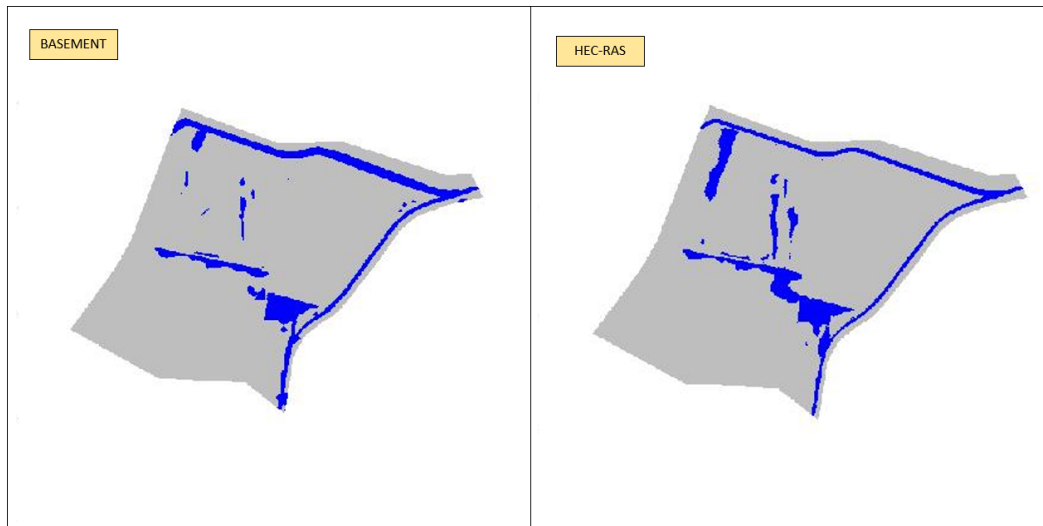


Figure 4.13: Mapping the top 10% of values for depth (blue) for BASEMENT and HEC-RAS 2D NACH scenario.

Velocity

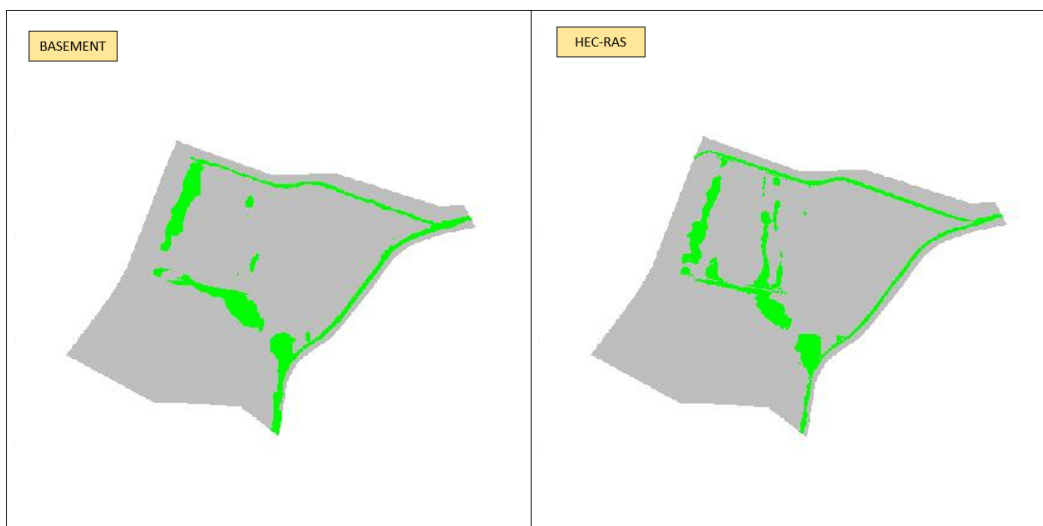


Figure 4.14: Mapping the top 10% of values for velocity (green) for BASEMENT and HEC-RAS 2D NACH scenario.

The top 10% values for depth(4.13) and velocity (4.14) were similar among both models for 2D NACH.

4.2.2 Metrics and Statistics

The 2D NACH study extent plus two key areas (fig. 4.15).

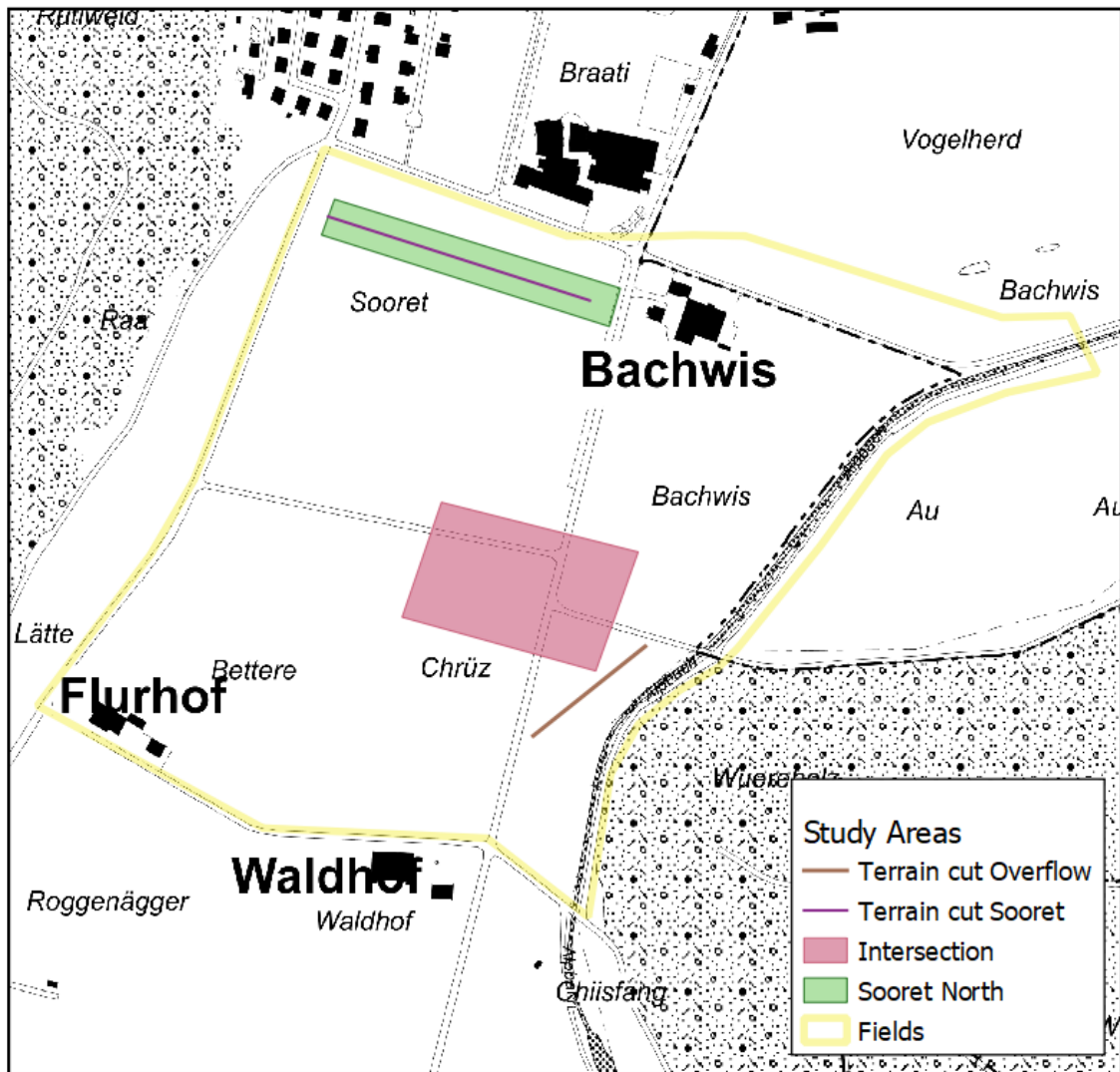


Figure 4.15: Main study area for the NACH scenario. An area stretching across the north of the Sooret field and the intersection located near the Alpbach are keys areas. A profile line has been extracted from within the Sooret field area and another from the area where the Alpbach overflows and are used to examine how the models behaved over time.

The contingency rasters (4.16) show mostly hits for 2D NACH.

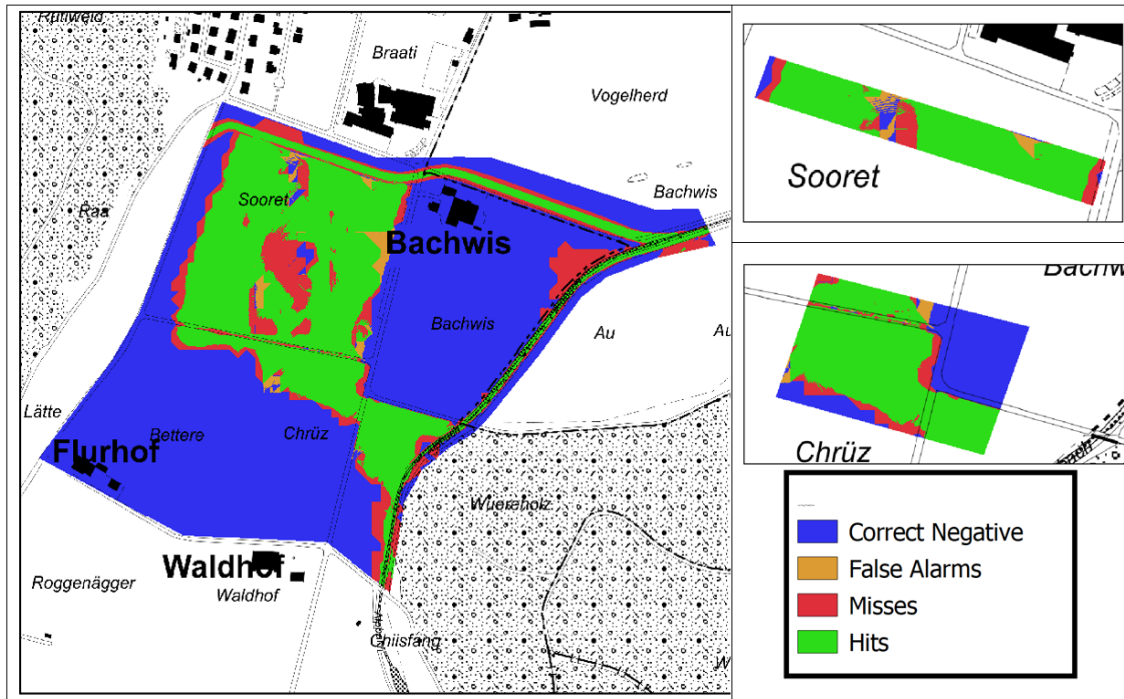


Figure 4.16: Hits, misses, false alarm and correct negatives for HEC-RAS compared to BASEMENT, assessed at 0.5m pixel size

Table 4.2 summarises the accuracy metrics and statistics for 2D NACH. The accuracy for this scenario was higher than for IST, which could be attributed to a better grid placement. The mean values and ranges are also similar between models, with the exception again of the HEC-RAS velocity having a greater range. The largest velocity values occur in the channels and it is possible the small 1m x 1m grid of HEC-RAS is better suited for representing small changes in the channel.

4.2.3 Residuals

Depth

The mapped depth residuals (fig. 4.17) and velocity residuals (fig. 4.18) indicate values near 0. At the area of the newly raised road, depth was predicted slightly higher by HEC-RAS.

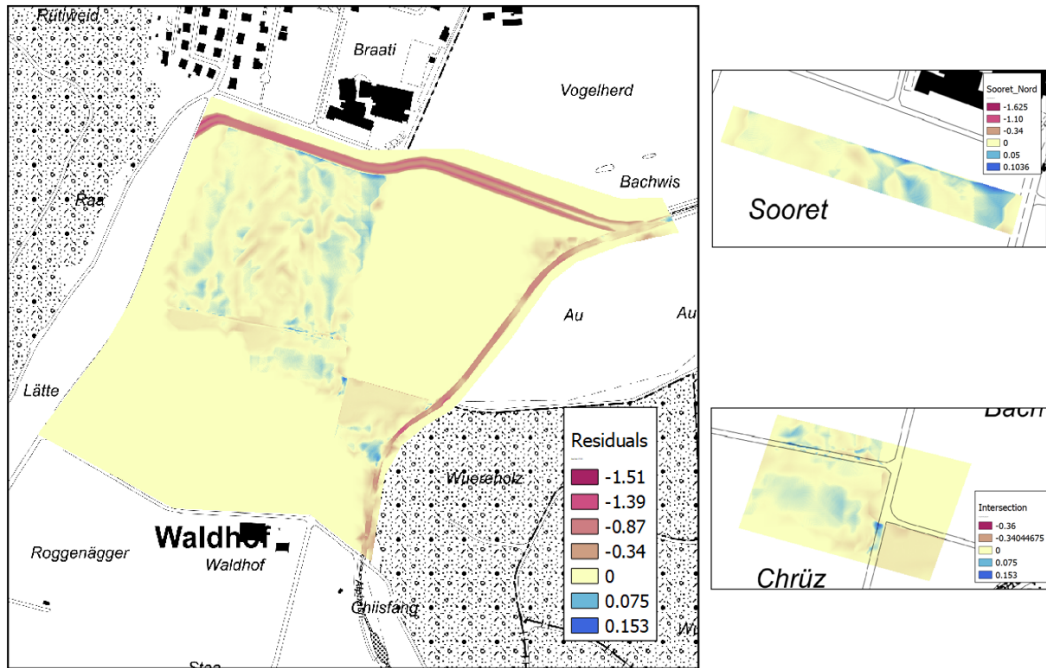


Figure 4.17: Depth residual values in metres for the NACH study area and key areas. Based on a pixel size of 0.5m.

Velocity

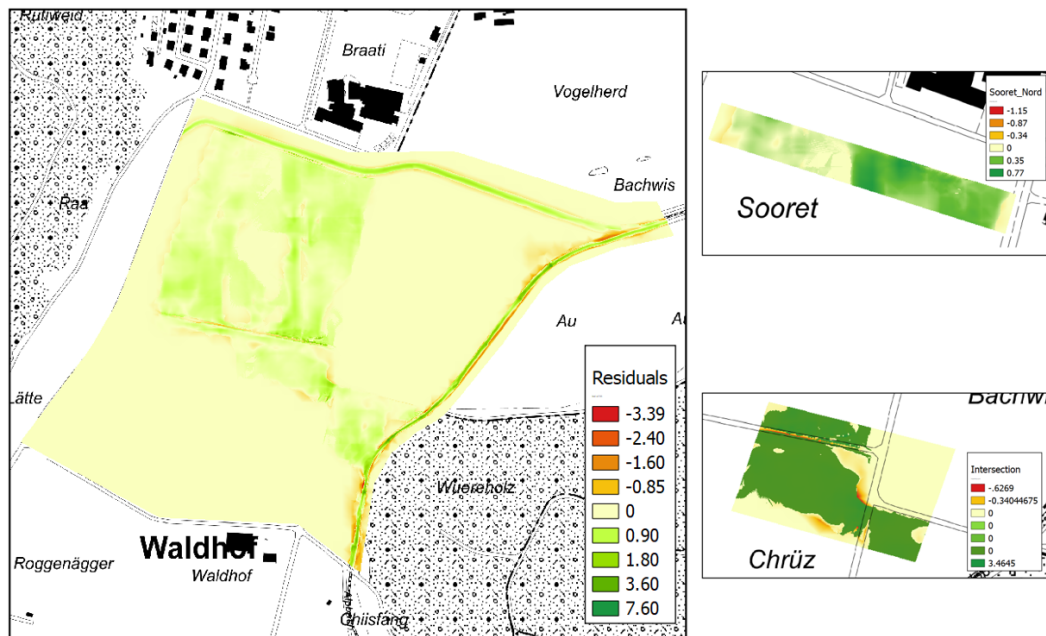


Figure 4.18: Velocity residual values in metres for the NACH study area and key areas. Based on a pixel size of 0.5m.

The histogram of depth residuals 4.19 and velocity residuals 4.20 show values to dominate near 0, like 2D IST.

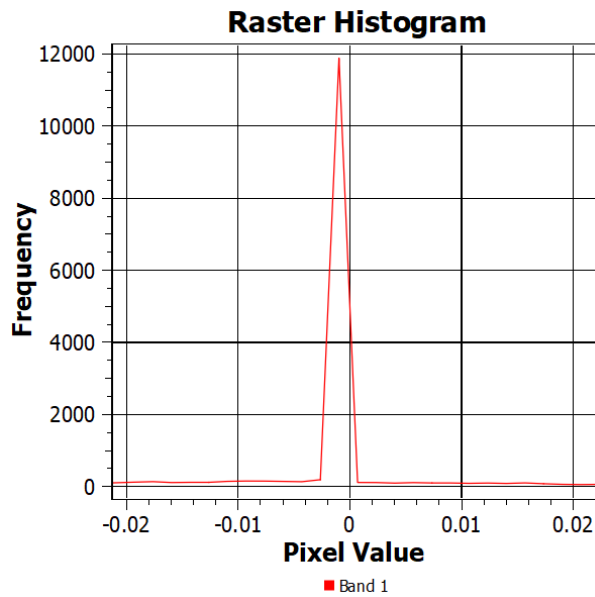


Figure 4.19: Histogram of residuals for depth for the 2D NACH scenario. Frequency indicates number of pixels.

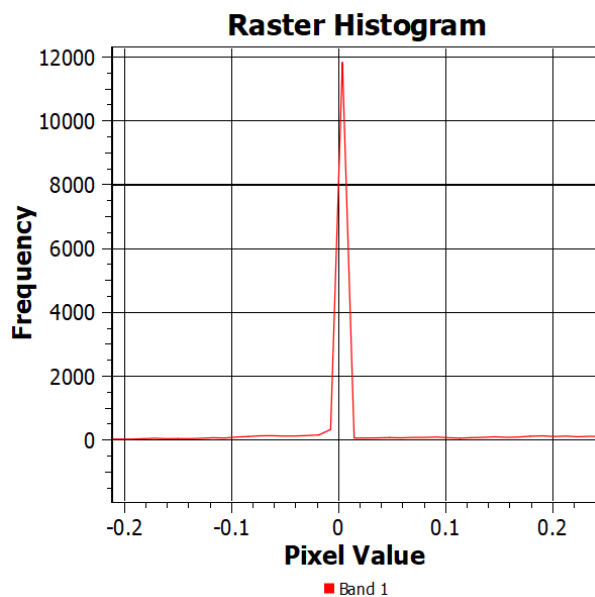


Figure 4.20: Histogram of residuals for velocity for the 2D NACH scenario. Frequency indicates number of pixels.

Including Time

The plots of the profiles lines for 2D NACH over model run time again point toward HEC-RAS being slightly lower for depth and slightly higher for velocity. With areas of lower terrain, mini valleys, showing the slightly higher residuals. This could be attributed to how the mesh and grid in the models is aligned at the small ridges. Gradually varied terrain shows a more uniform distribution of the residuals.

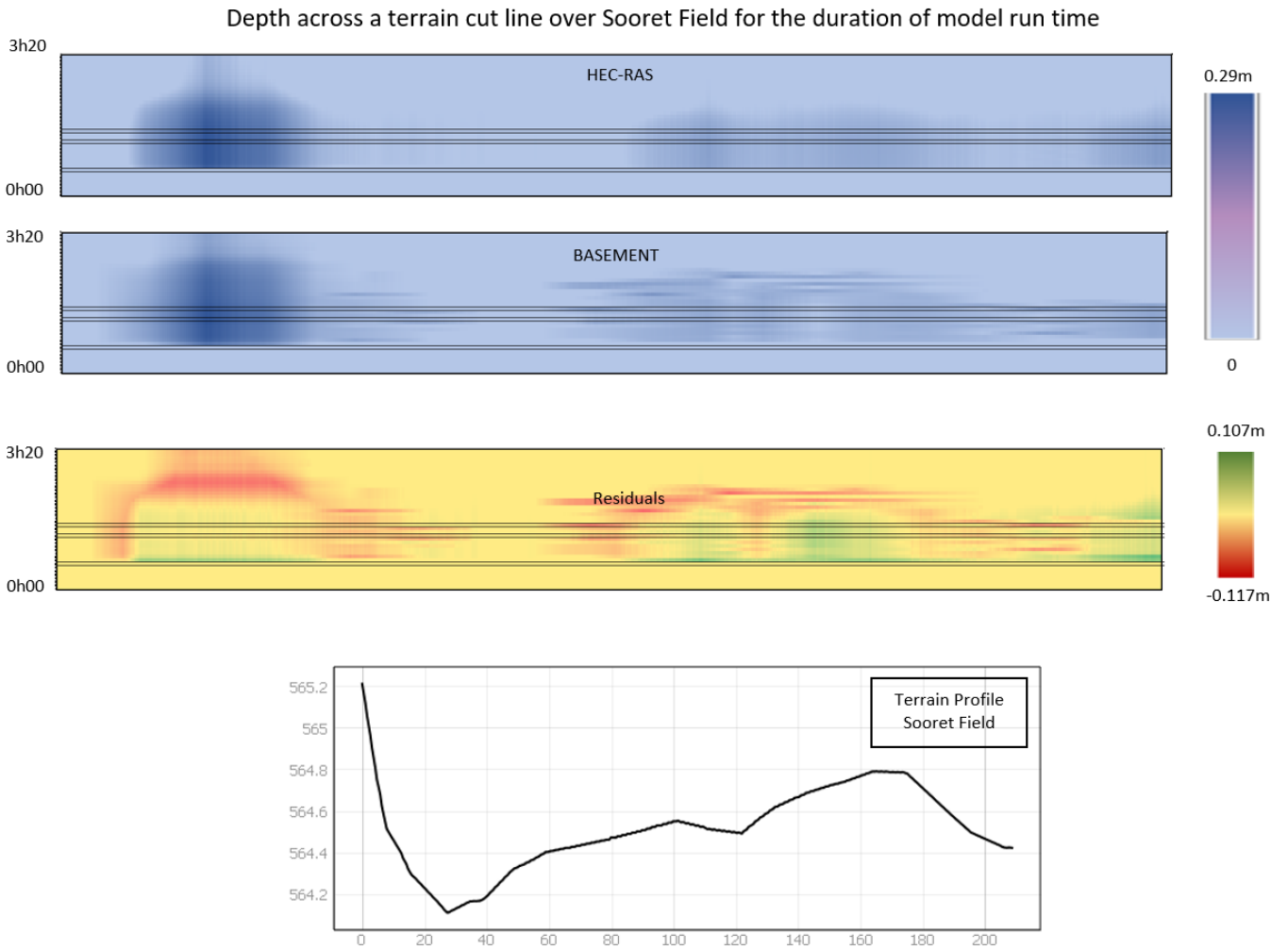


Figure 4.21: The y-axis for the plots represents model run-time and the x-axis represents distance along the profile line at the key area of the Sooret Field. The colour scale indicates the range of values. The horizontal markings are the start-, end- and post-peak flow times. The terrain profile is included for reference in the last plot.



Figure 4.22: The y-axis for the plots represents model run-time and the x-axis represents distance along the profile line at the key area of the Sooret Field. The colour scale indicates the range of values. The horizontal markings are the start-, end- and post-peak flow times. The terrain profile is included for reference in the last plot.

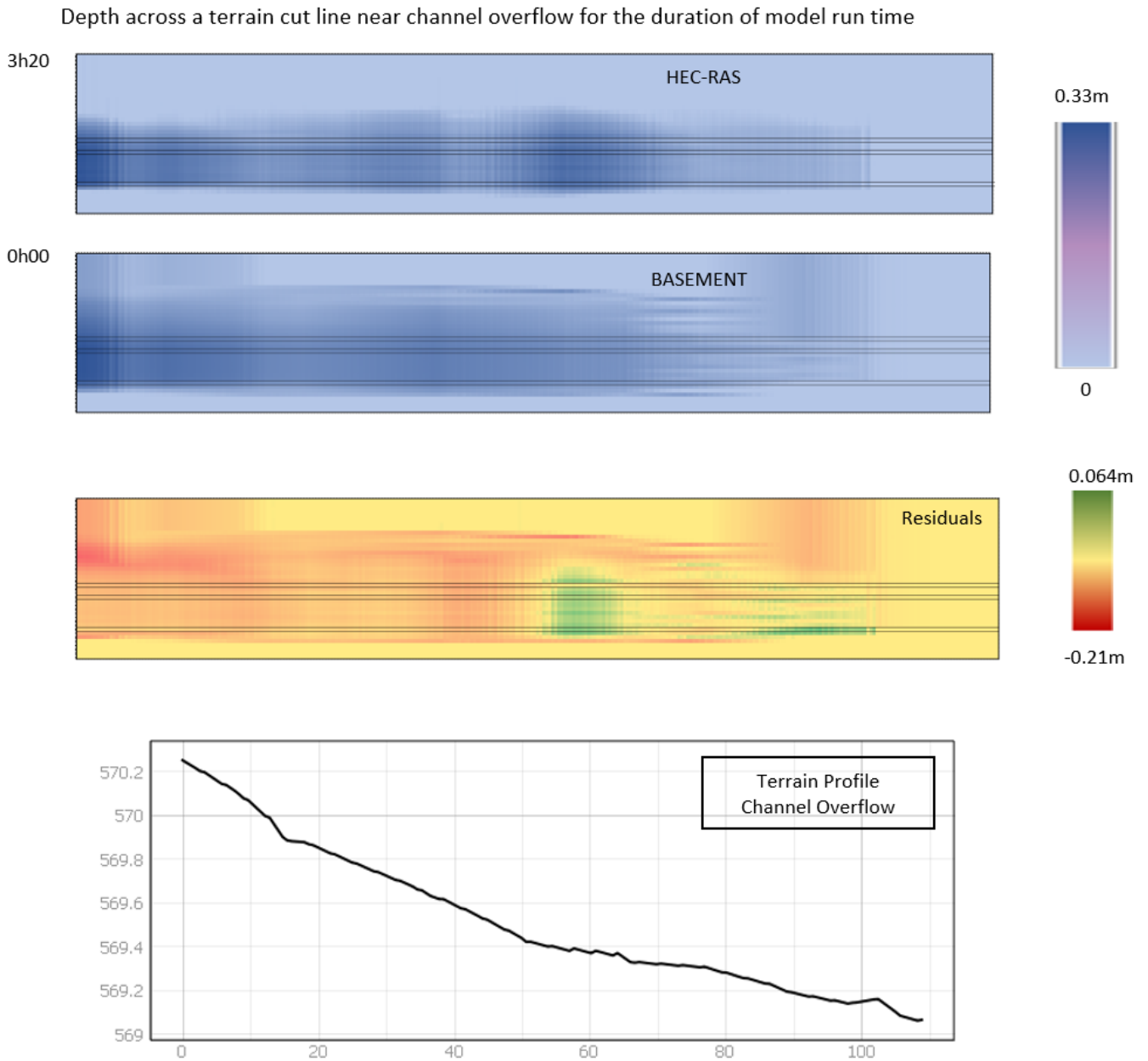


Figure 4.23: The y-axis for the plots represents model run-time and the x-axis represents distance along the profile line at the overflow area. The colour scale indicates the range of values. The horizontal markings are the start-, end- and post-peak flow times. The terrain profile is included for reference in the last plot.

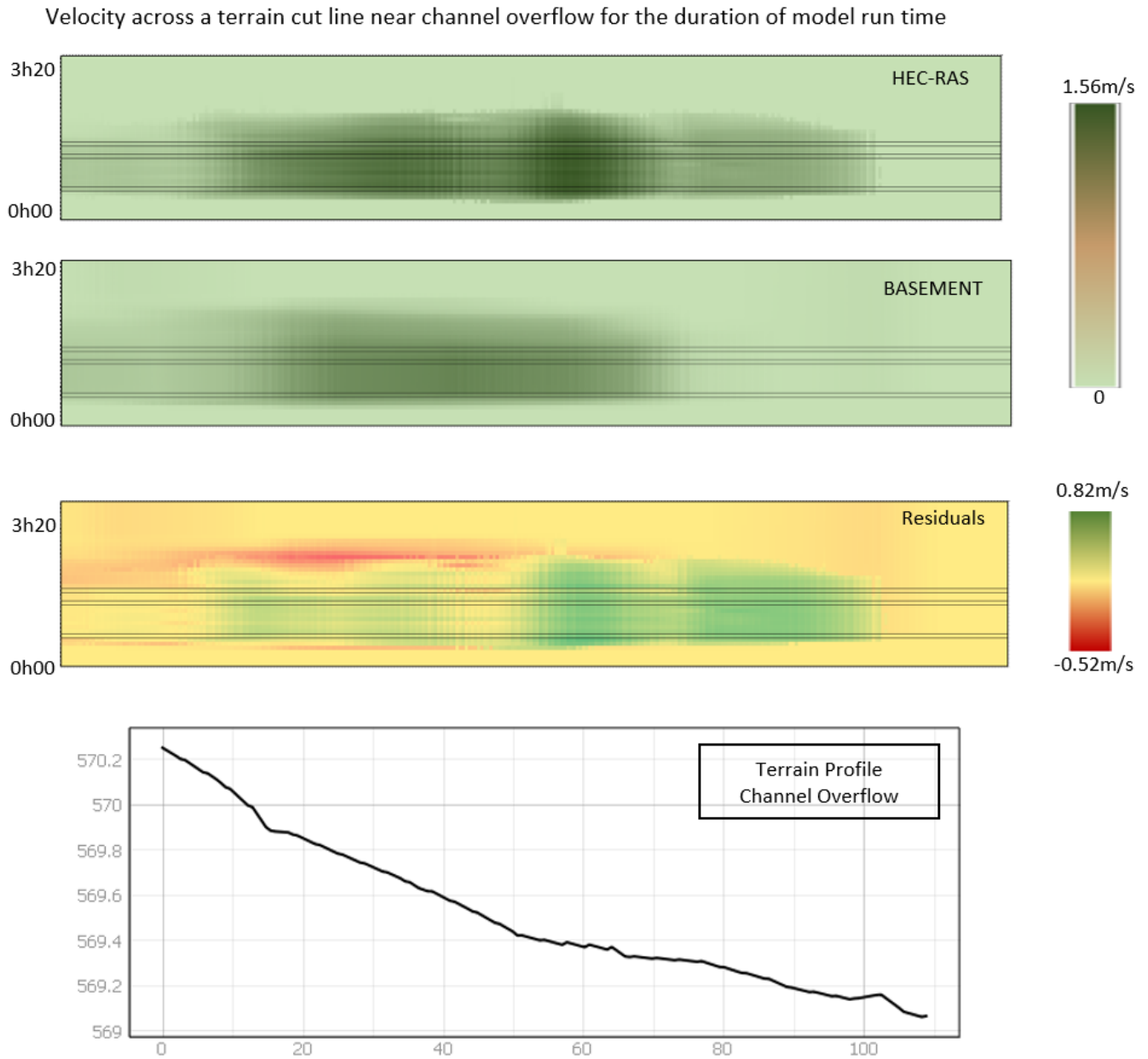


Figure 4.24: The y-axis for the plots represents model run-time and the x-axis represents distance along the profile line at the overflow area. The colour scale indicates the range of values. The horizontal markings are the start-, end- and post-peak flow times. The terrain profile is included for reference in the last plot.

4.2.4 Intense Hydrology

HQ1000

When increasing the hydrology to HQ1000, residuals of depth 4.25 and velocity 4.26 show a greater range but are still low. The most extreme values occur at pixels in the channels. The biggest change compared to the HQ300 is the depth residuals being positive

and larger for HEC-RAS in the area where flow overtops the raised road.

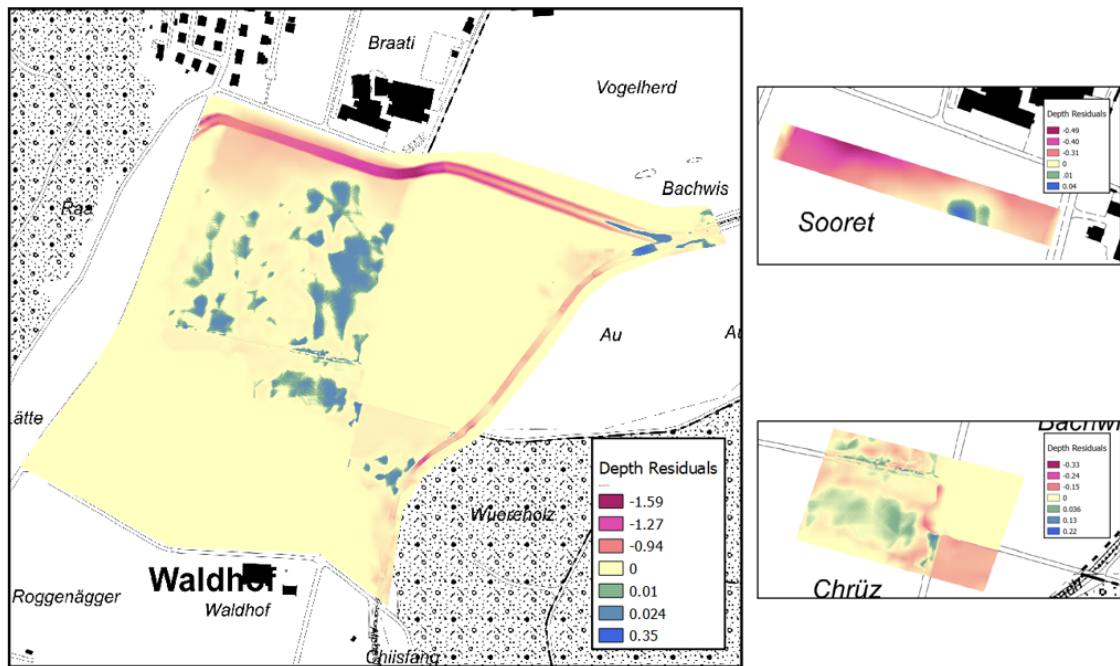


Figure 4.25: Depth residual values in metres for the NACH study area and key areas. Based on a pixel size of 0.5m.

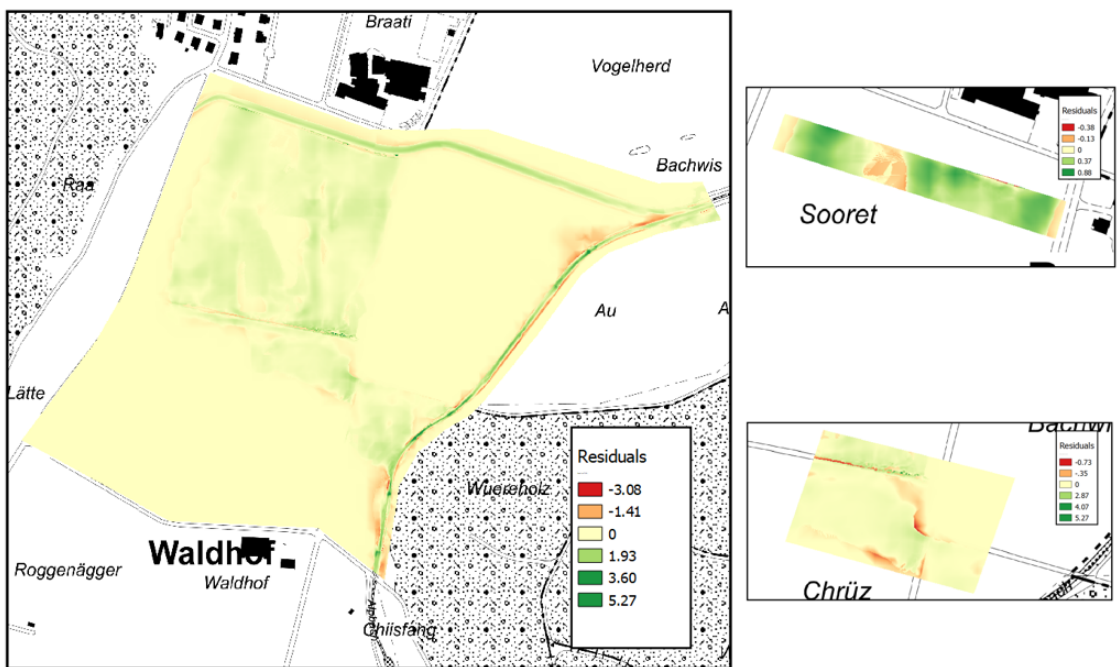


Figure 4.26: Velocity residual values in metres for the NACH study area and key areas. Based on a pixel size of 0.5m.

The histogram of depth residuals (4.27) and velocity residuals (4.28) show values being close to 0, with a slightly greater tendency toward negative values for the depth.

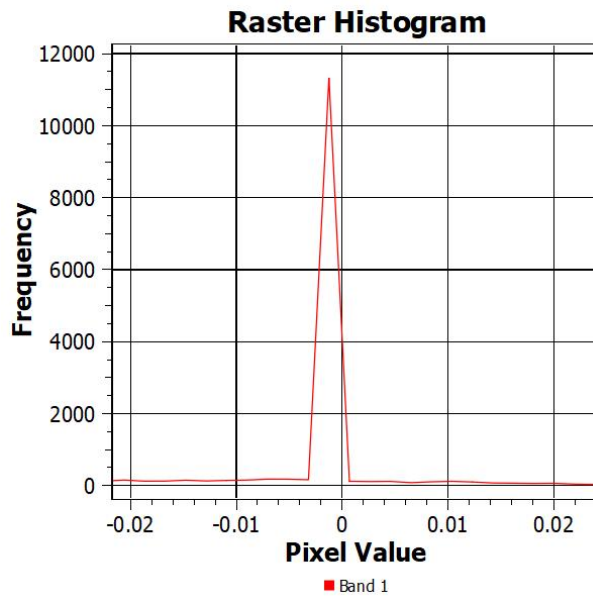


Figure 4.27: Histogram of residuals for depth for the 2D NACH scenario using an intense hydrology of HQ1000. Frequency indicates number of pixels.

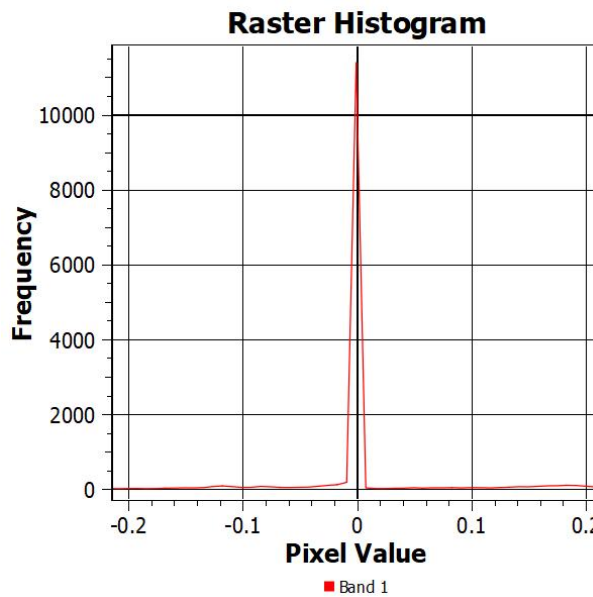


Figure 4.28: Histogram of residuals for velocity for the 2D NACH scenario using an intense hydrology of HQ1000. Frequency indicates number of pixels.

The residuals over time at the profile lines for HQ1000 hydrology show a similar output to those for HQ300.

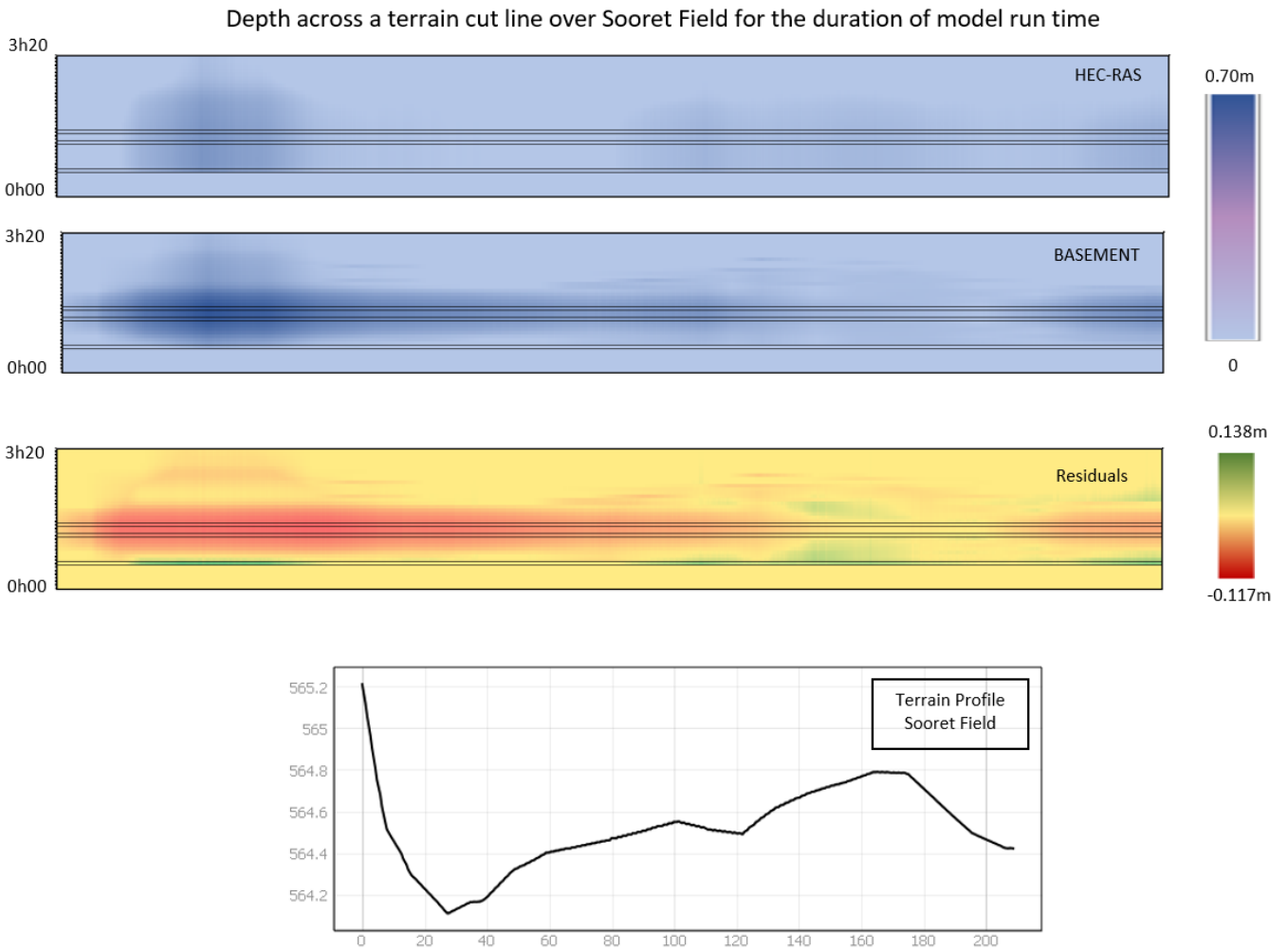


Figure 4.29: The y-axis for the plots represents model run-time and the x-axis represents distance along the profile line across the Sooret Field. The colour scale indicates the range of values. The horizontal markings are the start-, end- and post-peak flow times. The terrain profile is included for reference in the last plot.

Velocity across a terrain cut line over Sooret Field for the duration of model run time

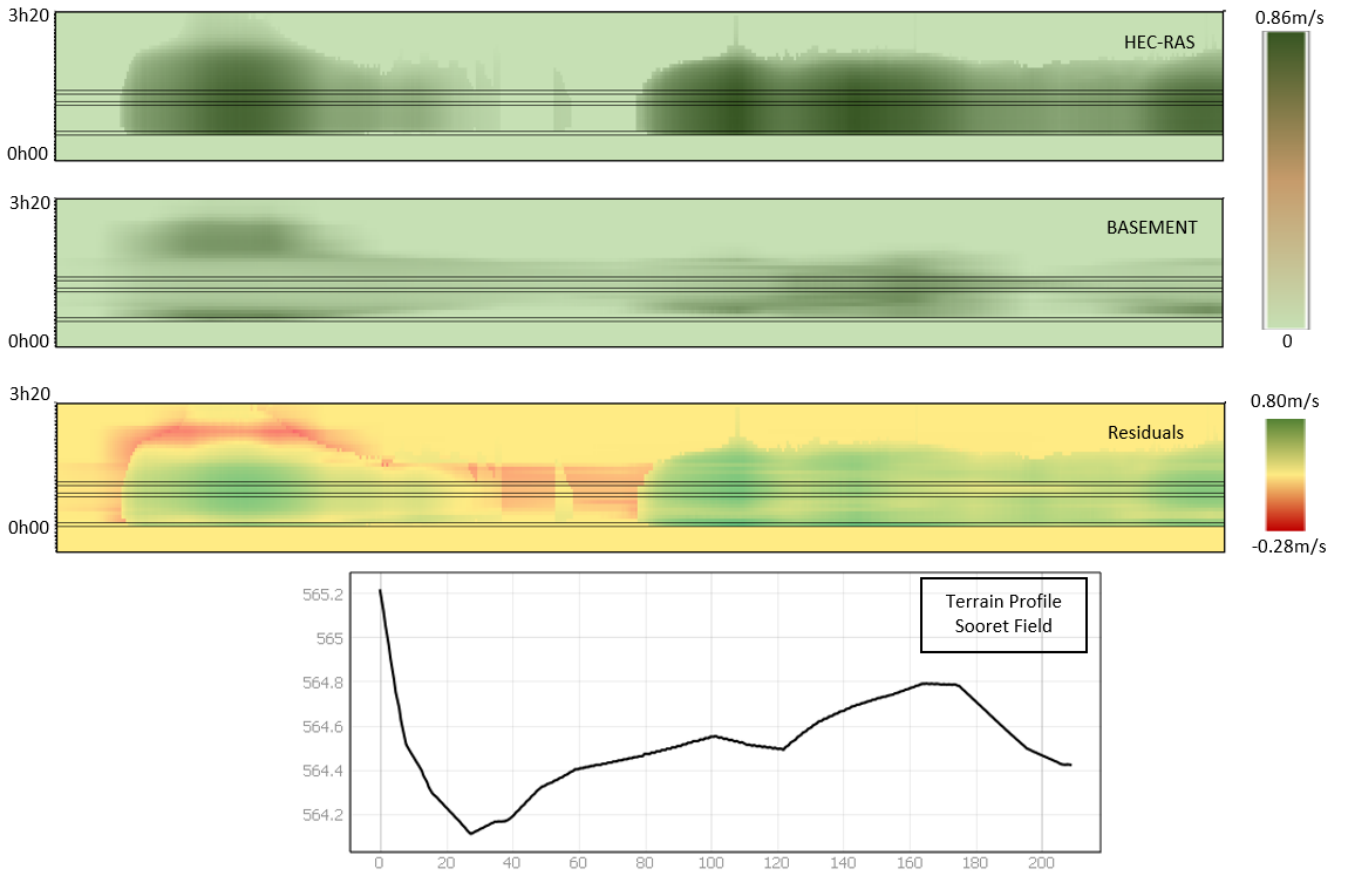


Figure 4.30: The y-axis for the plots represents model run-time and the x-axis represents distance along the profile line across the Sooret Field. The colour scale indicates the range of values. The horizontal markings are the start-, end- and post-peak flow times. The terrain profile is included for reference in the last plot.

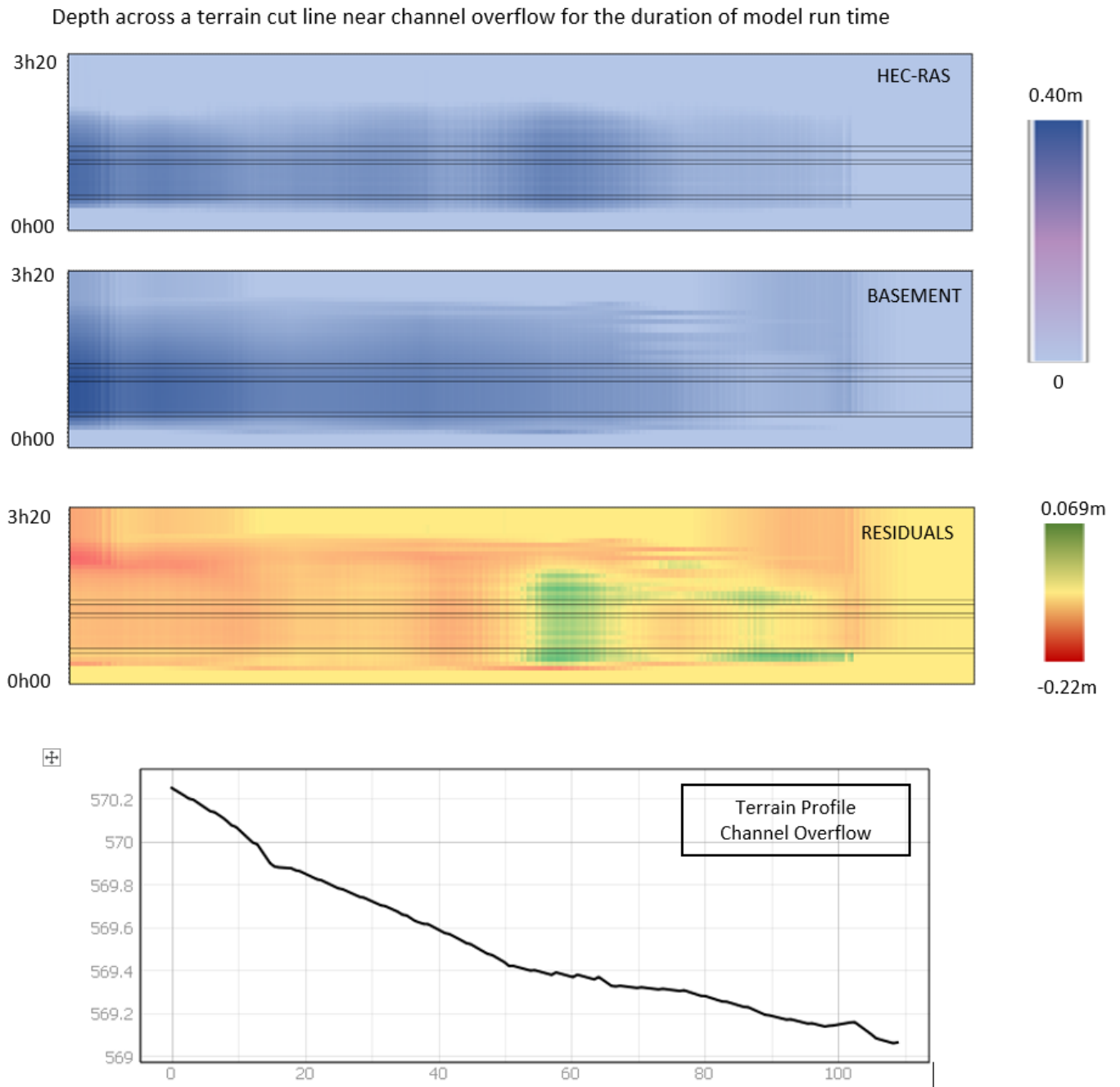


Figure 4.31: The y-axis for the plots represents model run-time and the x-axis represents distance along the profile line at the overflow area. The colour scale indicates the range of values. The horizontal markings are the start-, end- and post-peak flow times. The terrain profile is included for reference in the last plot.

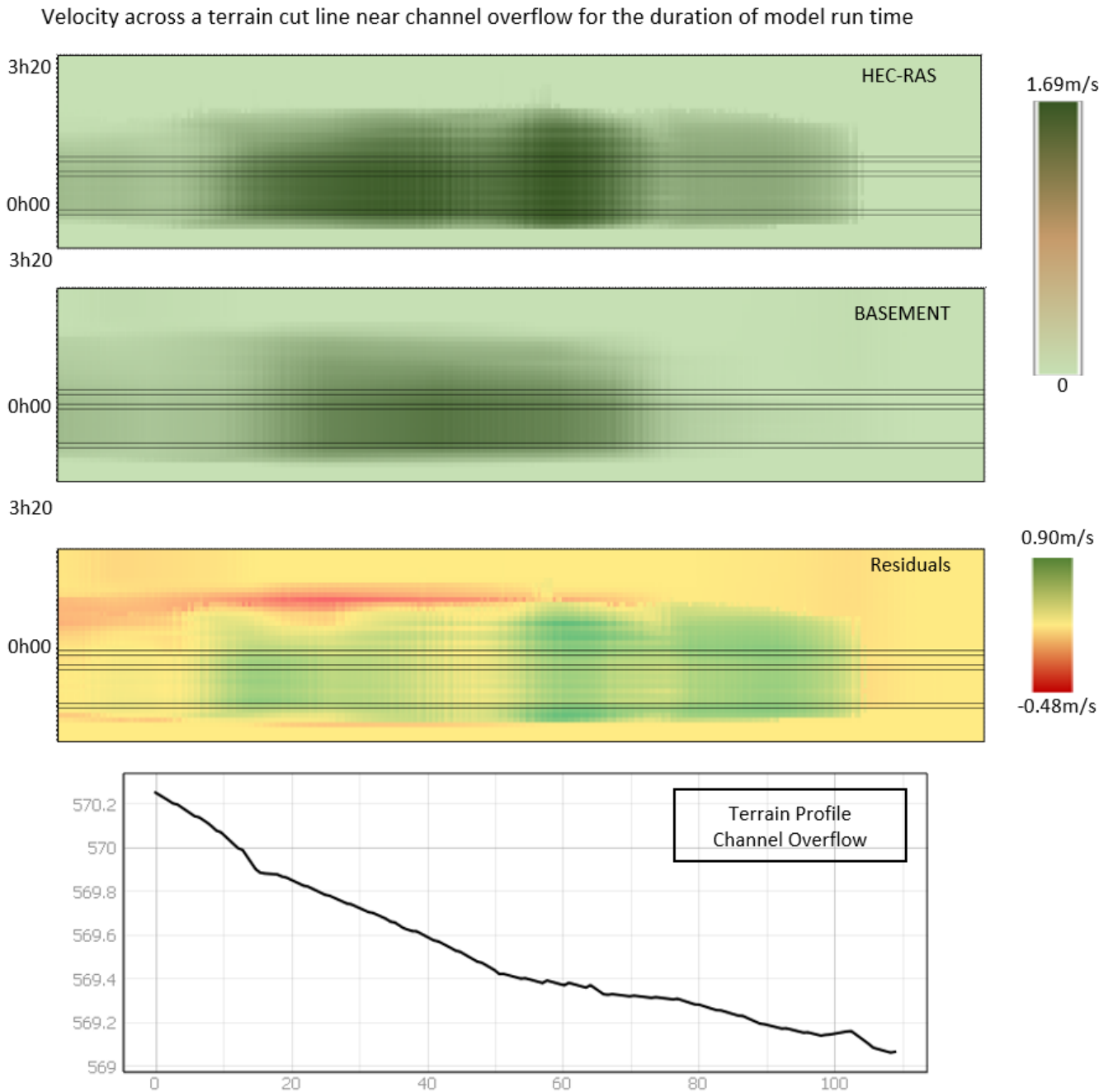


Figure 4.32: The y-axis for the plots represents model run-time and the x-axis represents distance along the profile line at the overflow area. The colour scale indicates the range of values. The horizontal markings are the start-, end- and post-peak flow times. The terrain profile is included for reference in the last plot.

Varying Hydrology – Junction

For the Huebbach, the hydrology was altered by increasing HQ1000 flow by 30% and 50% to represent a situation where only this catchment experienced intense rain and then how this effected outputs at the region of the confluence was observed.

When flow meets another stream the velocity decreases (see fig 4.33 and a lake effect could occur at this area. In the case of BASEMENT and HEC-RAS, both models had similar outcomes (see fig. 4.34 at the confluence area and even at 50% increased flow, water did not leave the channel in either model, aside from a very small amount on the south side of the channel in the HEC-RAS model).

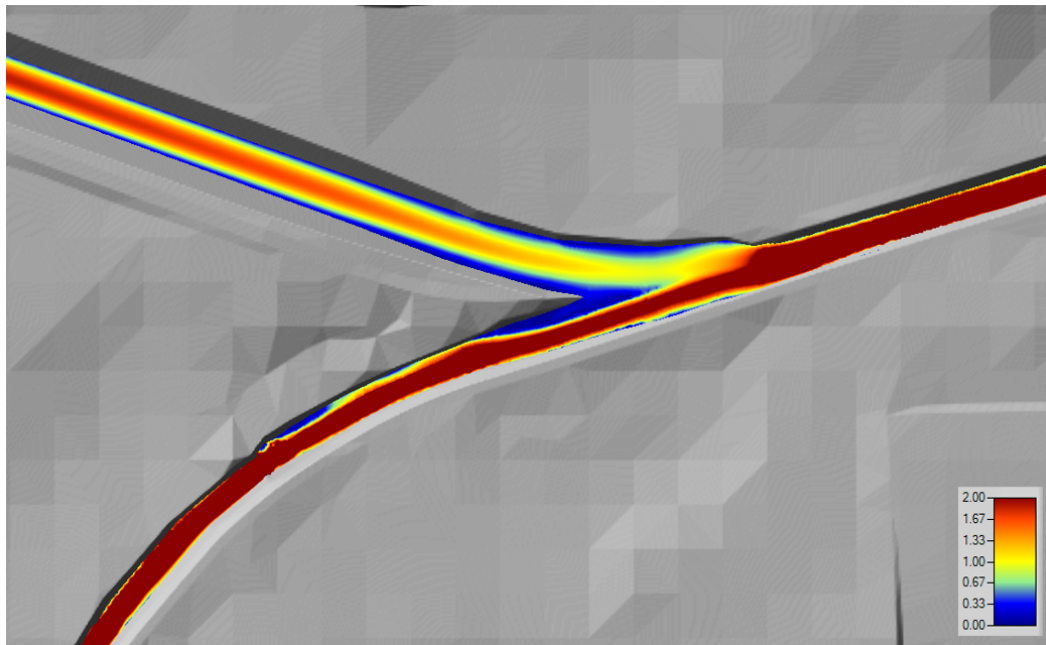


Figure 4.33: As the Huebbach flow joins the Alpbach its velocity is slowed at the stream junction as expected. An upwelling of water is possible into the Huebbach and a lake effect could be observed where the flows meet.

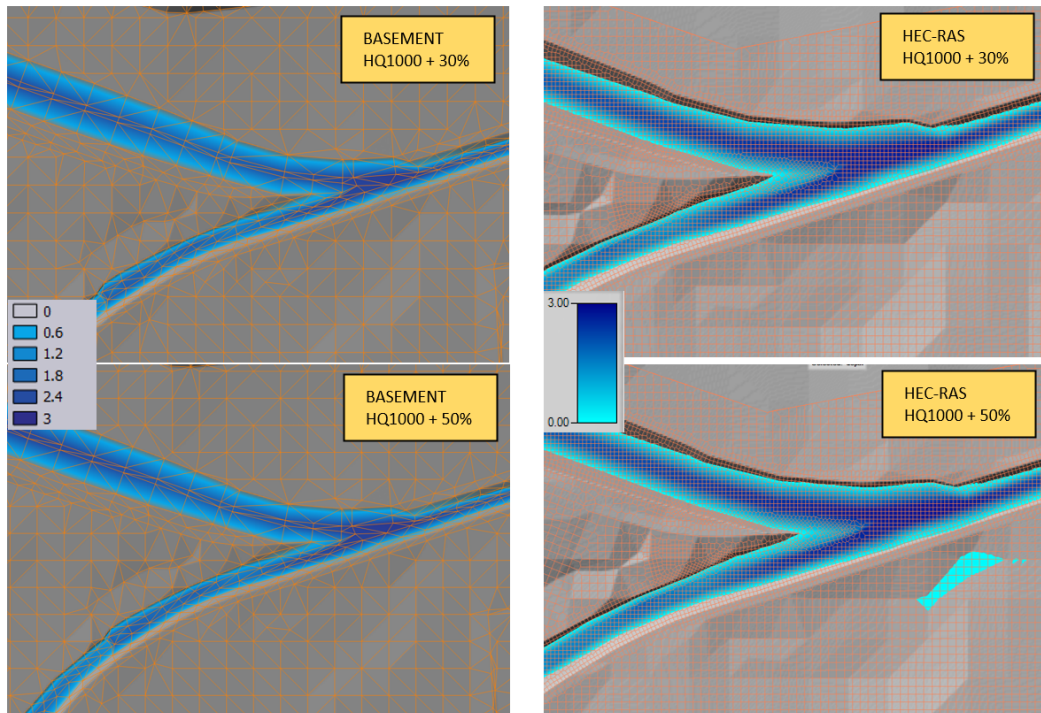


Figure 4.34: The two left images are for the BASEMENT models and the two on the right for HEC-RAS. Neither model produced a noticeable lake effect. Although a small amount of flow did leave the channel for the HEC-RAS HQ1000 + 50% scenario.

Table 4.1: Flood area index, accuracy metrics, contingency table and summary statistics for 2D IST scenario.

		Full Study Area	Outlet Wilen	Engistr 95
Total Area (m ²)		219,514	11,962	6,102
Flood Area Index		0.54	0.52	0.86
Contingency Table				
Hits		183156	22682	16198
Correct Negatives		536688	4398	5595
Misses		147357	19350	2019
False Alarms		10711	1196	591
Accuracy Metrics				
Accuracy		0.82	0.57	0.89
Bias		0.59	0.57	0.92
Hit Rate		0.55	0.54	0.89
False Alarm Ratio		0.06	0.05	0.04
False Alarm Rate		0.02	0.21	0.10
Critical Success Index		0.54	0.52	0.86
Success Index		0.58	0.32	0.56
Peak Difference		0.19	0.25	0.10
% Error Peak		6.45	37.26	18.01
Summary Statistics				
Depth (m)	Mean Value BASEMENT	0.08	0.25	0.09
	Mean Value HEC-RAS	0.04	0.06	0.07
	Range BASEMENT	2.96	0.68	0.58
	Range HEC-RAS	2.77	0.43	0.48
Velocity (m/s)	Mean Value BASEMENT	0.14	0.15	0.36
	Mean Value HEC-RAS	0.16	0.09	0.44
	Range BASEMENT	4.54	0.82	1.00
	Range HEC-RAS	7.30	0.97	1.32

Table 4.2: Flood area index, accuracy metrics, contingency table and summary statistics for 2D NACH scenario.

		Full Study Area	Sooret	Intersection
Total Area (m ²)		230,510	6,752	14,410
Flood Area Index		0.72	0.82	0.87
Contingency Table				
Hits		260313	20996	34650
Correct Negatives		561496	1296	17768
Misses		91150	3348	4458
False Alarms		8926	1360	757
Accuracy Metrics				
Accuracy		0.89	0.83	0.91
Bias		0.77	0.92	0.91
Hit Rate		0.74	0.86	0.89
False Alarm Ratio		0.03	0.06	0.02
False Alarm Rate		0.02	0.51	0.04
Critical Success Index		0.72	0.82	0.87
Success Index		0.67	0.46	0.60
Peak Difference		0.15	0.00	0.07
% Error Peak		5.14	-0.26	6.42
Summary Statistics				
Depth (m)	Mean Value BASEMENT	0.11	0.06	0.13
	Mean Value HEC-RAS	0.07	0.06	0.12
	Range BASEMENT	2.97	0.33	1.10
	Range HEC-RAS	2.81	0.33	1.03
Velocity (m/s)	Mean Value BASEMENT	0.14	0.06	0.27
	Mean Value HEC-RAS	0.23	0.06	0.47
	Range BASEMENT	4.78	0.33	1.33
	Range HEC-RAS	8.22	0.33	3.72

Chapter 5

Results and Discussion Q2

The intra-model dimensionality was explored in two sets. The channel was compared between the 2D and 1D models and the floodplain between the 1D2D and 2D. Although it has been featured in research [26], it is not appropriate to use 1D results to judge flow in a 2D domain, like a flood plain (expert opinion, personal communication).

5.1 1D and 2D – Channel

The thalweg was used as a profile line to plot the depth 5.1 and velocity 5.2 along the channel for the 1D and 2D models. Higher depth values are approximately the same between 1D and 2D, but the low values are much lower for the 2D. This is likely occurring because the channel was represented much smoother in the 1D model as the terrain between cross sections is interpolated. The steep drops or locations where the channel bed has been carved out by the streams and has a lower elevation, are not represented in the 1D terrain. Whereas the 1m x 1m grid along the channel was able to pick up this variation in elevation. The velocities between the two domains are also not equivalent because of this variation in terrain representation. However, the peak values for the 1D are similar at many points to the 2D. It is unclear why at approximately halfway along the channel the 1D velocity shows a strange result and hovers around 3m/s, this could be the area where the Alpbach bends and the channel terrain variation was too great to allow cross sections to be placed there, thus the interpolation distance is longer.

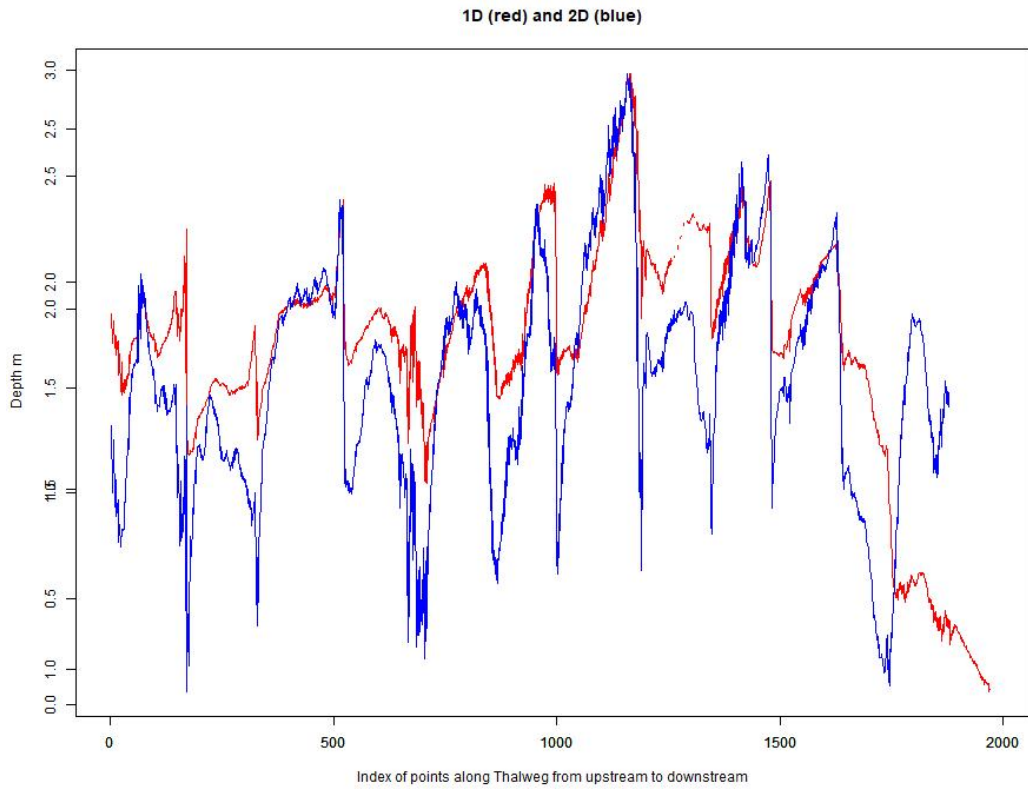


Figure 5.1: caption

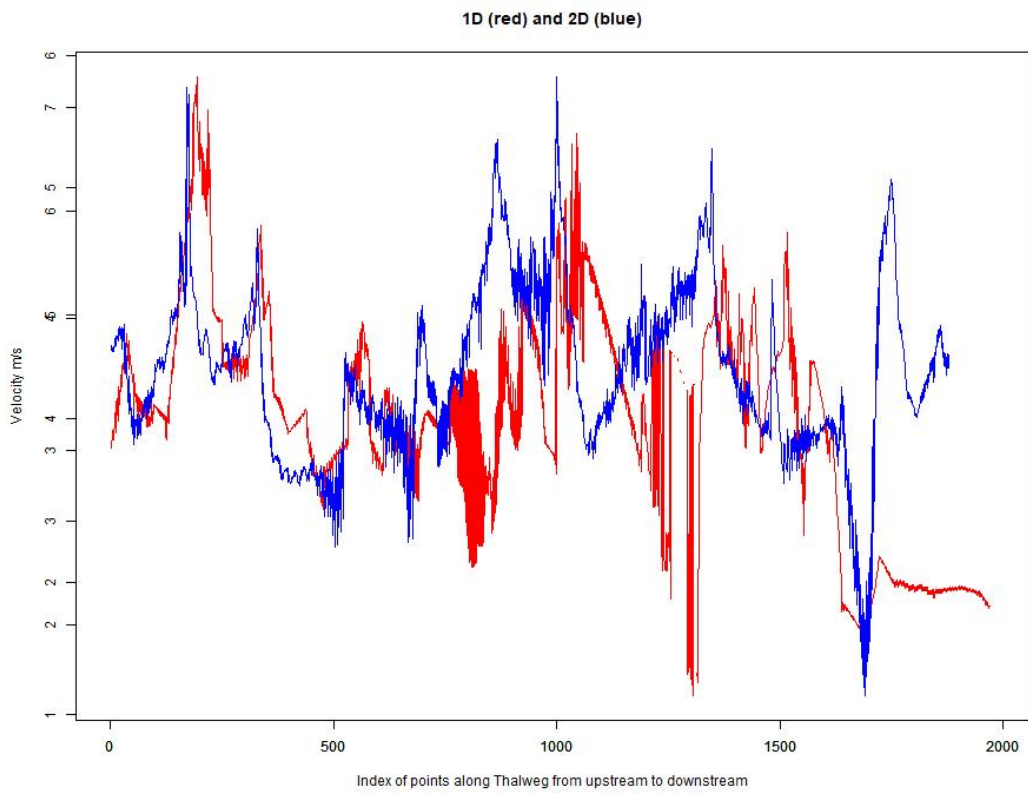


Figure 5.2: caption

As stated, the actual flood plain cannot be compared because the flow should not be modeled in 1D. Instead the depth over time at a point (see fig 5.3 in the area of overflow was plotted (see fig 5.4.) to gauge approximately how the 2 models compare in this region. The pattern of depth is similar between the two models, but the 2D depth was greater by a range of 0 - 0.23m. However, peak values are the same between both models.



Figure 5.3: Point selected to compare depth values over model run duration. For the 1D model this point is located along the channel bank but before the lateral structure

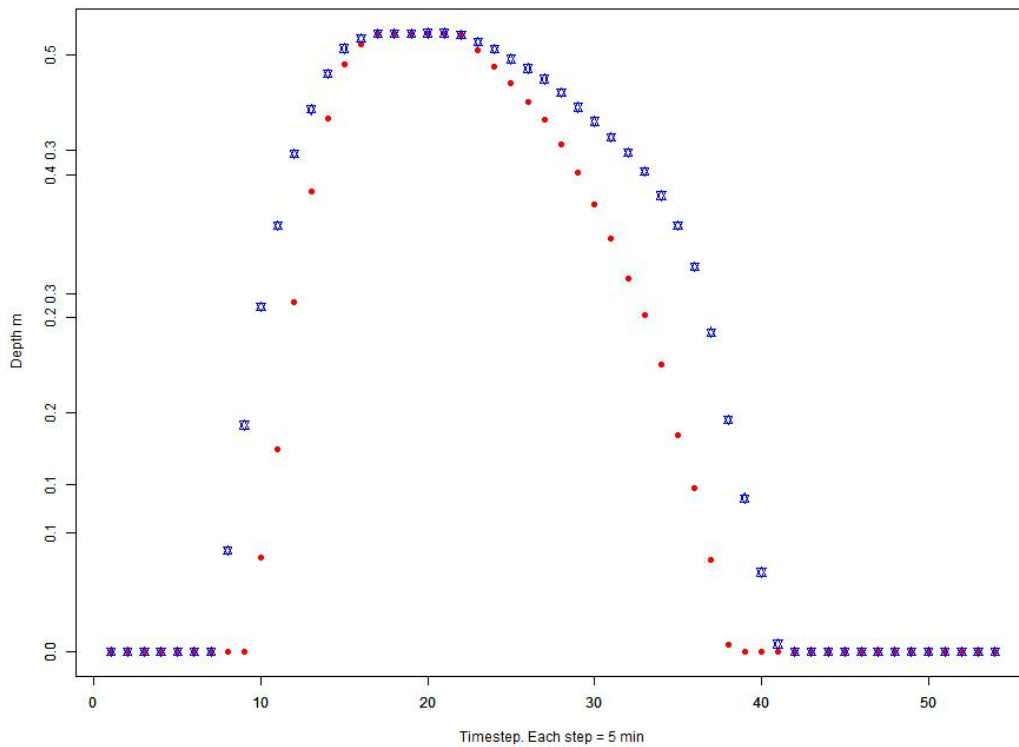


Figure 5.4: Depth values vs model run duration at a point located along the overflow region in the Alpbach. Red points represent values from the 1D model and blue points represent values from the 2D model.

5.2 1D2D and 2D – Floodplain

It was observed that between the 1D and 2D there was a similar pattern for depth, with 2D values being slightly higher than 1D during the pre and post peak flow times, but peak values being similar. At the time of peak flow the floodplain between the 2D and 1D/2D should not show great variation therefore. The residuals for depth and velocity were computed as 2D compared to the 1D2D and highlight pixels where the 2D output is greater than or less than the 1D2D.

The image of residuals shows that over the floodplain there was little variation between the models, aside from the 2D velocity being slightly greater in the overflow area compared to the 1D2D. The pixels over the channel have been included and the greater variation is visible there, but, for the histogram, as the floodplain area is far greater than the channel area, the channel pixels do not skew the clear result that residuals are hovering close to 0. For velocity, the histogram shows the highest frequency as being slightly above 0, which corresponds to the slightly higher values (green areas) when mapping the residuals.

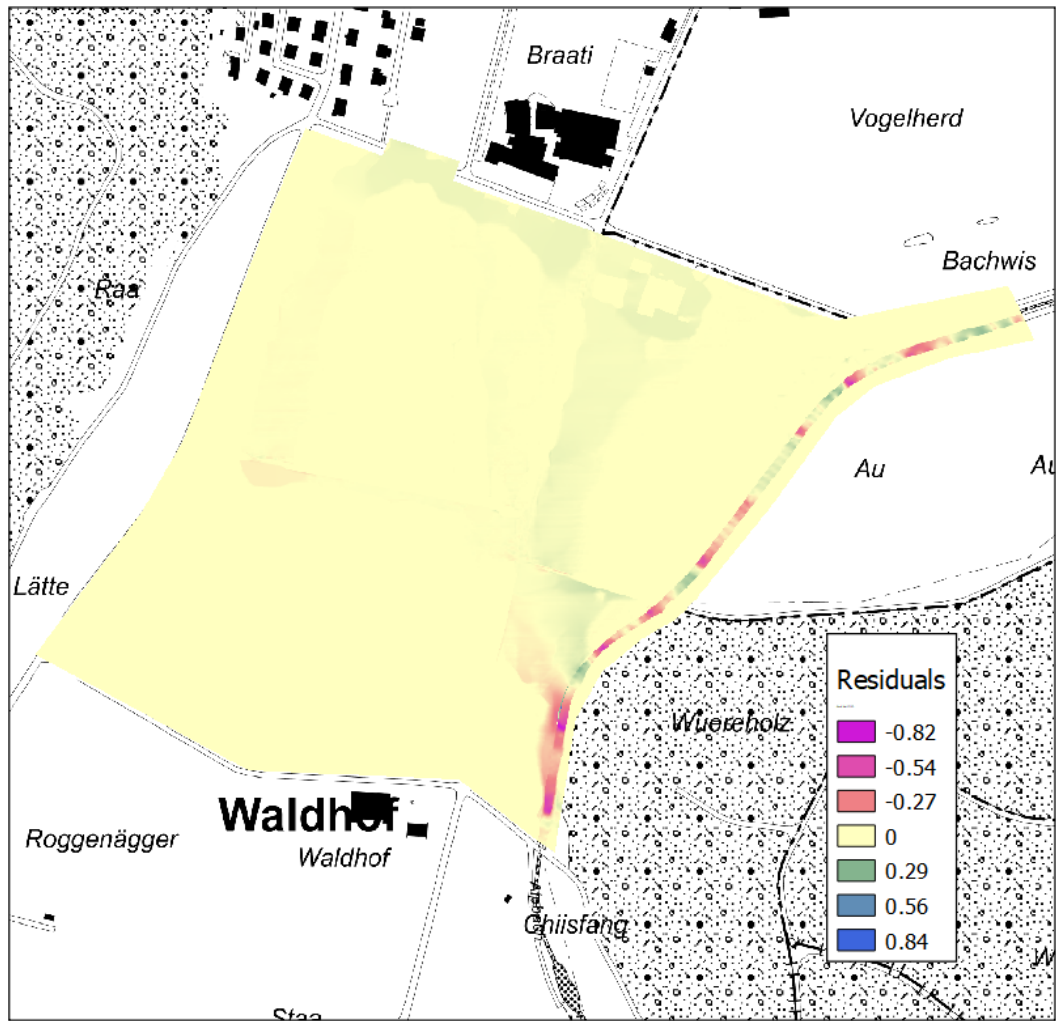


Figure 5.5: Depth residuals over the floodplain for 2D compared to 1D2D

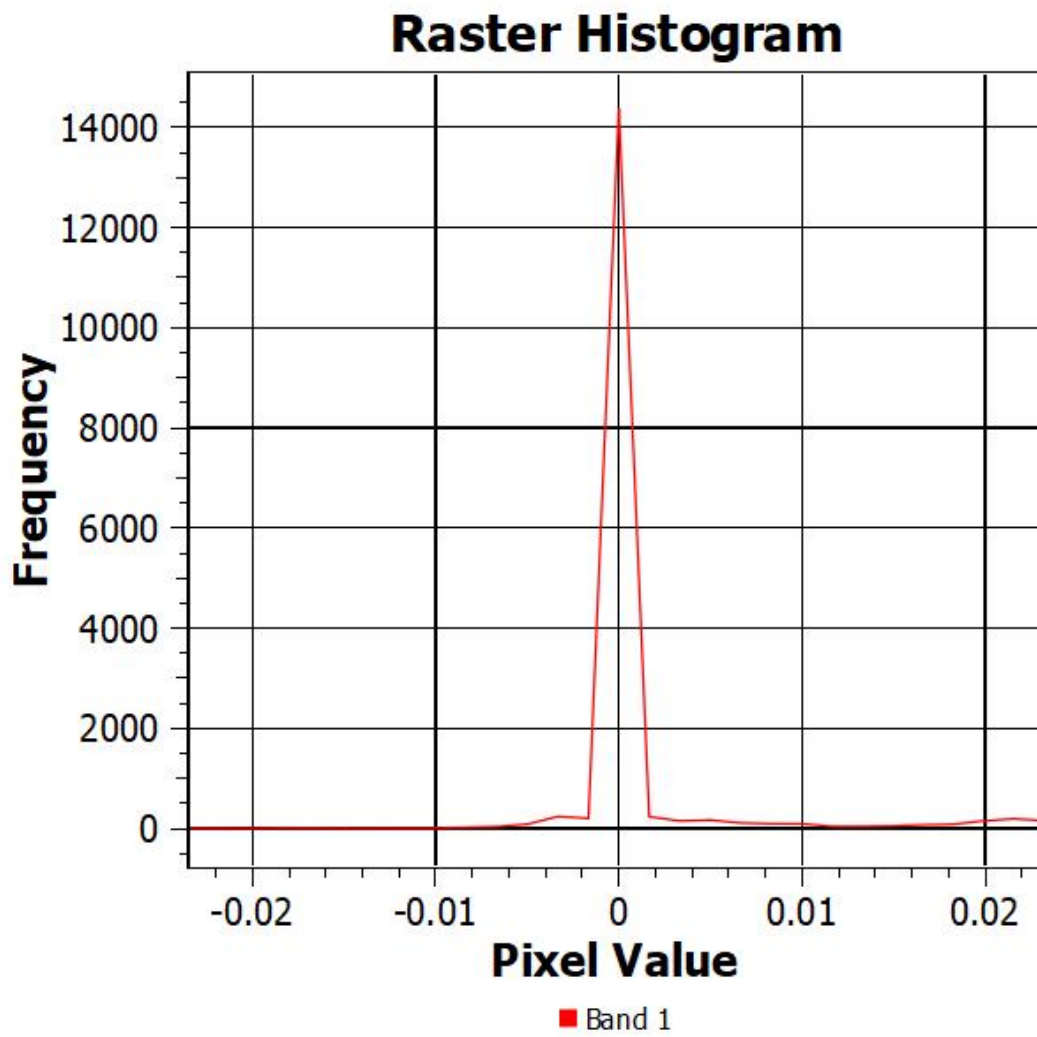


Figure 5.6: Histogram of depth residuals

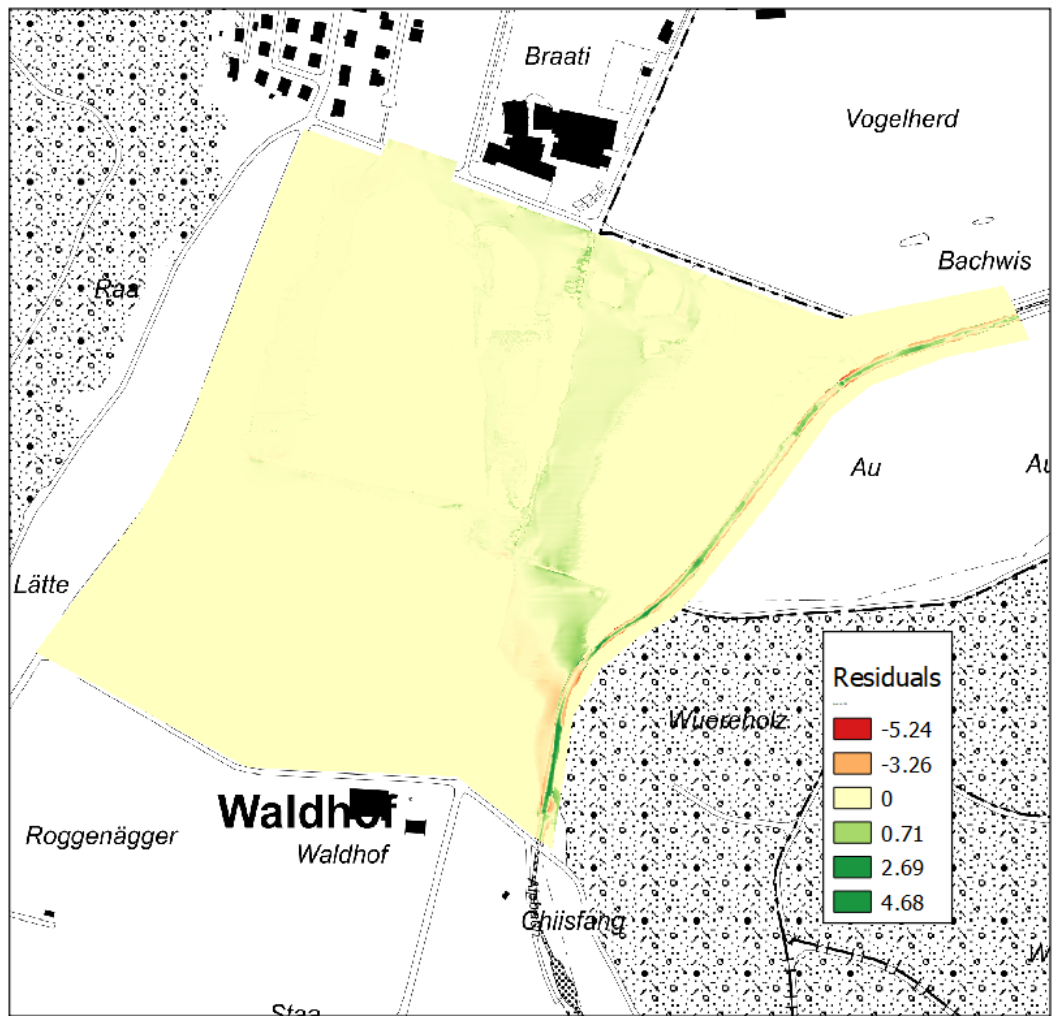


Figure 5.7: Velocity residuals over the floodplain for 2D compared to 1D2D

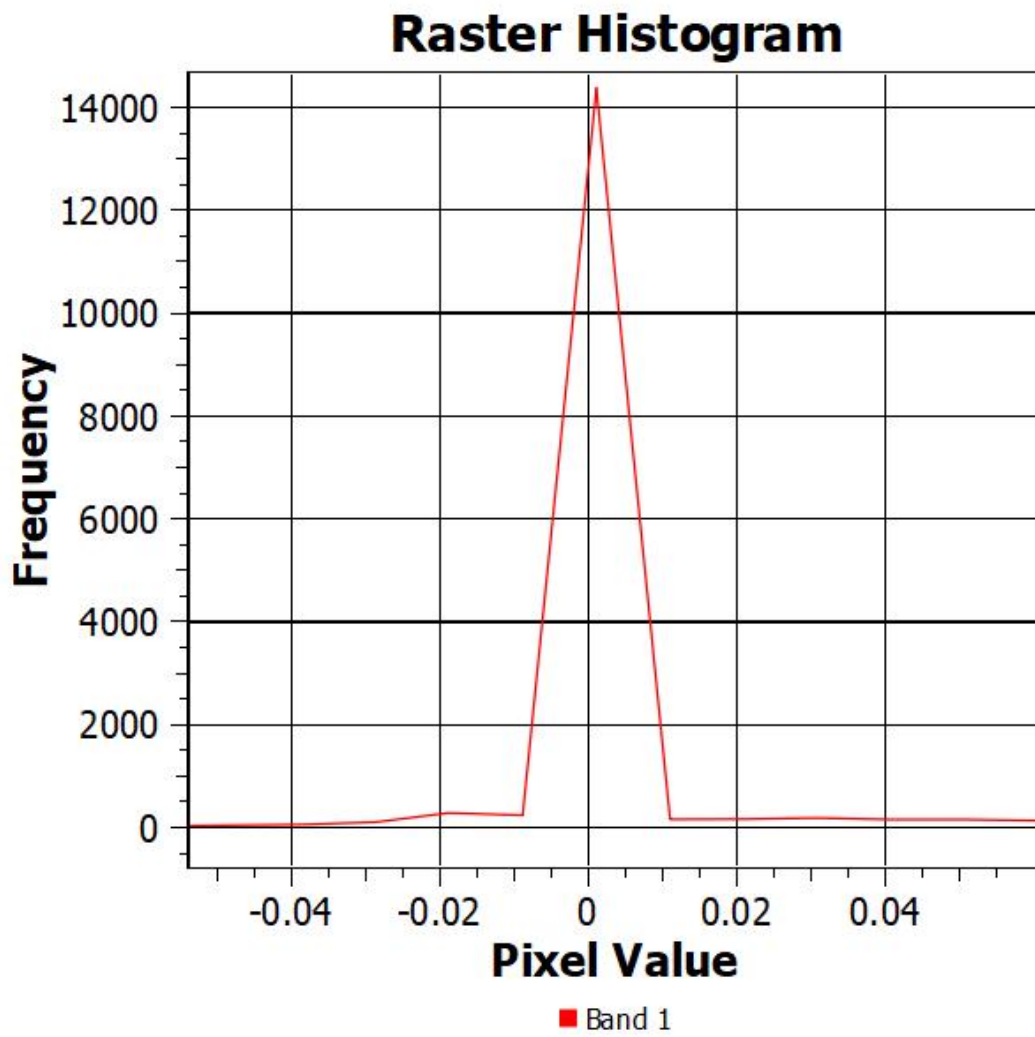


Figure 5.8: Histogram of velocity residuals

Chapter 6

Results and Discussion Q3

6.1 Roughness

In fig 6.1 the velocity at a profile line extracted from the overflow area is plotted. Decreasing the roughness value in intervals of 10% lead to an increase in velocity values at the profile line and increasing the roughness values lead to a decrease in velocity values. Fig 6.2 shows the flow for the duration of model run time over a profile line orientated in the direction of outflowing water. Decreasing the roughness value lead to a greater flow and increasing the roughness value lead to a reduced flow over the line. In these systematic cases, the model is behaving as expected as the manning's equation describes the relationship between velocity and surface roughness to be inversely related.

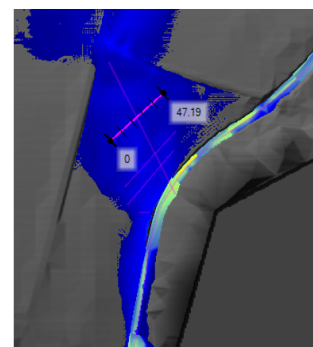
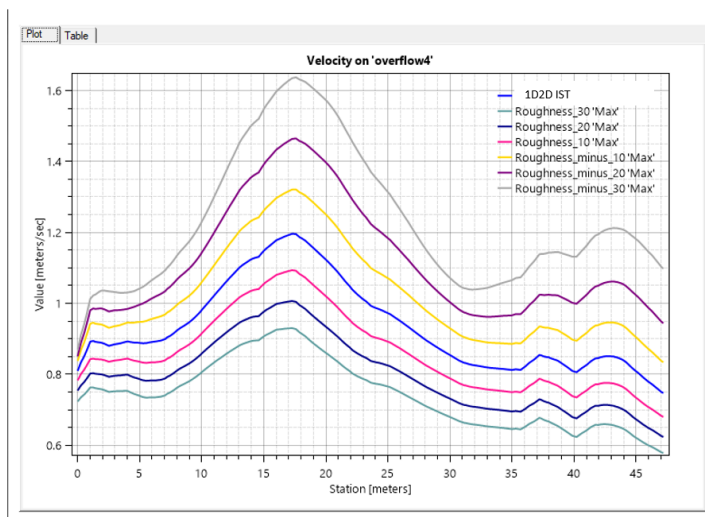


Figure 6.1: The max profile velocity is plotted over a profile line extracted from the overflow area.

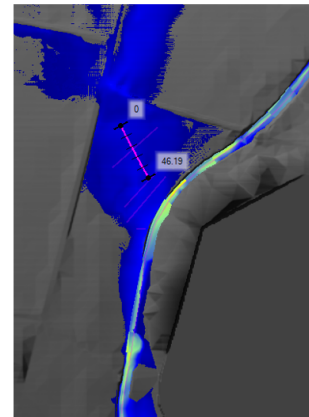
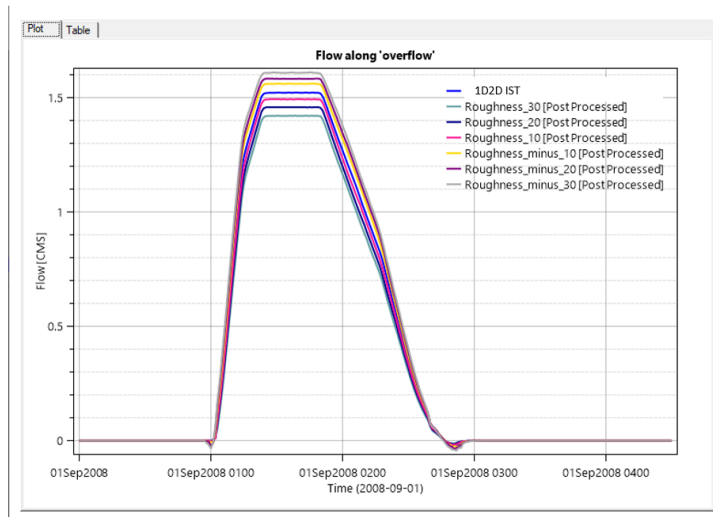


Figure 6.2: The flow along a profile line in the overflow area for the duration of model run-time

Ultimately, the flood extent between decreasing 30% and increasing 30% did not change substantially, as viewed in RAS-MAPPER (see fig 6.3)

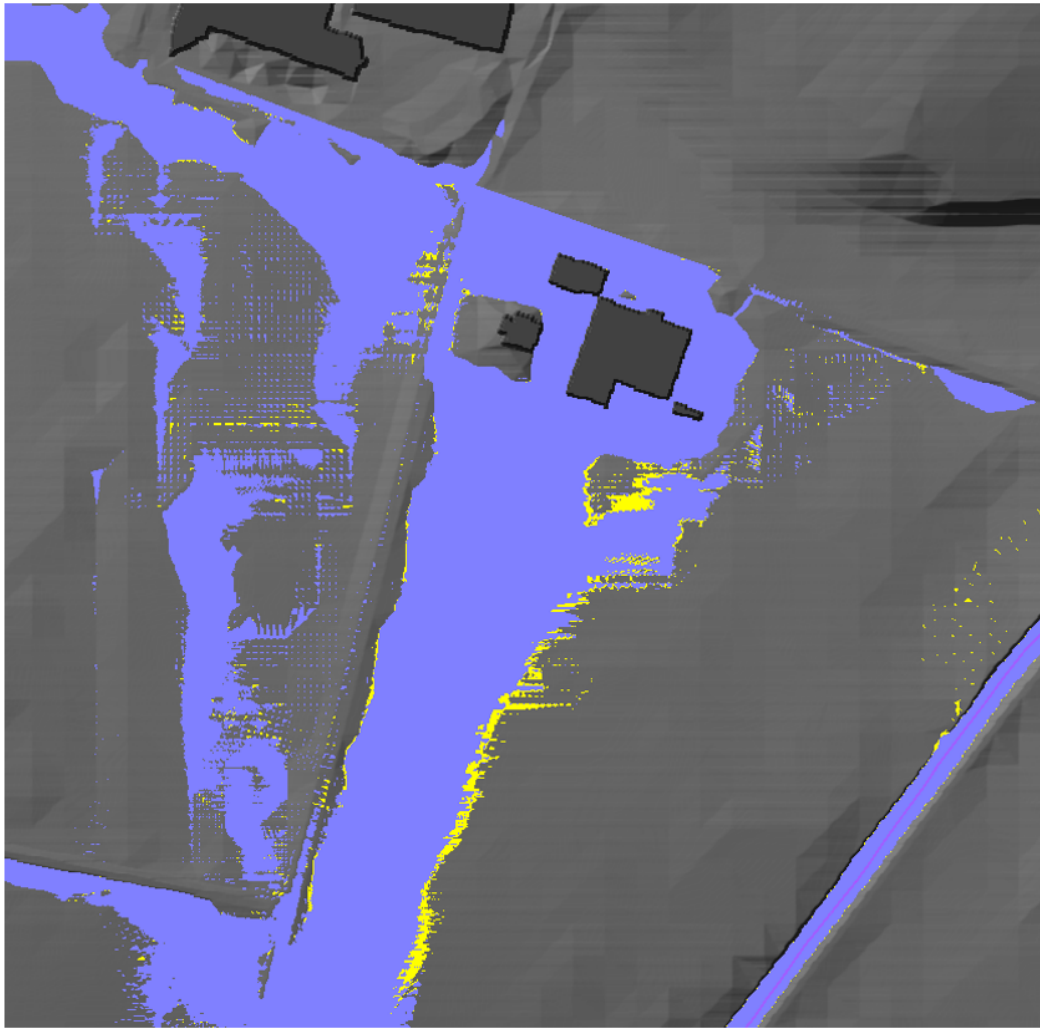


Figure 6.3: The purple region is decreasing Manning's n value by 30% and the yellow region is increasing by 30%.

6.2 Time

For the 2D model runs, a fixed time step of 2 seconds was used as it allowed for acceptable results within a manageable computation time. A 4.5 hour model run time could be computed within 1h45m35s. By switching this setting to allow the time step to be controlled by courant condition, with the courant range set from 0.5-3.0, the computation time substantially increased. A 1h45m model run time took 2h32m27s to compute. This could be expected because the smaller a grid cell, the smaller a time step is required to ensure flow crosses it within 1 time step. The channel and refinement region cells were 1m x 1m and in the base model scenarios the 2 second time step was long for these areas. By using the courant condition the time step was at times reduced to 0.625s. In this case, the results with a 2 second time step were still acceptable but should a modeller require more precision and have the computational resources available, then the courant condition should

be applied.

6.3 2D Equation

The 2D diffusive wave approximation was not an appropriate method for use on the Alpbach. This approximation is only valid when there is primarily sub-critical flow. In the case of the Alpbach, with its varied channel bed, there are many instances where water is flowing down a steep, and occasionally vertical slope. At these points the water is rapidly accelerated and the flow is super-critical, therefore any results generated by using this approximation would not be valid, even if the model remains stable until completion. When applying this approximation inappropriately, the results show no overflow from the channel and extremely high flow velocities.

6.4 Junction Equation

Using the energy balance method at the junction was tested. The model initially ran and at approximately 1 hour of model run time, it became unstable and crashed. This corresponds to the onset of peak flow. As the peak flow for the Alpbach is approximately 6 times greater than for the Huebbach, this imbalance meant the energy difference was likely too large for the model to handle and it was not able to find a balance which led to the eventual instability. However, the water surface elevation method does allow a stable model run and this is what was used in the 1D2D NACH scenario.

6.5 Weir Setup

The table of weir co-efficient results (6.1) shows the total flow crossing the lateral structures. A negative value indicates that flow was crossing the structure and entering the channel. Increasing the weir co-efficient leads to more flow moving from the 1D domain into the 2D domain and decreasing the co-efficient produces the opposite effect. The model appeared not to produce any obscure results in this systematic test.

6.6 Grid Size

The plots in fig 6.4 show the max profile velocities at 3 different lines. The models that included refined regions show velocity values behaving similarly in pattern. In the overflow

area the velocity increases as grid size increases. The dark blue line represents the 4m x 4m unrefined model. At the overflow area and after the raised road, this set-up is showing a much smaller velocity and unchanging (flat) velocity relative to the other models. At line C, the flow at the northern end of the field, the velocities are represented similarly, even for the large grid size. The smaller grid size obtained via refinement regions is necessary to capture hydraulic effects in areas where terrain is changing, as well as in the channel. In areas of relatively smooth terrain (line C, flat terrain), there is less variation in the flow and it is possible to utilise a larger grid size, as shown with the 4mx4m grid size producing a similar velocity.

Flood extent results are shown in figure 6.5. The different max depth profile extents are plotted over the flood plain, as viewed in RAS-MAPPER. As default cell size was increased, the flooded area decreased for the models that included the refinement region. For the model set up with only a 4m x 4m grid the flooded extent was similar to that of the 2m x 2m, except valleys in the terrain showed deeper water depths. The HEC-RAS manual [2] highlights that in the new 2D availability, the mesh can take into account underlying terrain. This can explain why the water can find its way to areas of lower elevation and pool there when viewing plots of all of the models. But, as depicted via the plots in fig ??, the large grid size over the relatively narrow channel is not appropriate to obtain accurate overflow.

Table 6.1: Table of values

Plan	Weir Co-eff	Alpbach Structure m ³ /s	Huebbach Structure m ³ /s
Weir Test 6	0.1	3.02	-2.98
Weir Test 5	0.2	4.82	-4.83
Weir Test 4	0.3	5.31	-5.39
Weir Test 3	0.4	5.22	-5.42
1D2D IST	0.5	6.3	-5.39

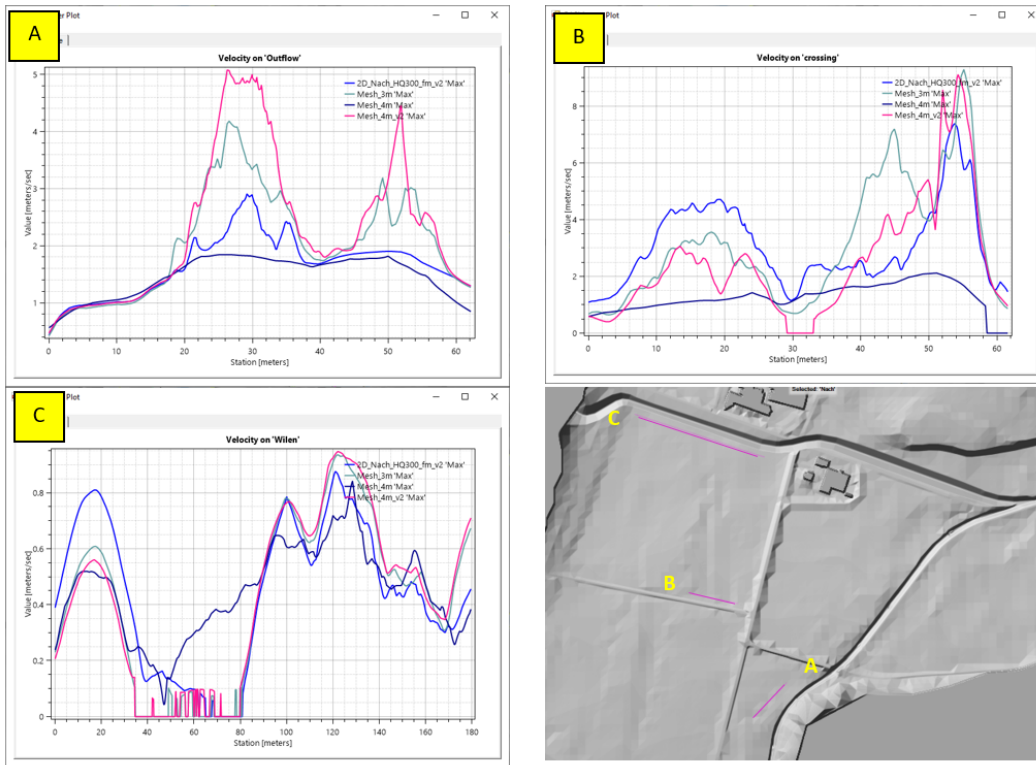


Figure 6.4: Max velocity profiles for the varying grid sizes extracted at three areas

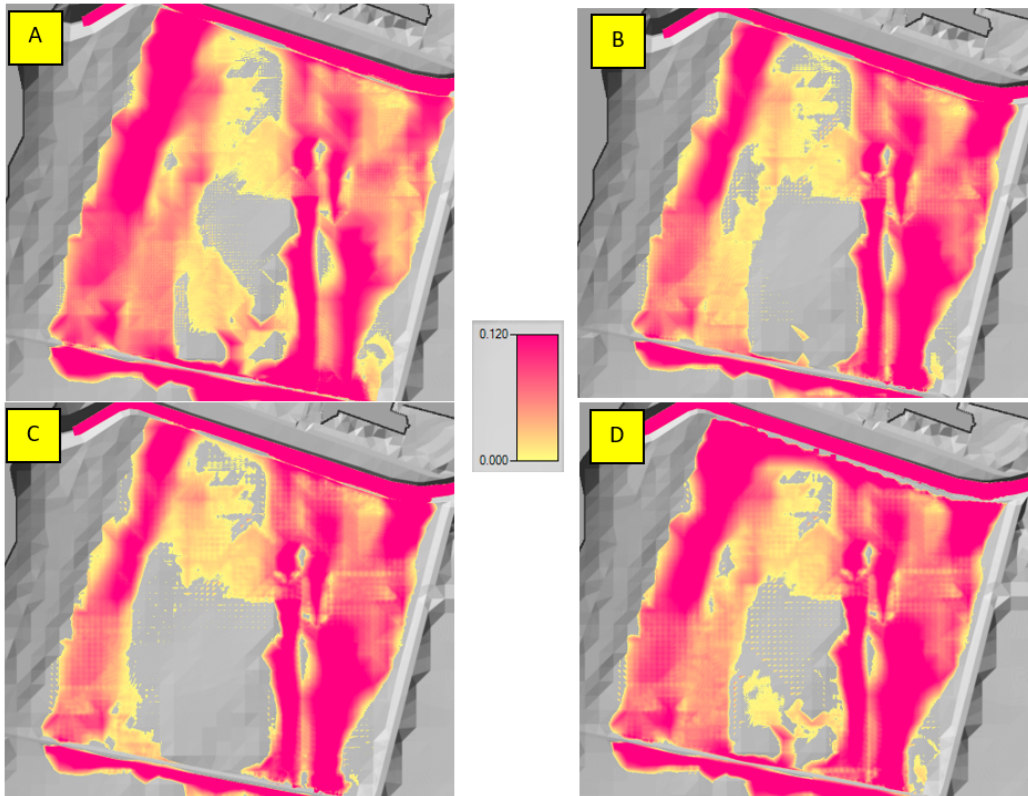


Figure 6.5: Image A is the 2m x 2m default grid. Image B is the 3m x 3m default grid. Image C is the 4m x 4m default grid. Images A-C had refinement regions of 1m x 1m in place over areas of hydraulic importance. Image D is a 4m x 4m grid size over the entire study extent, including channel

6.7 Grid Alignment

Alignment of cell edges was found to be very important and this was realised when setting up the models. The model reacts with high sensitivity to cell alignment and even though the HEC-RAS user's manual emphasises that the 2D grid can take into account underlying terrain, it also states cell faces should be aligned to high ground [2].

In setup of a 2D grid (figure 6.6), with only adding a channel refinement area, not even reducing the cell size, a big difference was observed in the flow being contained in the channel. This flow exceeding the channel in Image A was not for a flood event, but only a base flow to begin setting up and testing the geometry.

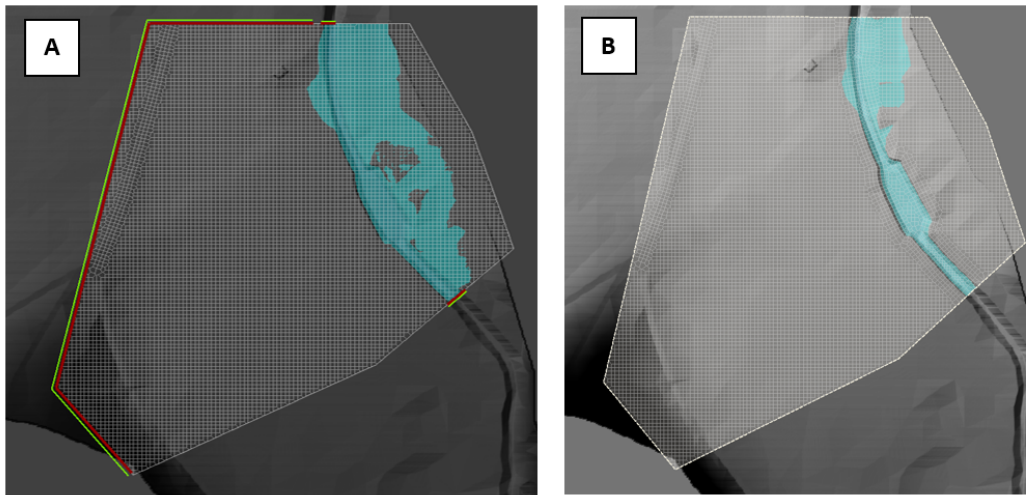


Figure 6.6: Images from setup phase of a 2D model. Image A shows the outcome with a grid laid over the channel area. Image B shows the outcome after a refinement region was added to align the cell edges along the channel bank and bed.

Images D and E in figure 6.7 illustrate overflow leaving the channel and flowing away from it or being directed back into the channel. Image D corresponds to the grid alignment in Image A, where the grid is connected to the structure but care was not taken to align the cell edges along the structure. Image E corresponds to the grid alignment in Image B, where a strip of cells are refined to have their edges parallel to the structure.

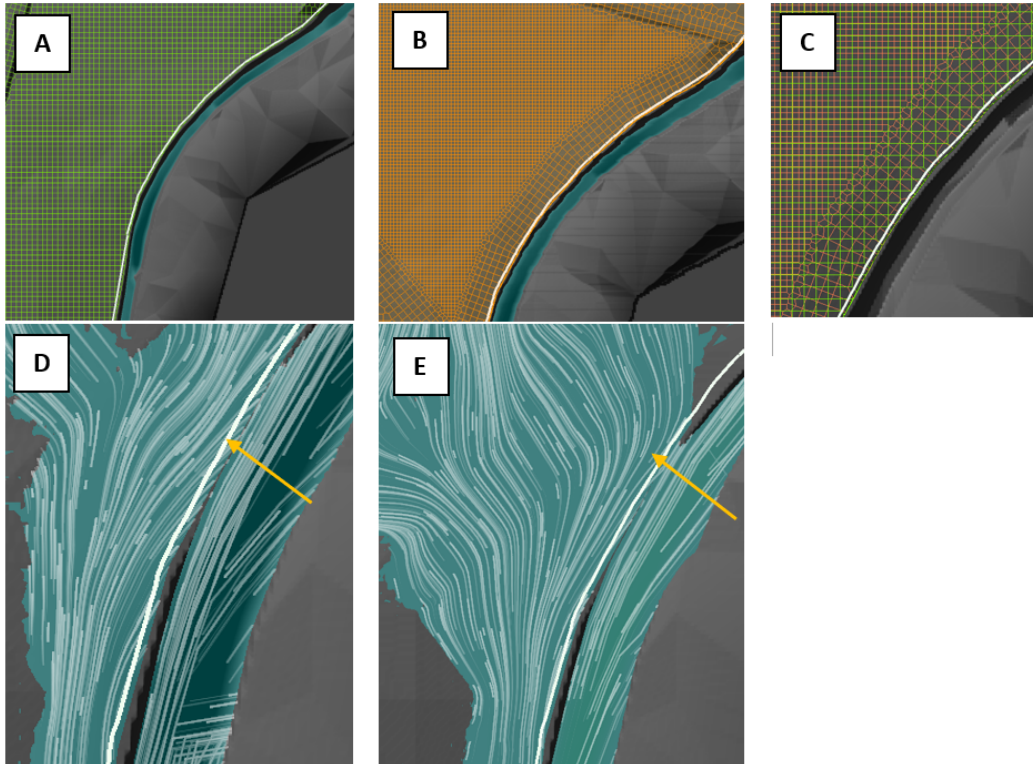


Figure 6.7: Image A is an unrefined grid along the 1D2D connection structure. Image B has a refinement done to the grid. Image C is a comparison of the refined/unrefined grids. Image D and E show the depth results for these models with particle tracing switched on. The particles in image D are leaving the channel and then curving back towards it a short distance later, while those in image E continue to move away from the channel.

Figure 6.8 shows the flow over the structure for the duration of model run time. The total flow is very limited in plot A (0 - .12) and corresponds to a grid not aligned to the structure and water being directed back into the channel (considered a negative direction over the structure). Whereas in plot B, which corresponds to a well aligned grid, the total flow is over $6\text{m}^3/\text{s}$. (y-axis scale is different in each plot).

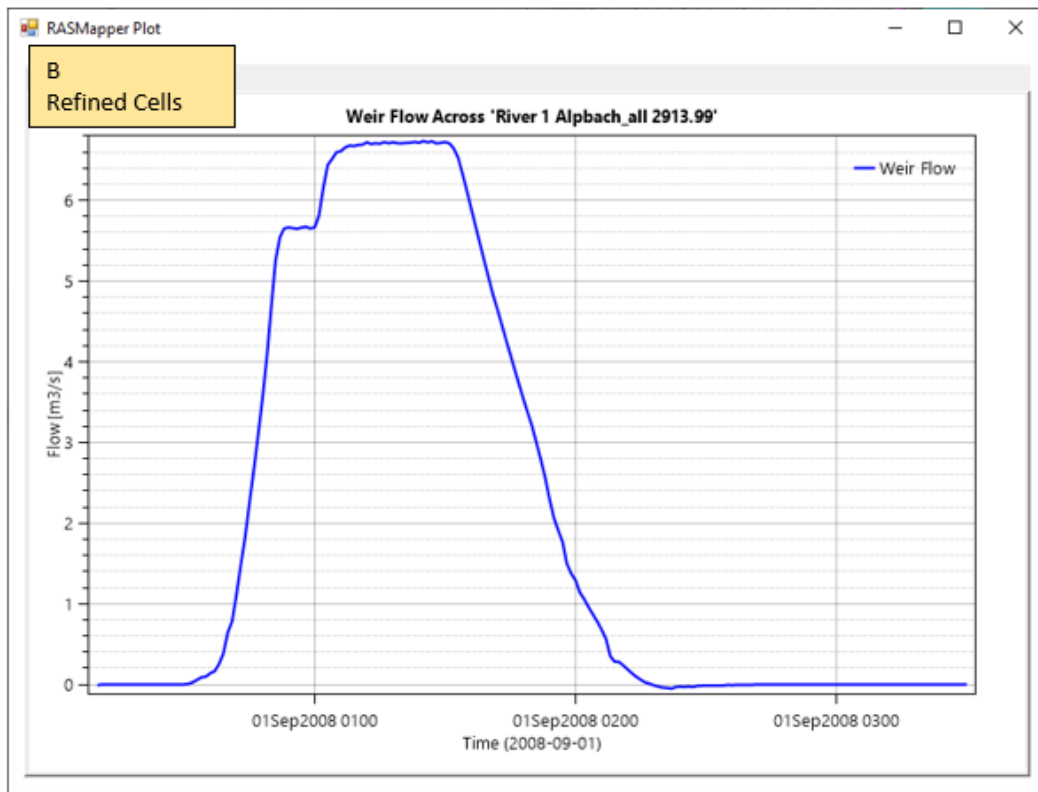
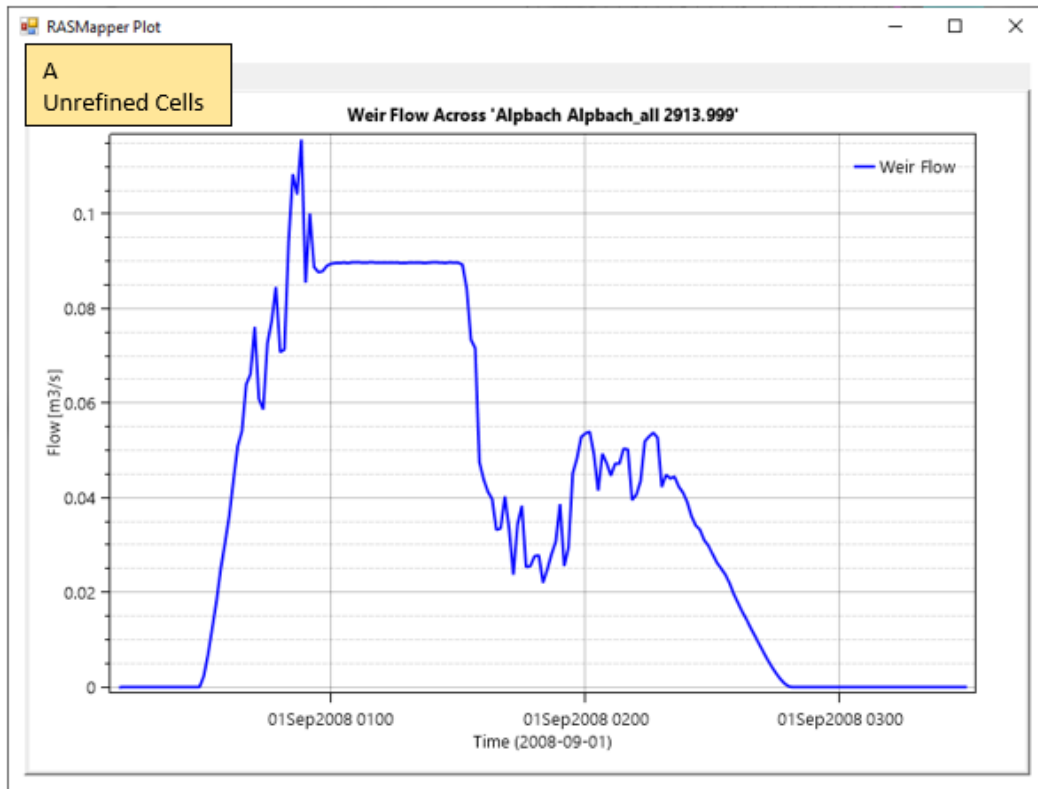


Figure 6.8: For the entire duration of the model run, Plot A shows the limited total flow over the connection structure between 1D and 2D when the cells are not refined and Plot B shows the total flow increase substantially

Chapter 7

Discussion

7.1 Further Discussion

When it comes to computation time, the full 2D NACH scenario took approximately 2.5 computational hour in HEC-RAS and approximately 2 hours in BASEMENT. The HEC-RAS was set to use a 2 second time-step to save on computation time and this was the biggest that could be used. So if using a smaller time step or courant condition then computation time will only increase. Also to mention is that the study area for this thesis amounted to less than 1% of the study area for the HWS, thus computation time would be very large for a fully 2D model covering the whole of HWS. The fully 1D model ran in 17s and if a fully 1D model can meet the modeling requirements, and a skilled modeler is working on the geometry placement, then this will save a lot of time and should be used.

Furthermore, the results need to be taken with caution as there was no accounting for atmospheric or land surface conditions during the model run. For example, during a flood event caused by heavy precipitation, it is likely that the surface would be saturated and an additional flood volume would be present from the precipitation directly falling on the land surface. As well, sediment was not modeled in these scenarios, but realistically, stream flow can contain high sediment loads.

It is difficult to compare exactly the use of both models, as the model set-up for BASEMENT was carried out at B+S AG. But what can be commented on is the features. HEC-RAS is more of an *all in one* software because it contains all of the features needed to set-up a functioning model with input conditions. This is a time saving benefit because for BASEMENT additional softwares would need to be downloaded and learned to set-up the model and process the results. As well, likely due to it being around longer, the community of users for HEC-RAS is very large and it is possible to troubleshoot many problems by searching online.

Chapter 8

Conclusion

In this thesis, the flood models HEC-RAS and BASEMENT were compared within a region contained in HWS, as well, the latest version of HEC-RAS examined in greater detail. The main findings are outlined in this section, grouped by the research questions.

How do the outputs of BASEMENT and HEC-RAS compare to one another?

For the IST scenario, velocity peak values were similar between both models and mainly occurred in the overflow area. Peak depth values between both models showed some variation, with BASEMENT modeling larger depths near the outflow to Wilen and HEC-RAS closer to Engistrasse 95. This was noticed in the contingency outputs with a lower accuracy over the Sooret field and at the outlet to Wilen. For the NACH scenario, there was less variation between the models and higher accuracy values. This could be attributed to greater care being taken in the NACH scenario to arrange the mesh and grid along the newly raised road. Model residuals in general were close to 0 in the study areas, with greatest variation occurring within the channel. In general, HEC-RAS outputs depth slightly less than BASEMENT and velocity slightly higher than BASEMENT. The models also behaved similarly when increasing the hydrology to extreme situations, especially at the junction. The mapping of residuals shows that the residuals over the floodplain intensified slightly.

How do intra-model results from using varying dimensionality in HEC-RAS compare to one another??

In the case of the Alpbach, the channel bed is varied and due to the need to stabilise the 1D model by strategic cross section placement, as well interpolation of terrain between cross sections, this terrain variation is dampened in the 1D model. Yet, the overflow depth over time between the 1D and 2D model was still found to be similar. And with this the outputs for depth and velocity over the floodplain between the 1D/2D and 2D were similar.

A drawback of the 1D model was the set-up time as the cross sections had to be placed to ensure a gradually decreasing channel slope representation. However, this time is gained back in computation time as the 1D model computational demand was miniscule compared to the 2D demand (17s vs 2h+). For an experienced modeler, a 1D model could be a quick and far less computationally intensive means to understand the channel dynamics and produce estimates for flood volume and timing. If it is necessary to model the flood plain then, for the area concerning this case study, the 1D2D results were very close to the 2D and 1D2D could be used to save on computational time.

How do intra-model results from varying parameters in HEC-RAS compare to one another?

Via exploring parameter settings in HEC-RAS, it was found that many parameters and settings are available in the software, but not all of them are applicable for every setting and careful consideration should be taken when setting up the model, to ensure that it suits the study area. In the case of the Alpbach in the HWS, it was found that using the diffusive wave approximation did not apply, even if computation time could be saved and results could be obtained, the results were not valid. As well, the junction equation could be tested but as these Alpbach and Huebbach have large flow discrepancies, only the water surface method could be applied. Adjusting surface roughness values and weir co-efficient values did not result in obscure results and these settings could be tested in calibration to arrive at a suitable value. Computational time step could also be tested and chosen by the modeler depending on their needs and resources. Allowing the model to determine the computational time step based on Courant condition could lead to lengthy computation times, especially when a small grid is used. Grid size should be determined based on the modeling needs and terrain as well. It is possible to use a larger grid size in flatter areas to allow for quicker computation, but in areas where flow is highly varied or greater details is needed from the outputs, the grid size should be reduced. The model was found to be incredibly sensitive to grid alignment. Results could be obtained with poor alignment but they were not valid. The modeler must take great care to study the terrain and set-up the geometry to ensure grid cells are aligned appropriately.

Overall, in this study area, the two softwares produced similar outputs. However, this study area is relatively small and the results here may not apply to larger areas or with different channels. What can be concluded via setting up model geometry, and especially via exploring parameters is that the models are performing computations at points which are ultimately determined by the modeler. Thus the model is highly dependent on how the modeler chooses to represent the system. The geometry set-up is an important link between reality and model results and care should be taken to ensure that study area is well understood by the modeler to provide an accurate as possible connection.

Chapter 9

References

Bibliography

- ¹M. Abily, N. Bertrand, O. Delestre, P. Gourbesville, and C. M. Duluc, "Spatial Global Sensitivity Analysis of High Resolution classified topographic data use in 2D urban flood modelling", *Environmental Modelling and Software* **77**, 183–195 (2016).
- ²U. S. A.C.E., *HEC-RAS River Analysis System*, February (2016).
- ³R. Ahmadian, R. A. Falconer, and J. Wicks, "Benchmarking of flood inundation extent using various dynamically linked one- and two-dimensional approaches", *Journal of Flood Risk Management* **11**, S314–S328 (2018).
- ⁴E. Ahmadisharaf and A. J. Kalyanapu, "A Coupled Probabilistic Hydrologic/Hydraulic Modelling Framework to Investigate the Uncertainty of Flood Loss Estimates", *Journal of Flood Risk Management*, e12536 (2019).
- ⁵L. Alfieri, F. Dottori, R. Betts, P. Salamon, and L. Feyen, "Multi-Model Projections of River Flood Risk in Europe under Global Warming", *Climate* **6**, 6 (2018).
- ⁶Amt fuer Umwelt des Kantons Thurgau, "Alpbach / Krebsbach / Huebbach Hochwasserschutz Vorprojekt", (2015).
- ⁷N. Andres and A. Badoux, "The Swiss flood and landslide damage database: Normalisation and trends", *Journal of Flood Risk Management* **12**, 1–12 (2019).
- ⁸H. Apel, G. T. Aronica, H. Kreibich, and A. H. Thielen, "Flood risk analyses - How detailed do we need to be?", *Natural Hazards* **49**, 79–98 (2009).
- ⁹M. Beniston, "Linking extreme climate events and economic impacts: Examples from the Swiss Alps", *Energy Policy* **35**, 5384–5392 (2007).
- ¹⁰M. Beniston and D. B. Stephenson, "Extreme climatic events and their evolution under changing climatic conditions", *Global and Planetary Change* **44**, 1–9 (2004).
- ¹¹N. D. Bennett, B. F. Croke, G. Guariso, J. H. Guillaume, S. H. Hamilton, A. J. Jakeman, S. Marsili-Libelli, L. T. Newham, J. P. Norton, C. Perrin, S. A. Pierce, B. Robson, R. Seppelt, A. A. Voinov, B. D. Fath, and V. Andreassian, "Characterising performance of environmental models", *Environmental Modelling and Software* **40**, 1–20 (2013).
- ¹²W. Bertoldi, A. Siviglia, S. Tettamanti, M. Toffolon, D. Vetsch, and S. Francalanci, "Modeling vegetation controls on fluvial morphological trajectories", *Geophysical Research Letters* **41**, 7167–7175 (2014).

-
- ¹³G. W. Brunner, "Benchmarking of the HEC-RAS Two-Dimensional Hydraulic Modeling Capabilities", (2018).
- ¹⁴L. Bures, R. Roub, P. Sychova, K. Gdulova, and J. Doubalova, "Comparison of bathymetric data sources used in hydraulic modelling of floods", *Journal of Flood Risk Management* **12** (2019) 10.1111/jfr3.12495.
- ¹⁵A. Cook and V. Merwade, "Effect of topographic data, geometric configuration and modeling approach on flood inundation mapping", *Journal of Hydrology* **377**, 131–142 (2009).
- ¹⁶S. Dhungel, M. E. Barber, and R. L. Mahler, "Comparison of one- And two-dimensional flood modeling in urban environments", *International Journal of Sustainable Development and Planning* **14**, 356–366 (2019).
- ¹⁷G. Di Baldassarre, G. Schumann, P. D. Bates, J. E. Freer, and K. J. Beven, "Cartographie de zone inondable: Un examen critique d'approches déterministe et probabiliste", *Hydrological Sciences Journal* **55**, 364–376 (2010).
- ¹⁸P. Dimitriadis, A. Tegos, A. Oikonomou, V. Pagana, A. Koukouvinos, N. Mamassis, D. Koutsyiannis, and A. Efstratiadis, "Comparative evaluation of 1D and quasi-2D hydraulic models based on benchmark and real-world applications for uncertainty assessment in flood mapping", *Journal of Hydrology* **534**, 478–492 (2016).
- ¹⁹G. Felder, A. Zischg, and R. Weingartner, "The effect of coupling hydrologic and hydrodynamic models on probable maximum flood estimation", *Journal of Hydrology* **550**, 157–165 (2017).
- ²⁰R. Ferguson, "Time to abandon the Manning equation?", *Earth Surface Processes and Landforms* **35**, 1873–1876 (2010).
- ²¹J. Fuhrer, M. Beniston, A. Fischlin, C. Frei, S. Goyette, K. Jasper, and C. Pfister, "Climate risks and their impact on agriculture and forests in Switzerland", *Climatic Change* **79**, 79–102 (2006).
- ²²J. Hall, B. Arheimer, G. T. Aronica, A. Bilibashi, M. Boháč, O. Bonacci, M. Borga, P. Burlando, A. Castellarin, G. B. Chirico, P. Claps, K. Fiala, L. Gaál, L. Gorbachova, A. Gül, J. Hannaford, A. Kiss, T. Kjeldsen, S. Kohnová, J. J. Koskela, N. MacDonald, M. Mavrova-Guirguinova, O. Ledvinka, L. Mediero, B. Merz, R. Merz, P. Molnar, A. Montanari, M. Osuch, J. Parajka, R. A. Perdigão, I. Radevski, B. Renard, M. Rogger, J. L. Salinas, E. Sauquet, M. Šraj, J. Szolgay, A. Viglione, E. Volpi, D. Wilson, K. Zaimi, and G. Blöschl, "A European flood database: Facilitating comprehensive flood research beyond administrative boundaries", *IAHS-AISH Proceedings and Reports* **370**, 89–95 (2015).
- ²³J. Hall, B. Arheimer, M. Borga, R. Brázdil, P. Claps, A. Kiss, T. R. Kjeldsen, J. Kriaučiūnienė, Z. W. Kundzewicz, M. Lang, M. C. Llasat, N. Macdonald, N. McIntyre, L. Mediero, B. Merz, R. Merz, P. Molnar, A. Montanari, C. Neuhold, J. Parajka, R. A. Perdigão, L. Plavcová, M. Rogger, J. L. Salinas, E. Sauquet, C. Schär, J. Szolgay, A. Viglione, and G. Blöschl, "Un-

-
- derstanding flood regime changes in Europe: A state-of-the-art assessment”, *Hydrology and Earth System Sciences* **18**, 2735–2772 (2014).
- ²⁴N. P. f. N. Hazards, *Vademecum - Hazard Maps - Swiss System Applied Abroad*.
- ²⁵F. E. Hicks and T. Peacock, “Suitability of HEC-RAS for Flood Forecasting”, *Canadian Water Resources Journal* **30**, 159–174 (2009).
- ²⁶E. Huțanu, A. Mișu-Pintilie, A. Urzica, L. E. Paveluc, C. C. Stoleriu, and A. Grozavu, “Using 1D HEC-RAS Modeling and LiDAR Data to Improve Flood Hazard Maps Accuracy: A Case Study from Jijia Floodplain (NE Romania)”, *Water* **12**, 1624 (2020).
- ²⁷L. Keller, A. P. Zischg, M. Mosimann, O. Rössler, R. Weingartner, and O. Martius, “Large ensemble flood loss modelling and uncertainty assessment for future climate conditions for a Swiss pre-alpine catchment”, *Science of the Total Environment* **693** (2019) 10.1016/j.scitotenv.2019.07.206.
- ²⁸N. Köplin, B. Schädler, D. Viviroli, and R. Weingartner, “Seasonality and magnitude of floods in Switzerland under future climate change”, *Hydrological Processes* **28**, 2567–2578 (2014).
- ²⁹Kourtis. I. M., Bellos. V., and Tsihrintzis. V. A., “Comparison of 1D-1D and 1D-2D urban flood models”, *Comparison of 1D-1D and 1D-2D urban flood models*, 1–6 (2017).
- ³⁰Z. W. Kundzewicz, S. Kanae, S. I. Seneviratne, J. Handmer, N. Nicholls, P. Peduzzi, R. Mechler, L. M. Bouwer, N. Arnell, K. Mach, R. Muir-Wood, G. R. Brakenridge, W. Kron, G. Benito, Y. Honda, K. Takahashi, and B. Sherstyukov, “Le risque d’inondation et les perspectives de changement climatique mondial et régional”, *Hydrological Sciences Journal* **59**, 1–28 (2014).
- ³¹D. Lea, K. Yeonsu, and A. Hyunuk, “Case study of HEC-RAS 1D-2D coupling simulation: 2002 Baeksan flood event in Korea”, *Water (Switzerland)* **11**, 1–14 (2019).
- ³²Z. Liu, V. Merwade, and K. Jafarzadegan, “Investigating the role of model structure and surface roughness in generating flood inundation extents using one- and two-dimensional hydraulic models”, *Journal of Flood Risk Management* **12** (2019) 10.1111/jfr3.12347.
- ³³B. Merz, J. Aerts, K. Arnbjerg-Nielsen, M. Baldi, A. Becker, A. Bichet, G. Blöschl, L. M. Bouwer, A. Brauer, F. Cioffi, J. M. Delgado, M. Gocht, F. Guzzetti, S. Harrigan, K. Hirschboeck, C. Kilsby, W. Kron, H. H. Kwon, U. Lall, R. Merz, K. Nissen, P. Salvatti, T. Swierczynski, U. Ulbrich, A. Viglione, P. J. Ward, M. Weiler, B. Wilhelm, and M. Nied, “Floods and climate: Emerging perspectives for flood risk assessment and management”, *Natural Hazards and Earth System Sciences* **14**, 1921–1942 (2014).
- ³⁴B. Merz, “Flood Risk Analysis”, in *Oxford research encyclopedia of natural hazard science* (Oxford University Press, 2017), pp. 1–24.

-
- ³⁵D. Molinari, K. M. De Bruijn, J. T. Castillo-Rodríguez, G. T. Aronica, and L. M. Bouwer, "Validation of flood risk models: Current practice and possible improvements", *International Journal of Disaster Risk Reduction* **33**, 441–448 (2019).
- ³⁶S. Néelz and G. Pender, *Delivering benefits thorough evidences: Benchmarking the Latest Generation of 2D Hydraulic Modelling Packages- SC120002*. (2013), Report–SC120002.
- ³⁷G. Papaioannou, L. Vasiliades, A. Loukas, and G. T. Aronica, "Probabilistic flood inundation mapping at ungauged streams due to roughness coefficient uncertainty in hydraulic modelling", *Advances in Geosciences* **44**, 23–34 (2017).
- ³⁸F. Pappenberger, K. Beven, K. Frodsham, R. Romanowicz, and P. Matgen, "Grasping the unavoidable subjectivity in calibration of flood inundation models: A vulnerability weighted approach", *Journal of Hydrology* **333**, 275–287 (2007).
- ³⁹F. Pappenberger, K. Beven, K. Frodsham, R. Romanowicz, and P. Matgen, "Grasping the unavoidable subjectivity in calibration of flood inundation models: A vulnerability weighted approach", *Journal of Hydrology* **333**, 275–287 (2007).
- ⁴⁰D. P. Patel, J. A. Ramirez, P. K. Srivastava, M. Bray, and D. Han, "Assessment of flood inundation mapping of Surat city by coupled 1D/2D hydrodynamic modeling: a case application of the new HEC-RAS 5", *Natural Hazards* **89**, 93–130 (2017).
- ⁴¹F. Peña and F. Nardi, "Floodplain Terrain Analysis for Coarse Resolution 2D Flood Modeling", *Hydrology* **5**, 52 (2018).
- ⁴²A. Petroselli, M. Vojtek, and J. Vojteková, "Flood mapping in small ungauged basins: a comparison of different approaches for two case studies in Slovakia", *Hydrology Research* **50**, 379–392 (2018).
- ⁴³A. Radice, E. Giorgetti, D. Brambilla, L. Longoni, and M. Papini, "On integrated sediment transport modelling for flash events in mountain environments", *Acta Geophysica* **60**, 191–213 (2012).
- ⁴⁴V. Röthlisberger, A. Zischg, and M. Keiler, "Spatiotemporal aspects of flood exposure in Switzerland", *E3S Web of Conferences* **7**, 0–4 (2016).
- ⁴⁵S. Saksena and V. Merwade, "Incorporating the effect of DEM resolution and accuracy for improved flood inundation mapping", *Journal of Hydrology* **530**, 180–194 (2015).
- ⁴⁶K. Schneeberger, O. Rössler, and R. Weingartner, "Spatial patterns of frequent floods in Switzerland", *Hydrological Sciences Journal* **63**, 895–908 (2018).
- ⁴⁷M. Siegrist and H. Gutscher, "Flooding risks: A comparison of lay people's perceptions and expert's assessments in Switzerland", *Risk Analysis* **26**, 971–979 (2006).
- ⁴⁸J. Teng, A. J. Jakeman, J. Vaze, B. F. Croke, D. Dutta, and S. Kim, *Flood inundation modelling: A review of methods, recent advances and uncertainty analysis*, 2017.

-
- ⁴⁹C. Volz, P. Rousselot, D. Vetsch, and R. Faeh, "Numerical modelling of non-cohesive embankment breach with the dual-mesh approach", *Journal of Hydraulic Research* **50**, 587–598 (2012).
- ⁵⁰A. E. K. Vozinaki, G. G. Morianou, D. D. Alexakis, and I. K. Tsanis, "Comparing 1D and combined 1D/2D hydraulic simulations using high-resolution topographic data: a case study of the Koiliaris basin, Greece", *Hydrological Sciences Journal* **62**, 642–656 (2017).
- ⁵¹World Economic Forum, *The Global Risks Report* (2018), p. 80.
- ⁵²R. Worni, M. Stoffel, C. Huggel, C. Volz, A. Casteller, and B. Luckman, "Analysis and dynamic modeling of a moraine failure and glacier lake outburst flood at Ventisquero Negro, Patagonian Andes (Argentina)", *Journal of Hydrology* **444–445**, 134–145 (2012).
- ⁵³A. P. Zischg, M. Mosimann, D. B. Bernet, and V. Röthlisberger, "Validation of 2D flood models with insurance claims", *Journal of Hydrology* **557**, 350–361 (2018).

Declaration of originality

I hereby declare that the submitted thesis is the result of my own, independent work. All external sources are explicitly acknowledged in the thesis.

Place, Date

Navjot Sidhu

Zürich,

A handwritten signature in blue ink, appearing to read 'Navjot', written in a cursive style.

Appendices

Appendix A

A.1 BASEMENT Computational Meshes

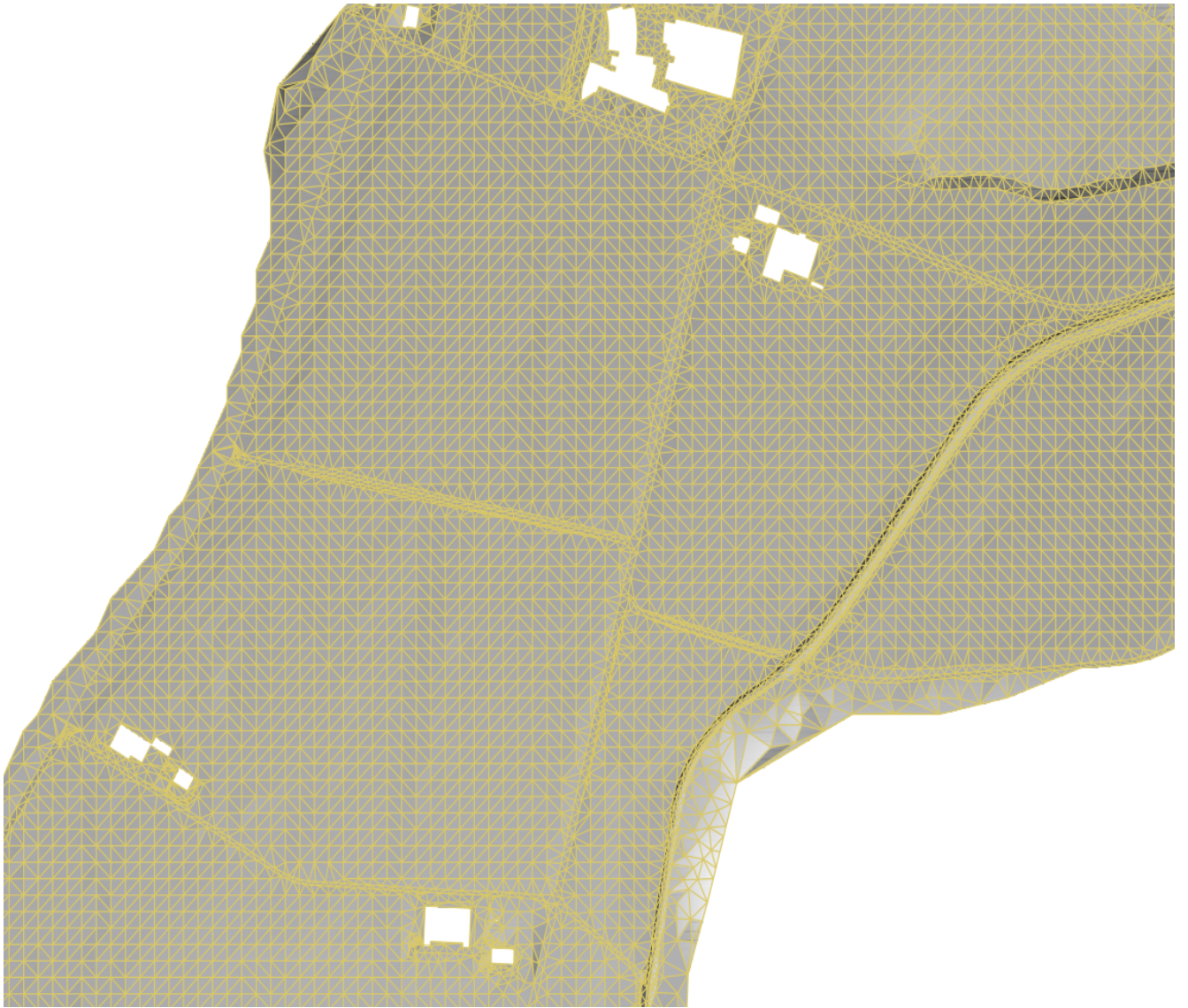


Figure A.1: Computational geometry for the BASEMENT IST scenario over the study area. As received from B+S AG.

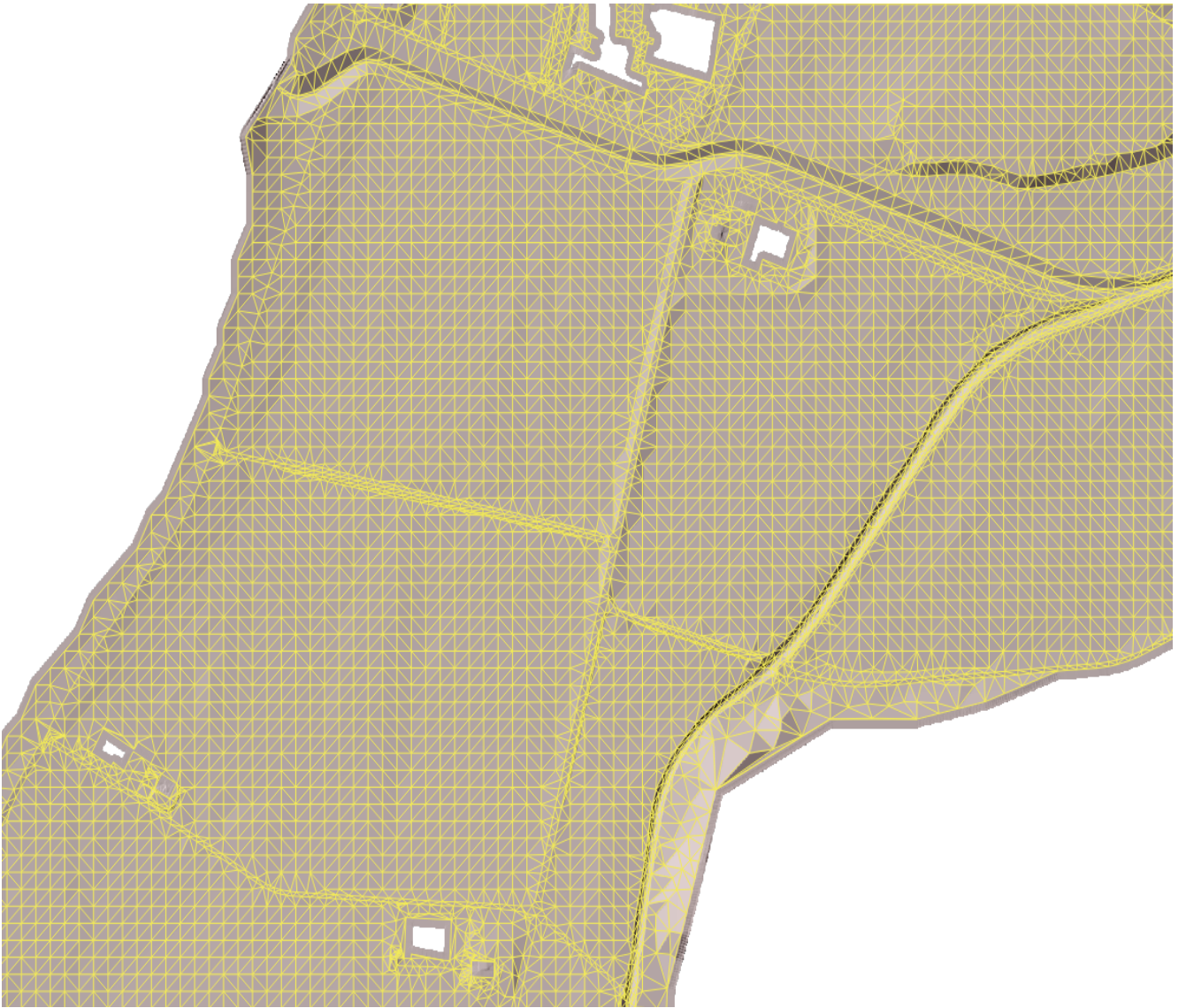


Figure A.2: Computational geometry for the BASEMENT NACH scenario over the study area. As received from B+S AG.

A.2 Flood area maps: start-, end-, and post-peak flow

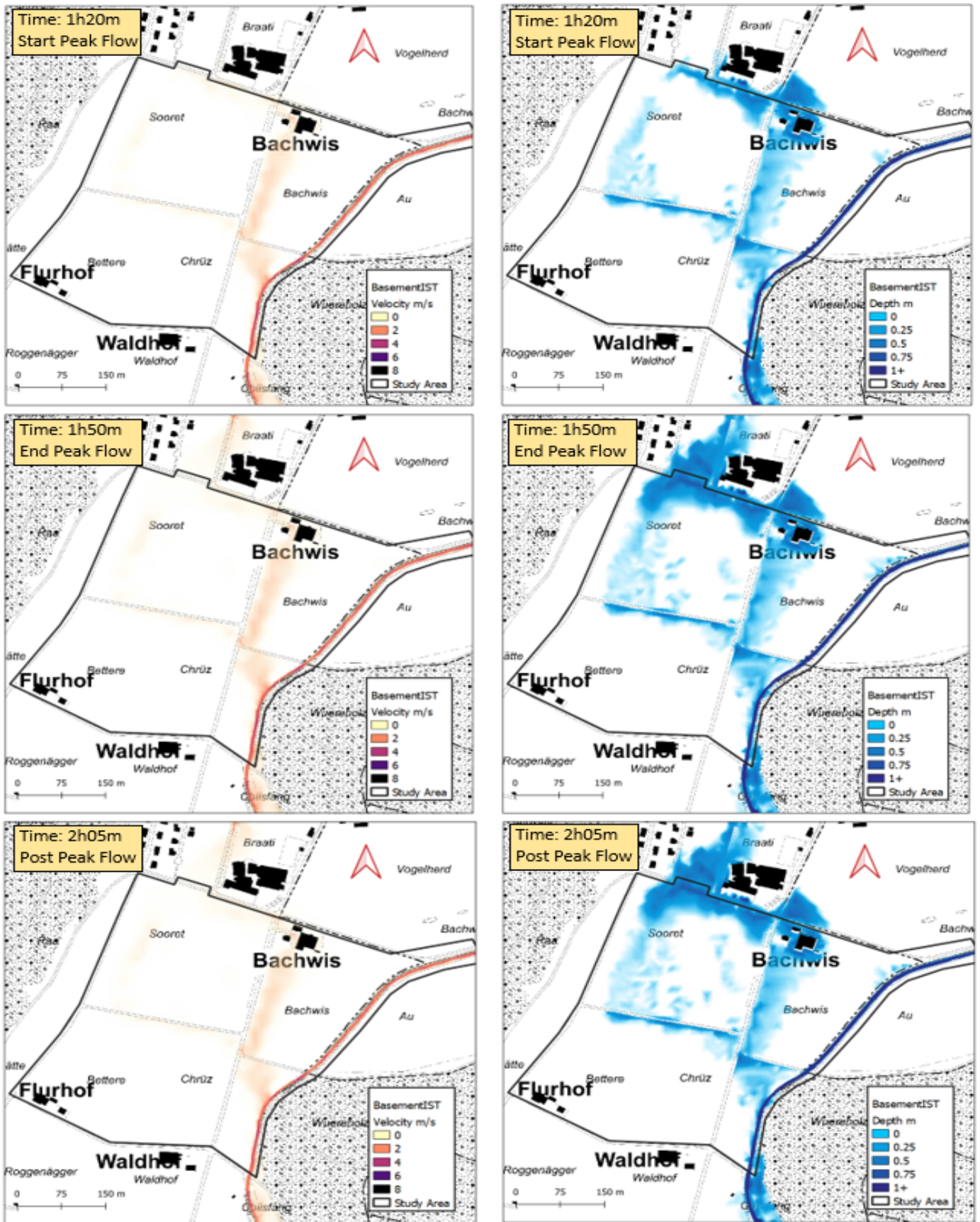


Figure A.3: Depth and Velocity outputs for the BASEMENT IST scenario.

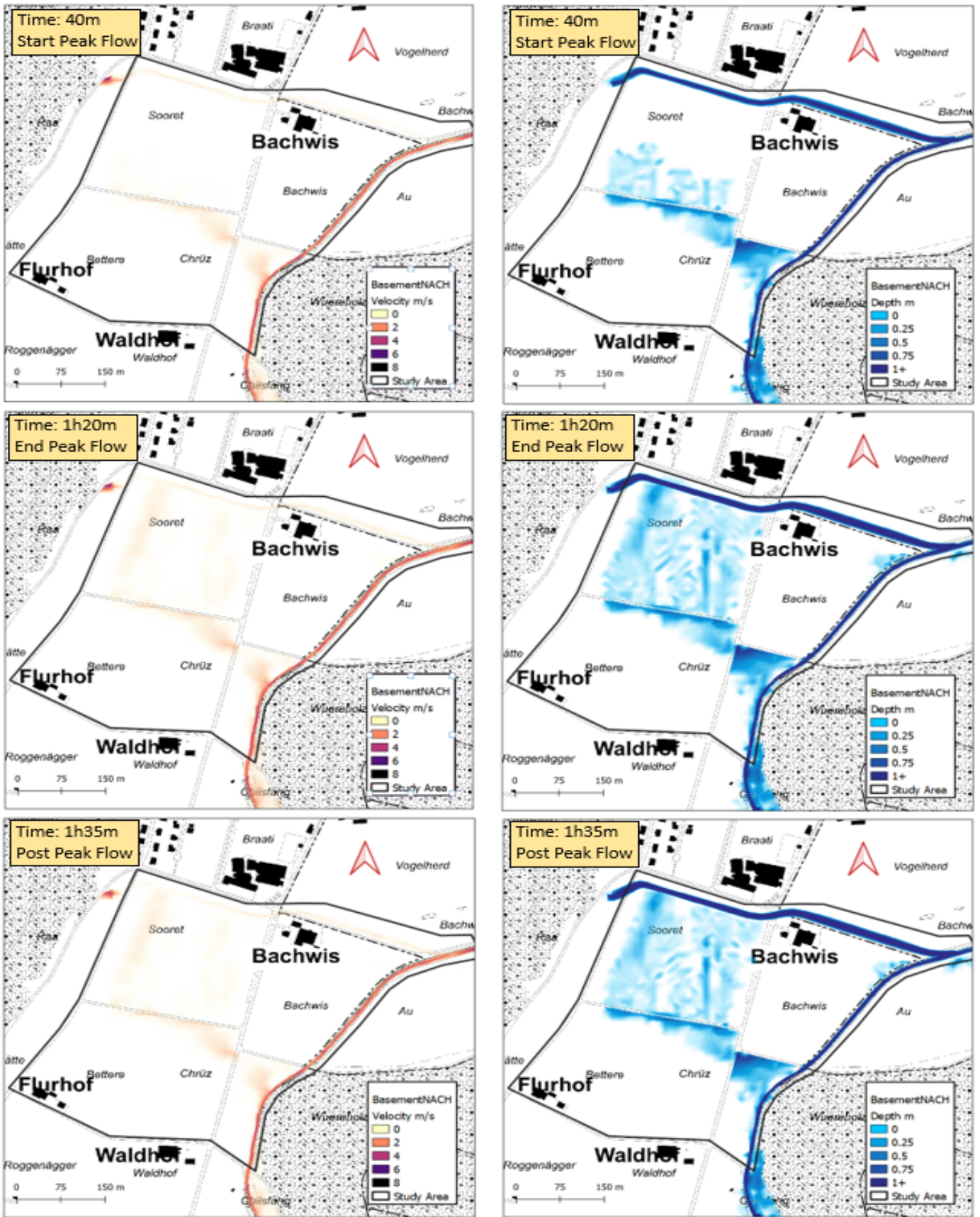


Figure A.4: Depth and Velocity outputs for the BASEMENT NACH scenario.

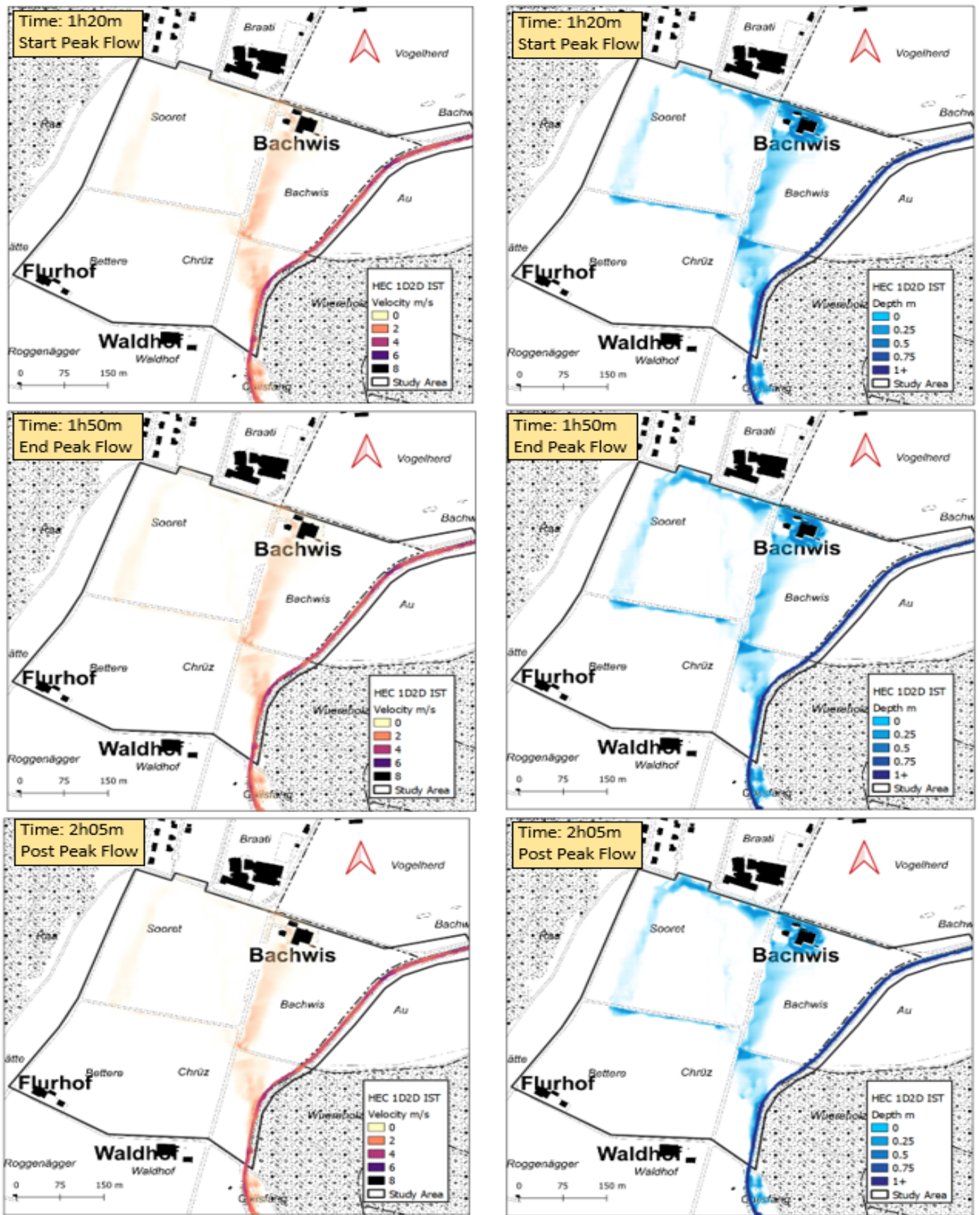


Figure A.6: Depth and Velocity outputs for the HEC-RAS 1D2D IST scenario.

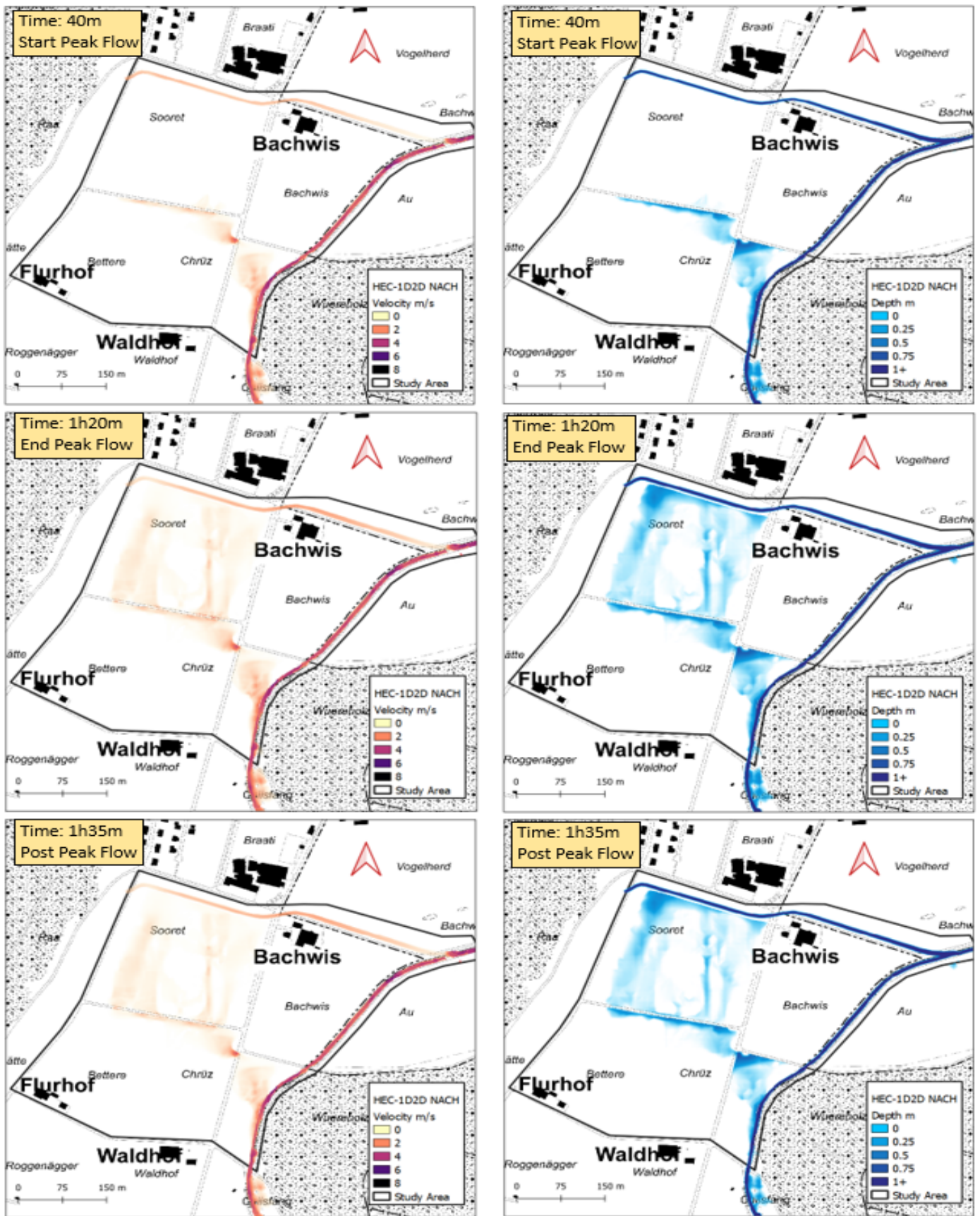


Figure A.7: Depth and Velocity outputs for the HEC-RAS 1D2D NACH scenario.

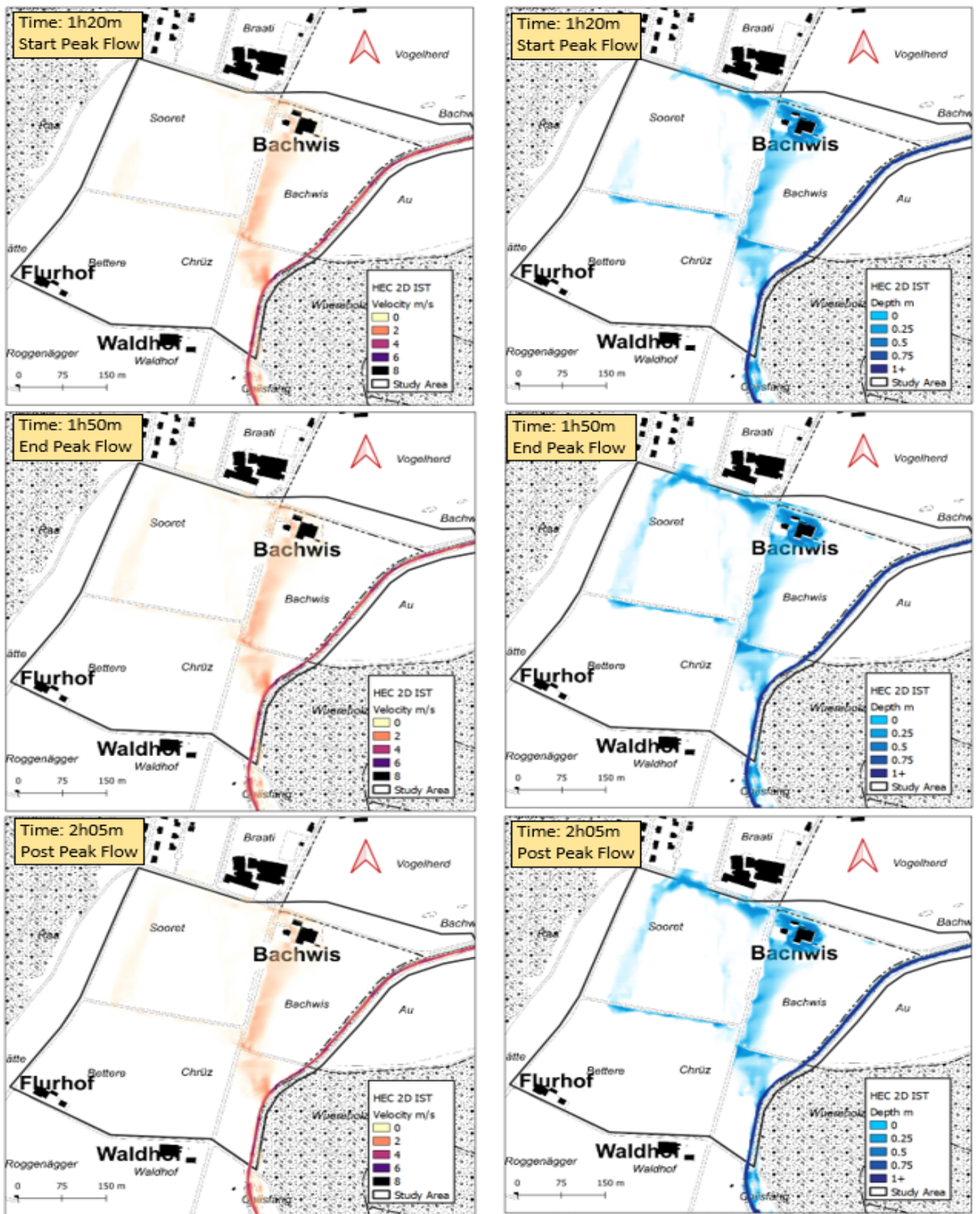


Figure A.8: Depth and Velocity outputs for the HEC-RAS 2D IST scenario.

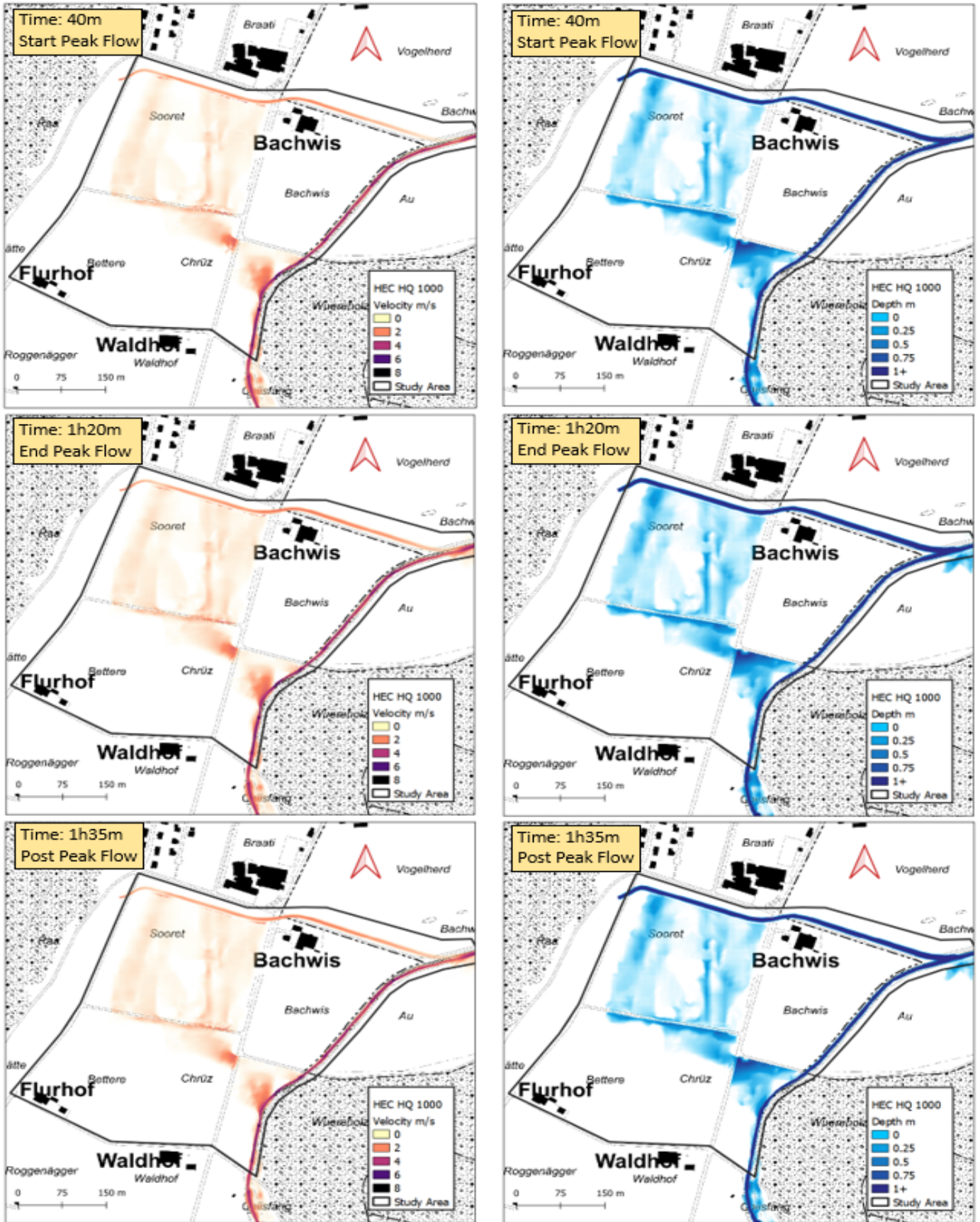


Figure A.10: Depth and Velocity outputs for the HEC-RAS NACH extreme flood scenario.